UNIVERSITY OF SOUTHAMPTON

FACULTY OF HUMANITIES

Archaeology

Volume 2 of 2

Innovation and Technological Change in the Archaeological Record: Conceptual Design in Mediterranean Maritime Technology from the Archaic to Late Antiquity

APPENDICES AND SUPPLEMENTARY DATA

by

Peter B. Campbell

Thesis for the degree of Doctor of Philosophy

March 2017

UNIVERSITY OF SOUTHAMPTON

ABSTRACT

FACULTY OF HUMANITIES

Archaeology

Thesis for the degree of Doctor of Philosophy

Innovation and Technological Change in the Archaeological Record: Conceptual Design in Mediterranean Maritime Technology from the Archaic to Late Antiquity

Peter B. Campbell

This thesis argues for an empirical approach to the study of innovation. Innovation has traditionally been approached as qualitative and therefore not identifiable in the archaeological record. The author uses engineering's principles of conceptual design to argue that fundamental technical concepts differentiate technologies and the level to which a new concept is dissimilar to previous concepts determines its level of innovation. By defining an innovation as the creation of a new conceptual design framework, the thesis explores an empirical view of innovation and how the creation and transfer of design concepts can be quantified and mapped.

In the past, mechanisms for technological change have been adapted to culture from determinism or natural analogies such as evolution. This thesis argues that, as conceptual designs, the most valid mechanism originates from social theories relating to the creation and transfer of concepts. The author introduces Technology-as-Concept as a means to explain the creation and transfer of design concepts as found in the archaeological record.

This approach is applied to three maritime technologies found in the Mediterranean that date from the Archaic Period through Late Antiquity: anchors, warship rams, and ships' hulls. Through identifying conceptual design traits in archaeological remains and interpreting the creation and spread of innovations, the findings challenge the current chronologies for these technologies.

The thesis discusses how Technology-as-Concept is a useful method for archaeology. It challenges cultural evolution and determinism as means for explaining technological change and demonstrates the explanatory ability of the latest social approaches. Finally, it argues for an empirical approach to innovation and the ability to identify innovation in the archaeological record.

DECLARATION OF AUTHORSHIP

I, Peter B. Campbell..

declare that this thesis and the work presented in it are my own and has been generated by me as the result of my own original research.

Innovation and Technological Change in the Archaeological Record: Conceptual Design in Mediterranean Maritime Technology from the Archaic to Late Antiquity..

I confirm that:

1. This work was done wholly or mainly while in candidature for a research degree at this University;
2. Where any part of this thesis has previously been submitted for a degree or any other qualification at this University or any other institution, this has been clearly stated;
3. Where I have consulted the published work of others, this is always clearly attributed;
4. Where I have quoted from the work of others, the source is always given. With the exception of such quotations, this thesis is entirely my own work;
5. I have acknowledged all main sources of help;
6. Where the thesis is based on work done by myself jointly with others, I have made clear exactly what was done by others and what I have contributed myself;
7. Parts of this work have been published as:
   Campbell, Peter B., 2012, A Roman Type IVB Wooden Anchor Found in the Corfu Channel, Albania. *International Journal of Nautical Archaeology* 41(2): 411-416.

Signed: ....

Date: ....

Acknowledgements

First and foremost I must thank my family. My parents have supported- even encouraged- my endless education and fieldwork without hesitation. If I accomplish anything with my life it is due to them. Many of ideas in this thesis have come from discussion with my brother Jonathan, a designer and innovation specialist, who pointed me to parts of the library that archaeologists rarely venture in to. He has always encouraged me to push boundaries and think outside the box. I would also like to thank my family in the United States and Denmark, who I feel as though I have neglected during the PhD. It is a problem I look forward to rectifying shortly.

I have been fortunate to have an extraordinary PhD supervisor, Lucy Blue, who is a brilliant archaeologist, but also a wonderful person. She has worked tirelessly for me, not only in regards to supervision, but locating PhD funding and offering career advice. She has done this not only for me, but many other PhD and Masters students at Southampton and elsewhere. This will prove Lucy's lasting legacy, as she has been sowing the seeds for the future of maritime archaeology through the Centre for Maritime Archaeology, Alexandria Centre for Maritime Archaeology, MAST, and Honor Frost Foundation. The field will reap the benefits long into the future.

I am grateful for the advice of Simon Keay, who has been a terrific advisor on my PhD. My supervisory committee, composed of Ian Croudace, Julian Whitewright, Dominic Hudson, Stephen Turnock, and Jon Downes, provided excellent support. Ian even trekked across Italy with me, from Sicily to Pisa, to sample artefacts. I am also grateful for the advice of Archaeology faculty members such as Clive Gamble and Yannis Hamilakis, who were always happy to discuss ideas.

The faculty of the Centre for Maritime Archaeology provided endless help and support: Jon Adams, Julian Whitewright, Helen Farr, Jesse Ransley, and Fraser Sturt. Without these five, and Lucy, this thesis would look very different. I also must thank the student members of the CMA and Archaeology department, who have been invaluable for bouncing ideas around. I'm not going to try to list everyone or I am bound to forget someone, but you know who you are.

I am indebted to Jeff Royal, a tireless mentor who encouraged all my research proposals from Sicily to Croatia, and RPM Nautical Foundation, especially George Robb, James Goold, Howard Phoenix, and Michael Blades. Sebastiano Tusa and the Soprintendenza Del Mare's office were very accommodating. Thanks to William Murray for help in Rome and professional advice.

A great deal of other fieldwork contributed to this research, including the field schools I co-directed in Albania, Montenegro, and Croatia. Thank you to Auron Tare, Derek Smith, Chris Begley, Petra Zdravkovic, Derek Irwin, Luka Bekic, Mladen Pesic, and Lee Pape who helped run these projects. Chris has advised me on all things professional and his mentorship has greatly shaped my career. I would also like to thank the many students that attended our field schools.

There are a number of museums and museum staffs that I am indebted to: the staff of the Kanellopoulous Museum, the staff of the Piraeus Museum, Musée Petit Palais, A.D. Trendall Research Centre at La Trobe University, Dirk Booms, Ross Thomas, and the Department of Greece and Rome at the British Museum, and Marianne Hamiaux and Ludovic Laugier at Musée Louvre.

I am indebted to Greg Votruba, who made his PhD on ancient anchors available to me. While in the midst of my own reconstruction and testing of ancient anchors, I heard of Greg's World Anchors Reconstruction and Experimentation Project with its ambitious full-scale reconstruction of ancient anchor designs. Greg's research and our discussions contributed to my own work.

A great deal of analysis was undertaken for this thesis and I am appreciative of the work by the National Oceanography Centre, Ship Science, Mu-VIS facility (Engineering) at the University of Southampton, Winchester School of Art, and University of Kentucky. The finite elemental analysis was conducted by engineering interns Yannick Mathias and Sylvain Gimenez. Similarly, 3D modelling was conducted by Mateuz Polakowski, James Miles, and Grant Cox, and I am indebted for their help. Larry Hassebrook and Eli Crane from the University of Kentucky dragged several 3D scanners out to archaeological sites to help out. Mark Mavrogordato, the Mu-VIS staff, and James Miles ran the x-ray tomography. Anna Wilma helped with Greek translations.

This research was possible through funding from several groups. I am indebted to the Southampton Marine and Maritime Institute for my studentship. Fieldwork was funded by the Honor Frost Foundation, Historical Metallurgy Society, Explorers Club, and Breuckmann GmbH.

Damian Robinson, the external examiner for the viva, provided a helpful critique that greatly improved the thesis. His advice and help is greatly appreciated.

Finally, I would like to thank my mentors. Over the last fifteen years I have been privileged to have a number of brilliant minds shape my professional career. Foremost are Lucy Blue, Chris Begley, and Jeff Royal who were mentioned earlier, but also Jon Henderson, Nic Flemming, Fred Hocker, Larry Babits, Nathan Richards, David Stewart, Maria Jacobsen, Grant Gilmore, Craig Williams, and Susie Jansen. Thank you all.

Discussions at conferences and pubs over the years have been very fruitful to the ideas expressed in this thesis. Each interaction offers challenges and improves ideas. It is a delight to study people in the past, but the real pleasure is working through ideas with the people in the present. I am indebted to this small field of archaeology and hope to continue to contribute.

Contents

Appendices

This volume contains the appendices and supplementary data for the thesis *Innovation and Technological Change in the Archaeological Record: Conceptual Design in Mediterranean Maritime Technology from the Archaic to Late Antiquity,* presented in Volume I.

Appendix 1 is a table of known ancient anchors from dateable contexts.

Appendix 2 is a copy of the author's article "A Roman Type IVB Anchor Found in the Corfu Channel, Albania" in the *International Journal of Nautical Archaeology*.

Appendix 3 is a description of the rams that have been found in the archaeological record.

Appendix 4 is an account of analysis and testing of the Egadi warship rams.

Appendix 5 is a chronology of the available evidence for warship rams including bronze rams, iconography, numismatics, monuments, and other sources.

Appendix 6 contains the hydrostatic results of the hull reconstructions.

Appendix 1. Table of Ancient Anchors

Anchor Database					
Site/Shipwreck	*Anchors*	*Location*	*Material*	*Date*	*Source*
Aci Trezza 1	Multiple	Italy	Iron & lead	1-400 AD	Strauss 2013:9030
Agde A	A	France	Iron	200-150 BC	Bouscaras 1954
Algajola	A	France	Lead	150-100 BC	Liou 1973
Algajola	B		Lead		
Algajola	C		Lead		
Algajola	D		Lead		
Algajola	E		Lead		
Algajola	F		Lead		
Alonnisos	A	Greece	Lead	420-400 BC	Hadjidaki 1996:561-593
Anataş Adacik	A	Turkey	Iron	1000-1100 AD	Günsenin 1998:312
Antidragonera	A	Greece	Stone	350-300 BC	Strauss 2013:8658
Antidragonera	B		Stone		
Antidragonera	C		Stone		
Antidragonera	D		Stone		
Antidragonera	E		Stone		
Antidragonera	F		Stone		
Antidragonera	G		Stone		
Antidragonera	H		Stone		
Antidragonera	I		Stone		
Antikythera A	A	Greece	Lead	c. 80 BC	Throckmorton 1970:10
Antikythera B	A	Greece	Lead	100 BC- 500 AD	Dumas 1972
Arles IV	A	France	Lead	25-40 AD	Long 1993:30-31
Arles IV	B		Iron		
Artemision	A	Greece	Lead	200-80 BC	Kallipolitis 1972:419-426
Ashkelon	A	Israel	Iron	400-1450 AD	Strauss 2013:8847
Ashkelon	B	Israel	Iron		
Ashkelon Hellenistic	A	Israel	Iron	200-1 BC	Galili *et al.* 2010:125-145
Ashkelon Hellenistic	B		Iron		
Ashkelon Hellenistic	C		Iron		
Ashkelon Hellenistic	D		Iron		
Ashkelon Byzantine	Multiple		Iron	400-1450 AD	Galili and Sharvit 1998:102
Ashkelon Late Roman	A	Israel	Stone	300-500 AD	Galili and Sharvit 1998:101
Ashkelon Late Roman	B		Stone		
Ashkelon Roman	A	Israel	Lead	1-200 AD	Strauss 2013:8855
Atalanti	A	Greece	Lead	1-100 AD	Touchais 1985:831
Avidmou Bay	A	Cyprus	Stone	450-500 AD	Leidwanger 2007:308-316
Avidmou Bay	B		Stone		
Avidmou Bay	C		Stone		

Avidmou Bay	D		Stone		
Avidmou Bay	E		Stone		
Avidmou Bay	F		Stone		
Avidmou Bay	G		Stone		
Avidmou Bay	H		Stone		
Avidmou Bay	I		Stone		
Avidmou Bay	J		Stone		
Avidmou Bay	K		Stone		
Balise de Rabiou	Multiple	France	Unknown	40-100 AD	Dangreaux 1993:50
Bateguier	Multiple	France	Iron	900-1000 AD	*Bilan Scientifique* 1993:52
Bozburun Byzantine	A	Turkey	Iron	875-900 AD	Harpster 2009:297-313
Bozburun Late Antique	A	Turkey	Iron	500-600 AD	Royal 2006:195-218
Bozburun Late Antique	B		Iron		
Bozburun Late Antique	C		Iron		
Bozburun Late Antique	D		Iron		
Bozburun Late Antique	E		Iron		
Bozburun Late Antique	F		Iron		
Bozburun Late Antique	G		Iron		
Bozburun Late Antique	H		Iron		
Bozburun Late Antique	I		Iron		
Bumbiste	A	Croatia	Lead	30 BC-200 AD	Jurišić 2000:4
Butrint 1	A	Albania	Lead	300-275 BC	Royal 2008:29-31
Cala del Diavolo	A	Italy	Iron	120-10 BC	Strauss 2013:8983
Cala del Falco 2	A	Italy	Lead	25-50 AD	Strauss 2013:9056
Cala del Falco 2	B		Lead		
Cala Minnola	A	Italy	Lead	100-50 BC	Strauss 2013:8722
Çamalti Burnu 1	A	Turkey	Iron	120-1280 AD	Günsenin 2001:117-133
Çamalti Burnu 1	B		Iron		
Çamalti Burnu 1	C		Iron		
Camarina A	A	Italy	Iron	175-200 AD	Parker 1976:25-29
Cap Bear B	A	France	Iron	100-300 AD	Strauss 2013:7593
Cap Bear B	B		Iron		
Cap Bear B	C		Iron		
Cap Bear B	D		Iron		
Cap Bear B	E		Iron		
Cap Bear B	F		Iron		
Cap Bear B	G		Lead		

Cap Gros C	A	France	Lead	50-1 BC	Gauthier 1992:55
Cap Gros C	B		Lead		
Cap Gros C	C		Lead		
Cap Gros C	D		Iron		
Cap Taillat	A	France	Iron	110-90 BC	Strauss 2013:7623
Cape Gelidonya A	A	Turkey	Stone	1200-1150 BC	Strauss 2013:7631
Cape Glavat	A	Croatia	Lead	75-100 AD	Jurišić 2000:10
Capo Granitola A	A	Italy	Iron	225-275 AD	Gianfrotta and Pomey 1980:219
Capo Granitola A	B		Lead		
Capo Granitola D	A	Italy	Iron	200-400 AD	Purpura 1987
Capo Granitola D	B		Iron		
Capo Granitola D	C		Iron		
Capo Granitola D	D		Lead		
Capo Palinuro	A	Italy	Lead	150 BC-400 AD	Strauss 2013:8811
Capo Testa	A	Italy	Iron	1-75 BC	Strauss 2013:7680
Cavalière	A	France	Lead	110-90 BC	Charlin *et al.* 1978:9-93
Cefalu	A	Italy	Lead	400-600 AD	Strauss 2013:7715
Cefalu	B		Iron		
Cefalu	C		Stone		
Chretienne C	A	France	Lead	175-150 BC	Pomey and Guibal 1996:102
Chretienne D	A	France	Iron	325-375 AD	Joncheray 1994:54
Chretienne D	B		Iron		
Comlek Burun	A	Turkey	Iron	1000-1200 AD	Royal 2006:195-218
Coscia di Donna	A	Italy	Lead	75-100 AD	Strauss 2013:149
Dhokos	A	Greece	Stone	2210-2190 BC	Strauss 2013:7780
Dhokos	B		Stone		
Dhrapi	A	Greece	Lead	250-50 BC	Papathanassopoulos 1980:164-167
Dor D	A	Israel	Stone	550-600 AD	Kahanov and Royal 2001:257
Dor D	B		Stone		
Dor D	C		Stone		
Dramont C	A	France	Lead	125-100 BC	Joncheray 1994:5-51
Dramont C	B		Lead		
Dramont C	C		Lead		
Dramont C	D		Lead		
Dramont D	A	France	Lead	40-50 AD	Tchernia 1969:469-470
Dramont D	B		Iron		
Dramont D	C		Iron		
Dramont D	D		Iron		
Dramont E	Multiple	France	Iron	425-455 AD	Santamaria 1995
Dramont F	A	France	Iron	390-410 AD	Joncheray 1975:91-132
Ein Gedi	A	Israel	Lead	200-1 BC	Hadas *et al.* 2005:299

Gallipoli 1	A	Italy	Iron	1-400 AD	Strauss 2013:8694
Gallipoli 1	B		Iron		
Gallipoli 1	C		Iron		
Gallipoli 1	D		Iron		
Gallipoli 1	E		Iron		
Gallipoli 1	F		Iron		
Gallipoli 1	G		Iron		
Grado	A	Italy	Lead	300-200 BC	Strauss 2013:8885
Grado	B		Lead		
Grado (Julia Felix)	A	Italy	Iron	117-150 AD	Picozzi 1988:46-50
Grand Rouveau	A	France	Lead	25-75 AD	Marlier 2008:176-192
Grand Rouveau	B		Lead		
Grand Rouveau	C		Iron		
Herzliya Beach	A	Israel	Iron	1-400 AD	Strauss 2013:8856
Hishuley Carmel	A	Israel	Stone	1450-1350 BC	Strauss 2013:7917
Hof Hacarmel A	A	Israel	Lead	160-170 AD	Raban 1969:71
Isis	A	Int'l	Iron	375-425 AD	McCann and Freed 1994
Isis	B		Iron		
Isis	C		Iron		
Isis	D		Iron		
Isla Pedrosa	A	Spain	Iron	150-140 BC	Strauss 2013:7934
Isola di Monte Cristo	A	Italy	Iron	400-300 BC	Gianfrotta and Pomey 1980
Jaz Islet	A	Croatia	Iron	50-1 BC	Jurišić 2000:23
Kefar Shamir	A	Israel	Stone	1400-1200 BC	Strauss 2013:7952
Kizilburun	A	Turkey	Iron	125-25 BC	Rash 2012
Kizilburun	B		Lead		
Kizilburun	C		Lead		
Kizilburun	D		Lead		
Kizilburun	E		Lead		
Kocayemişilik	A	Turkey	Iron	1000-1100 AD	Günsenin 1998:312
Kocayemişilik	B		Iron		
Kopa	A	Croatia	Lead	25 BC-75 AD	Jurišić 2000:28
Kuyu Burnu	A	Turkey	Iron	600-700 AD	Günsenin 1998:312
Kuyu Burnu	B		Iron		
Kyrenia	A	Cyprus	Lead	310-300 BC	van Duivenvoorde 2012
La Giraglia	A	France	Lead	15-25 AD	Sciallano 1996:60
La Madonnina	A	Italy	Stone	325-300 BC	Strauss 2013:8022
La Madonnina	B		Stone		
Ladispoli B	A	Italy	Lead	25-100 AD	Gianfrotta 1981:27-31
Ladispoli B	B		Lead		
Lake Nemi	A	Italy	Iron	35-50 AD	Speziale 1931
Lake Nemi	B	Italy	Lead		
Laurons C	A	France	Lead	200-275 AD	Strauss 2013:7991
Laurons D	A	France	Lead	310-340 AD	Strauss 2013:7992

Le Miladou	A	France	Lead	125-50 BC	Dumontier and Joncheray 1991:109-174
Le Scole	A	Italy	Iron	300-400 AD	Rendini 1982:50
Le Scole	B		Lead		
Le Scole	C		Lead		
Les Mouettes	A	France	Iron	150-200 AD	*Bilan Scientifique* 1998:27
Les Mouettes	B		Iron		
Les Riches Dunes 4	A	France	Iron	50-1 BC	*Bilan Scientifique* 2002:47
Ma'agan Mikha'el	A	Israel	Lead	430-390 BC	Kahanov and Linder 2003
Maguelone	A	France	Iron	1-100 AD	*Bilan Scientifique* 2003:56
Mahdia	A	Tunisia	Lead	90-60 BC	Kapitän 1983
Mahdia	B		Lead		
Mahdia	C		Lead		
Mahdia	D		Lead		
Mal di Ventre	A	Italy	Lead	75-25 BC	Salvi 1992:237-248
Mal di Ventre	B		Lead		
Mal di Ventre	C		Lead		
Mala Palagruza	A	Croatia	Iron	1-100 AD	Jurišić 2000:39
Mala Palagruza	B		Lead		
Mali Frasker	A	Croatia	Lead	25 BC-75 AD	Jurišić 2000:40
Mazarron 2	A	Spain	Lead	650-600 BC	Negueruela 2005
Minorca	A	Spain	Unknown	1-300 AD	Strauss 2013:8100
Mlin	A	Croatia	Lead	1-200 AD	Jurišić 2000:45
Mlin	B	Croatia	Lead		
Moudros Bay	Multiple	Greece	Lead	325-25 BC	Strauss 2013:96
Mucurune	A	Italy	Unknown	200-50 BC	Strauss 2013:8826
Newe Yam Roman	A	Israel	Iron	150 BC-400 AD	Galili and Sharvit 1999:100
Newe Yam Roman	B		Iron		
Newe-Yam	A	Israel	Stone	1200-900 BC	Galili and Sharvit 1999:100
Newe-Yam	B		Stone		
Newe-Yam	C		Stone		
Newe-Yam	D		Stone		
Newe-Yam	E		Stone		
Newe-Yam	F		Stone		
Newe-Yam	G		Stone		
Newe-Yam	H		Stone		
Newe-Yam	I		Stone		
Newe-Yam	J		Stone		
Newe-Yam	K		Stone		
Newe-Yam	L		Stone		
Pabuç Burnu	A	Turkey	Stone	575-550 BC	Polzer 2004
Pabuç Burnu	B		Stone		
Pigne	A	Italy	Unknown	1000-1500 AD	Strauss 2013:8692
Pisa E	A	Italy	Lead	30-1 BC	Neilson 2002:248
Plane C	Multiple	France	Iron	900-1000 AD	*Bilan Scientifique* 2001:60

Plavac A	A	Croatia	Iron	10 BC-15 AD	Jurišić 2000:56
Plavac A	B		Iron		
Plemmirio B	Multiple	Italy	Iron	175-225 AD	Gibbins 1997:457-459
Plocice	A	Croatia	Lead	150 BC-400 AD	Jurišić 2000:58
Plytra - Xyli Bay	Multiple	Greece	Iron	150 BC-400 AD	Strauss 2013:8997
Polyaigos	A	Greece	Unknown	420-350 BC	Strauss 2013:8984
Porticello	Multiple	Italy	Lead	425-400 BC	Strauss 2013:8262
Porto Ercole A	A	Italy	Lead	150-100 BC	Rendini 1982:43-44
Pseira	A	Greece	Stone	1800-1675 BC	Strauss 2013:8986
Punta Licosa 1	A	Italy	Lead	100-1 BC	Beltrame 2002:459
Punta Mazza	A	Italy	Lead	200-250 AD	Freschi 1997:60-65
Punta Scaletta	A	Italy	Iron	140-130 BC	Lattanzi 2007:50-51
Punta Scaletta	B		Iron		
Punta Scaletta	C		Iron		
Punta Scaletta	D		Lead		
Punta Scaletta	E		Lead		
Punta Scaletta	F		Lead		
Punta Scaletta	G		Lead		
Qaitbay 1	Multiple	Egypt	Stone	75-25 BC	Strauss 2013:65
Qaitbay 2	Multiple	Egypt	Stone, iron, lead	200-1 BC	Strauss 2013:131
Saintes-Maries 11	A	France	Iron	150 BC-400 AD	*Bilan Scientifique* 1998:36
Saintes-Maries 25	A	France	Lead	50 BC-50 AD	*Bilan Scientifique* 2003:65-66
Saintes-Maries 25	B		Iron		
Saintes-Maries 3	A	France	Iron	1-100 AD	Long 1995:42
Saraylar	A	Turkey	Iron	1000-1100 AD	Günsenin 1998:315
Sciacca	A	Italy	Lead	150 BC-400 AD	Strauss 2013:8723
Secca Del Bagno	A	Italy	Lead	100-180 BC	Will 1982:352
Secca di Capistello	A	Italy	Iron	300-280 BC	Lattanzi 2007:123
Secca di Capistello	B		Lead		
Secca di Capistello	C		Lead		
Secche della Circe	A	Italy	Iron	400-500 AD	Strauss 2013:8721
Serçe Limani A	A	Turkey	Iron	1025-1030 AD	Bass *et al*. 2004
Serçe Limani A	B		Iron		
Serçe Limani A	C		Iron		
Serçe Limani A	D		Iron		
Serçe Limani A	E		Iron		
Serçe Limani A	F		Iron		
Serçe Limani A	G		Iron		
Serçe Limani A	H		Iron		
Serçe Limani A	I		Iron		
Sette Fratelli	A	Italy	Stone	400-300 BC	Strauss 2013:9027
Skerki Bank B	A	Italy	Lead	50-100 AD	McCann and Oleson 2004:128-154

Skerki Bank D	A	Italy	Lead	80-50 BC	McCann and Oleson 2004:40-90
Skerki Bank D	B		Lead		
Skerki Bank F	A	Italy	Iron	25-75 AD	McCann and Oleson 2004:90-118
Skerki Bank G	A	Italy	Lead	25-75 AD	McCann and Oleson 2004:118-128
Skerki Bank G	B		Lead		
Skerki Bank G	C		Lead		
Sud Lavezzi 5	A	France	Iron	50-150 AD	*Bilan Scientifique* 2005:94-96
Sud Lavezzi 5	B		Iron		
Sud Lavezzi 5	C		Iron		
Sud Lavezzi 5	D		Iron		
Sud Lavezzi 5	E		Iron		
Sud Lavezzi 5	F		Iron		
Sud Lavezzi 5	G		Iron		
Sud Lavezzi 5	H		Iron		
Tantura F	A	Israel	Iron	700-750 AD	Strauss 2013:8848
Tantura F	B		Iron		
Taranto C	A	Italy	Lead	1-100 AD	Throckmorton 1970:10
Taranto C	B		Lead		
Taranto C	C		Lead		
Taranto C	D		Lead		
Taranto C	E		Lead		
Tekmezar Burnu 1	A	Turkey	Iron	1000-1100 AD	Günsenin 1998:311-312
Tekmezar Burnu 1	B		Iron		
Tekmezar Burnu 1	C		Iron		
Tekmezar Burnu 1	D		Iron		
Tekmezar Burnu 1	E		Iron		
Tekmezar Burnu 1	F		Iron		
Tekmezar Burnu 2	A	Turkey	Iron	1000-1100 AD	Günsenin 1998:311-312
Tekmezar Burnu 2	B		Iron		
Tektaş Burnu	A	Turkey	Lead	440-425 BC	Trethewet 2001:109-114
Tektaş Burnu	B		Lead		
Tektaş Burnu	C		Lead		
Tektaş Burnu	D		Lead		
Tektaş Burnu	E		Lead		
Tell Hreiz II	A	Israel	Iron	400-1450 AD	Galiki and Sharvit 1999:98
Tijascica	A	Croatia	Lead	60-1 BC	Jurišić 2000:78
Tijascica	B		Iron		
Tour du Castellas 1	A	France	Lead	315-275 BC	*Bilan Scientifique* 2003:41-42
Tour du Castellas 1	B		Iron		
Tour-Fondue	A	France	Lead	225-200 BC	Dangreaux 2012:5-36

Uluburun	A	Turkey	Stone	1350-1300 BC	Pulak 1998:216
Uluburun	B		Stone		
Uluburun	C		Stone		
Uluburun	D		Stone		
Uluburun	E		Stone		
Uluburun	F		Stone		
Uluburun	G		Stone		
Uluburun	H		Stone		
Uluburun	I		Stone		
Uluburun	J		Stone		
Uluburun	K		Stone		
Uluburun	L		Stone		
Uluburun	M		Stone		
Uluburun	N		Stone		
Uluburun	O		Stone		
Uluburun	P		Stone		
Uluburun	Q		Stone		
Uluburun	R		Stone		
Uluburun	S		Stone		
Uluburun	T		Stone		
Uluburun	U		Stone		
Uluburun	V		Stone		
Uluburun	W		Stone		
Uluburun	X		Stone		
Uluburun	Y		Stone		
Valle Ponti	A	Italy	Iron	25-1 BC	Ruscito 1982:19-26
Vele Orjule	A	Croatia	Lead	110 BC-170 AD	Jursic 2000:80
Vele Orjule	B		Lead		
Verudica	A	Croatia	Lead	1-100 AD	Jursic 2000:83
Yassi Ada A	A	Turkey	Iron	625-630 AD	van Alfen 1996:189-213
Yassi Ada A	B		Iron		
Yassi Ada A	C		Iron		
Yassi Ada A	D		Iron		
Yassi Ada A	E		Iron		
Yassi Ada A	F		Iron		
Yassi Ada A	G		Iron		
Yassi Ada A	H		Iron		
Yassi Ada A	I		Iron		
Yassi Ada A	J		Iron		
Yassi Ada A	K		Iron		

Appendix 2. *International Journal of Nautical Archaeology* Publication

Cooper, J. P., and Zazzaro, C., forthcoming, The Mares Project survey of Jizan and the Farasan Islands, Part II: Archaeology, *Atlal*.
Davies, S. and Morgan, E., 2002, *Red Sea Pilot*. St Ives, Cambridgeshire.
Frost, H., 1969, The stone anchor of Byblos, *Mélanges de l'Université Saint-Joseph* **45**, 425–42.
Frost, H., 1991, Anchors sacred and profane. Ugarit-Ras Shamra, 1986; the stone anchors revised and compared, in M. Yon (ed.), *Ras Shamra-Ougarit VI: Arts et Industries de la Pierre*, 355–410. Paris.
Gaur, A. S., Sundaresh, Sila Tripati, Gudigar, P., Vora, K. H. and Bandodker, S. N., 2001, A group of 20 stone anchors from the waters of Dwarka, on the Gujarat Coast, India, *IJNA* **30**.1, 95–108.
Grossmann, E. and Kingsley, S. A., 1996, A three-hole stone anchor with wood remains from Crusader Arsuf (Apollonia), Israel, *IJNA* **25**.1, 49–54.
Hall, M., Llewellyn, O, Miller, A., al-Abbasi, T., al-Wetaid, A., al-Harbi, R. and al-Shammari, K., 2010, Important Plant Areas in the Arabian Peninsula: 2. Farasan Archipelago, *Edinburgh Journal of Botany* **67**.2, 189–208.
Keay, S. and Williams, D., 2005, Roman Amphorae: a digital resource, University of Southampton, doi:10.5284/1000021.
Marion de Procé, S. and Phillips, C., 2010, South Arabian inscriptions from the Farasān Islands (Saudi Arabia), *Proceedings of the Seminar for Arabian Studies* **40**, 277–82.
Mortensen, P., 1986, The Barbar Temple: its Chronology and Foreign Relations Reconsidered, in S. H. Al Khalifa and M. Rice (eds), *Bahrain Through the Ages: the Archaeology*. London and New York.
Phillips, C., Villeneuve, F. and Facey, W. A., 2004, A Latin Inscription from South Arabia, *Proceedings of the Seminar for Arabian Studies* **34**, 239–50.
Raban, A., 1975, The 'Naamah-south' expedition, *Sefunim* **IV**, 33–9.
Raban, A., 1990, Medieval anchors from the Red Sea, *IJNA* **19**.4, 299–306.
Shaw J. W., 1995, Two three-holed stone anchors from Kommos, Crete: their context, type and origin, *IJNA* **24**.4, 279–91.
Sila Tripati and Gaur, A. S., 1997, Stone anchors from Sindhudurg Fort on the west coast of India, *IJNA* **26**.1, 51–7.
Sundaresh, Gaur, A. S., Gudigar, P., Tripati Sila, Vora, K. H. and Bandodker S. N., 1999, Stone anchors from the Okhamandal Region, Gujarat Coast, India, *IJNA* **28**.3, 229–52.
Tibbetts, G. R., 1971, *Arab Navigation in the Indian Ocean before the Coming of the Portuguese*. London.
Van Hecke, J., Bossue, B., De Buck, V. and Carpentier, E. (eds), 1861, *Acta Sanctorum X Octobris die vigesima quarta*. Brussels.
Villeneuve, F., 2004, Une inscription latine sur l'archipel Farasân, Arabie Séoudite, Sud de la mer Rouge, *Comptes Rendus de l'Académie des Inscriptions et Belles-Lettres*, 419–29.
Villeneuve, F., 2007a, L'armée romaine en mer Rouge aux IIe-IIIe siècles après J-C.: à propos des inscriptions de Farasân, in A. Lewin (ed.), *Proceedings of the Conference L'esercito romano tardo-antico nel Vicino Oriente, Università della Basilicate, Potenza-Matera, 12–15 May 2005*, 13–27. Oxford.
Villeneuve, F., 2007b, Farasan Latin inscriptions and Bukharin's ideas: no pontifex Herculis! and other comments, *Arabia* **4**, 289–96.
Villeneuve, F., 2008, Deux inscriptions militaires latines découvertes aux îles Farasan (mer rouge méridionale, Arabie saoudite). Rome, Alexandrie, Pétra et le commerce oriental au IIe siècle après J-C, in A. R. Al-Ansary, K. I. Al-Muaikel and A. M. Alsharekh (eds), *Proceedings of the Conference 'The City in the Arab World in Light of Archaeological Discoveries', Sakaka, 5–7 December 2005*, 167–80. Riyadh.
Villeneuve, F., Phillips, C. and Facey, W., 2004, Une inscription latine de l'archipel Farasan (sud de la mer rouge) et son contexte archéologique et historique, *Arabia* **2**, 143–90.
Vine, P. and Casey, P., 1992, *Kuwait: A Nation's Story*. London.
Vosmer, T., 1999, Indo-Arabian stone anchors in the western Indian Ocean and Arabian Sea, *Arabian archaeology and epigraphy* **10**, 248–63.
Wachsmann, S., 1998, *Seagoing Ships and Seamanship in the Bronze Age Levant*, College Station TX.
Zarins J., Murad, A. and Al-Yaish K., 1981, Part I(a): The Second Preliminary Report on the Southwestern Province, *Atlal* **5**, 9–42.
Zazzaro, C. and Abdel Maguid, M. M., 2006, Ancient Egyptian anchors: new results from Wadi Gawasis, in E. el-Saeed, E. Mahfuz and A. M. Megahed (eds), *Festschrift Volume presented to Prof. Abdel Monem Abdel Haleem Sayed*, 139–62. Alexandria.
Zazzaro, C. and Abdel Maguid, M. M., forthcoming, Ancient Egyptian stone anchors from Mersa Gawasis, *Proceedings of the Conference The Red Sea in Pharaonic Times. Recent Discoveries along the Red Sea Coast. Cairo—Ayn Soukhna. 11–12 Jan 2009. Bulletin de l'Institut français d'archéologie orientale*.

A Roman Type IVB Wooden Anchor Found in the Corfu Channel, Albania

Lead components of a wooden anchor were discovered during the 2011 field season of the Albanian Coastal Survey Project, part of the Illyrian Coastal Exploration Program, a co-operative effort between RPM Nautical Foundation, the Albanian Institute of Archaeology, and the Albanian Ministries of Culture and Defence. Since 2007 an intensive survey for submerged cultural material has completed

Figure 1. Map of the northern Ionian Sea, the Corfu Channel and the location of the anchor. (P. Campbell)

over 25 km of shoreline. This survey reaches out to the 100-m contour and consists of two components: a multibeam sonar survey and a diver-based survey (see Royal, 2012 for Roman finds up to 2009).

Haldane (1984: 3–4) identifies this type of anchor as a Type IVA; but later (1990: 21) as IVB, which is the categorisation used here. This type corresponds to Kapitän's removable stock type 2b (1984: 39). The anchor was located at the entrance to a small bay on the Albanian side of the Corfu Channel (Fig. 1). This narrow strait between the island of Corfu and the mainland offers mariners relatively tranquil conditions for sailing between the Ionian and Adriatic seas compared to west of the island. The bay is located at the channel's narrowest point, has a maximum depth of 43 m with a sandy bottom and steeply sloping sides and offers the safest anchorage along the section of coast between Saranda Bay and Lake Butrint. The interior of the bay is protected, but the area outside marks the confluence of weather funnelled into the strait from the north-west and the steady southern wind, which causes mixed conditions in an otherwise safe passage. Ringing the bay to the south-west is a rocky reef, the exterior of which is covered in nets and anchors from various periods.

The anchor was situated at the entrance to the bay in 29 m depth. The absence of related cultural material suggests that the anchor was not stowed, but deposited during use. The sandy surface is not conducive to hanging up, so it is uncertain whether the vessel wrecked or whether the anchor was deposited due to other curcumstances. The orientation of the anchor suggests that the vessel would have been inside the bay and sheltered from weather coming up the strait; but it would have been exposed to the quick changing weather that comes from the north-west through Saranda Bay.

A light scatter of pottery from various periods begins at 36 m depth and continues up the slope to 5 m. The pottery is primarily composed of amphora sherds with some tableware found in shallower areas. The amphoras include Corinthian B dating to the 5th century BC, Dressel 28 (1st century AD), and Late Roman Adriatic amphoras (4th century AD), all typical finds for this region. The main concentration is located along the shore in 5 m, *c*.60 m from the anchor location. No complete amphoras are present, and shallower concentrations would have been exploitable by free divers both in Antiquity and today. Scuba diving was outlawed under the former communist government and remains rare to this day, so it is unlikely that deeper deposits were cleared. The pottery, therefore, is probably not related to the anchor, but does provide evidence of the bay being used as an anchorage.

Following documentation, Dr Adrian Anastasi from the Albanian Institute of Archaeology recovered the anchor for display in the Durrës Archaeological Museum, where it joins a Type IIA anchor located during the 2010 season.

The anchor

Without associated cultural material it is difficult to determine dates or origin of the Corfu Channel anchor. However, Type IV anchors were used from the 2nd century BC to the 4th century AD (Haldane, 1984: 13). Frost (1972: 114) associates them with Sicily and North Africa, while Haldane (1990: 22) states that this type is typically found in the eastern Mediterranean. The stock (Fig. 2) was located 120 cm from the closest

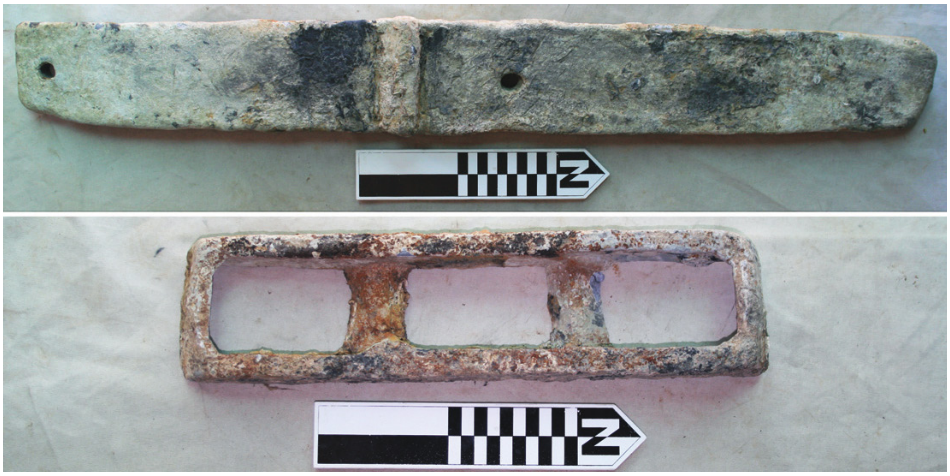

Figure 2. Removable lead stock and collar from the Corfu Channel anchor. (P. Campbell)

point on the collar, a lead piece used to reinforce wooden arms which have begun to loosen (Hadane, 1986: 163–4). Judging from these relative positions, the anchor came to rest with the heavier stock flat and the arms in the vertical position until the wooden elements began to disintegrate, at which point the shank or arms broke from the stock and came to rest flat down the slope. Correcting for movement, the distance between the stock and collar is estimated at 165 cm (Fig. 3). Interestingly, Frost's reconstruction of a removable-stock anchor in Sicily has a nearly-identical measurement between the stock-fitting and the collar (1972: 115). With the additional components above and below the stock and collar, the overall length would have been *c*.240 cm.

There is no surviving wood, nor evidence of the iron or bronze 'teeth' often found fitted to the ends of the arms, making the lead components the only remaining pieces of the anchor. The stock measures 922 mm across the top (as determined from its orientation to the collar *in situ*) and 904 mm across the bottom. The ends are *c*.90 mm sided, while the centre is 115 mm at the shank-block. The thickness varies between 32 and 43 mm across its length. The stock weighs *c*.39.5 kg. The collar measures 455 by 105 mm and varies in thickness from 37 to 45 mm. The fittings for the arms are *c*.120 × 75 mm, while the shank-fitting is 112 × 70 mm.

The arms exited the collar at a 28° angle relative to the shank. Acute arm-angles are common on ancient anchors (Haldane, 1986: 165). This is probably due to the working weight of the anchor being located in the stock. This drives the arms vertically into the ground as the stock comes to rest parallel to the bottom. In later anchors, constructed of iron with wooden or iron stocks, the weight is centred at the crown. This results in the arms coming to rest parallel to the bottom with the stock in the vertical position. Pressure

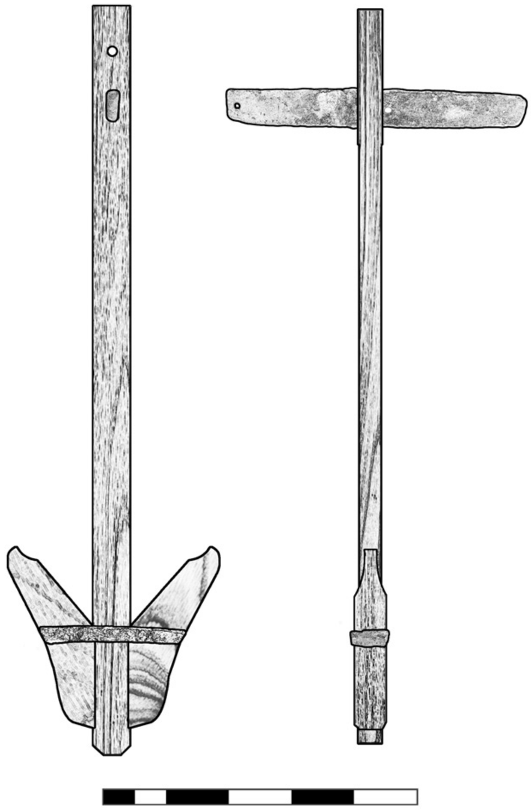

Figure 3. Reconstruction of the Corfu Channel anchor (scale: 1 m). (P. Campbell)

exerted on the stock causes the anchor to cant, resulting in a fluke catching the bottom (Knight, 1833: 505). These two conceptual approaches fundamentally differ, resulting in separate anchor designs that are identifiable by comparing physical characteristics. Light-stock anchors require a wider angle to catch when canted, while heavy-stock anchors do not require flukes since the 'teeth' of the arms are driven directly into the bottom.

Type IVB wooden anchors feature a removable lead stock. Removable stocks have previously been found only in isolation or with iron anchors, though other evidence suggested that Type IV stocks were used on wooden anchors. Use of removable stocks on wooden anchors denotes a significant transitional phase in anchor design and manufacture. The presence of a lead collar indicates that the Corfu Channel anchor was wooden, marking the first time a removable stock for a wooden anchor has been found in context (Haldane, 1984: 9). The Type IVB differs from type IVA due to the use of a stop or block to keep the shank in place, as well as a hole for the anchor-line or buoy-line (Haldane, 1984: 30–31). The block is offset to balance the anchor, with the opposite end thinning to allow the shank to be fitted over it. This thinner end is is extended 7 cm further than the block end, which is *c*.1 cm thicker along its length. The block partners with a hole for a pin which would have kept the shank from sliding off the stock. The lack of a pin on site implies that it was organic, probably wooden, as Kapitän suggests (1984: 38). The line-fitting is located at one end of the stock and would have been used to disengage the anchor from a hang or snag. The diameter of both holes is 17 mm.

Discussion

Type IV lead stocks from archaeological contexts are limited to iron anchors from the Punta Scaletta vessel and have not previously been found with wooden anchors (Lamboglia, 1964: 253; Haldane, 1984: 9). Frost (1972: 114–16) discovered remains of a wooden anchor designed to accept a removable stock, but no stock was found on site. Similarly, a wooden anchor from Elba had a fitting for a removal stock, but it is fashioned for an unknown square-shaped stock (Maggiani, 1982: 63). Though no wood survives on the Corfu Channel site, the lead collar attests to the Type IVB stock being fitted on a wooden anchor.

The Type IVB wooden anchor is a significant transitional stage for wooden anchors. Removable stocks are a clear divergence from wooden anchors with fixed stocks which were filled with lead, such as a Type IIA found on a rocky reef near the entrance to Lake Butrint during the 2010 field season. This type dates between the 5th and 2nd centuries BC (Haldane, 1984: 13). It consists of two lead pieces which were poured into a wooden stock, and a lead collar (Fig. 4), as well a fourth lead piece that appears to have been poured into the shank. Even though this type is thought to be the earliest form of lead composite anchor, Type IIA anchors were produced until the 2nd century BC when removable stocks and iron anchors were already in use.

Substantial developments took place in anchor manufacturing around the 2nd century BC. Mariners shifted to easily-stowable anchors by using removable stocks on both iron and wooden anchors. In fact, stowable anchors were considered a major development when re-invented as admiralty anchors during the 18th century (Casson, 1995: 253 n.113). Removable stocks on wooden anchors either mimicked contemporary iron anchors or were designed to fit both iron and wooden anchors interchangeably (Haldane, 1984: 9). For this reason, the Type IV anchor is the final phase of wooden anchor development, though it and earlier wooden anchor designs would continue to be used alongside iron anchors for several centuries.

Removable lead stocks were also the final development of anchors with their working weight set above the crown. Use of lead stocks declined with the arrival of lunate-shaped anchors with iron or wooden stocks by the Imperial Period (Casson, 1995: 253 n.114). The decline of lead-weighted anchors could be due to issues with sources of lead, or to improved ironworking (Haldane, 1984: 13); however two Hellenistic iron anchors found off the coast of Israel suggest that that a shift toward crown-weighted anchors occurred around the 1st or 2nd century BC (Galili *et al*., 2010: 143). The Hellenistic anchors were found among a shipwreck assemblage with their removable iron stocks stowed next to the shanks (Galili *et al*., 2010: 126). The crown provides the working weight, while the arms are set out from the shank at 90° before angling outwards at 34°. Additionally, the ends of the arms are slightly widened like proto-flukes (Galili *et al*., 2010: 128), rather than narrowed like the teeth of wooden anchors (Haldane, 1986: 166). The combination of these physical characteristics; working-weight centred in the crown, greater angle of arms, widening of the ends of arm-tips, and lighter stock, all indicate that these anchors were designed using the crown-weighted conceptual approach. Casson notes that iron anchor arms become lunate during the Roman Imperial period, but does not connect this shift to the development of flukes during the same period (1995: 253 notes 114, 116). The two Nemi barge anchors included a wooden anchor with a lead stock and a lunate iron anchor, which illustrates this transition continuing into the 1st century AD (Casson, 1995: figs 183–4). During the 3rd and 4th centuries AD the presence of iron anchors increases in archaeological contexts (Haldane, 1984, 13; Casson, 1995: 253 n.114).

Use of Type IVB stocks on both iron and wooden anchors demonstrates the degree of variability present during this period. Though a progression of lead composite anchors can be generally traced (Haldane, 1984: 13), there were clearly multiple designs being produced concurrently. Wood and lead composite anchors appear some time around the 6th century BC (Benoit,


Figure 4. Disconnected lead stocks, shank-filling and collar from a Type IIA anchor found during the 2010 survey. (H. Phoenix and P. Campbell)

1961: 170), while iron appears at least by the 5th century BC (Haldane, 1990: 23). Athenian naval records mention iron and lead composite anchors which date this practice to at least the 4th century BC (Casson, 1991: 89: Casson, 1995: 256 n.131). Some vessels, such as the Nemi barge and Hiero's super-freighter (Casson, 1995: 253 n. 115), carried both iron and wooden anchors, as did more traditional merchant vessels (Haldane, 1990: 23). Use of multiple anchor-types indicates that certain types of anchors may have been preferred in certain conditions. Haldane (1984: 33) suggests that lighter iron anchors were favoured for everyday use. Stock-weighed anchors may have been more effective in a soft sea-floor, such as the sandy slope where the Corfu Channel anchor was found, rather than rocky surfaces where the crown-weighted anchors may be more effective. Anchors suited to specific conditions may explain the variability of examples found on shipwrecks.

Conclusion

The Corfu Channel anchor provides physical evidence of a significant transitional type whose existence has been suggested by scholars for some time. The removable lead stock was the culmination of wooden anchor development, but ultimately wood's use dwindled as iron became prevalent. The use of wood and iron anchors together demonstrates how the Type IVB removable stock was a versatile product from a period when variability was pervasive, illustrating just how complex and mutable the past could be. Perhaps the most significant aspect of the Corfu Channel anchor is that it marks the end of the development of stock-weighted anchors, as the preference for crown-weighted anchors increased. In fact, the victory of iron over wood may have been more about the efficiency of crown-weighted anchors over stock-weighted anchors than issues of the weakness or shorter durability of wood.

Peter B. Campbell
Centre for Maritime Archaeology, University of Southampton, SO17 1BJ UK
RPM Nautical Foundation, 7009 Shrimp Road, Key West, Florida 33040 USA

Acknowledgements

The author would like to thank project collaborators including RPM Nautical Foundation, Albanian Institute for Archaeology, and Albanian Center for Marine Research, specifically principal investigators Dr Jeff Royal and Dr Adrian Anastasi, George Robb, Howard Phoenix, Auron Tare, Ardiola Alikaj, Enkeleida Qendro, and sharp-eyed Derek Smith.

References

Benoit, F., 1961, *L'Épave du Grand Congloué à Marseille*. Gallia supplement xiv, Paris.
Casson, L., 1991, *The Ancient Mariners: Seafaring and Sea Fighters of the Mediterranean in Ancient Times*. 2nd edn, Princeton.
Casson, L., 1995, *Ships and Seamanship in the Ancient World*. 2nd edn, Baltimore.
Frost, H., 1972, The discovery of a Punic ship, *IJNA* 1, 113–17.
Galili, E., Sussman, V., Stiebel, G. and Rosen, B., 2010, A Hellenistic/Early Roman Shipwreck Assemblage off Ashkelon, Israel, *IJNA* **39**.1, 125–45.
Haldane, D., 1984, The Wooden Anchor, unpublished Master's dissertation, Dept of Anthropology, Texas A&M University, College Station.
Haldane, D., 1986, Wooden anchor arm construction, *IJNA* **15**.2, 163–6.
Haldane, D., 1990, Anchors of Antiquity, *The Biblical Archaeologist* **53**.1, 19–24.
Kapitän, G., 1984, Ancient anchors—technology and classification, *IJNA* **13**.1, 33–44.
Knight, C., 1833, *The Penny Cyclopedia of the Society for the Diffusion of Useful Knowledge, Vol. 1*. London.
Lamboglia, N., 1964, La Campagna 1963 sul relitto di Punta Scaletta all'Isola de Giannutri, *Rivista di Studi Liguri* **30**.**1**, 229–57.
Maggiani, A., 1982, Isola d'Elba, *Bolletino d'Arte, 4th Supplement Archeologia Subaquea*, 62–4.
Royal, J., 2012, The Illyrian Coastal Exploration Program (2007–09): the Roman and Late-Roman Finds and their Contexts, *American Journal of Archaeology*, in press.

A Roman Nautical Lead Brazier: its decoration and origin, and comparable coastal finds

One of the most unusual technological artefacts present on Roman ships was the lead brazier (Fig. 1). About 20 such braziers have been recovered off the coast of Israel, most of them off the Carmel coast, with others from off Tel Ridan, Ashkelon and Yavneh-Yam (Fig. 2) (Galili and Sharvit, 1996; 1999a; 1999b; 1999c; Galili *et al.*, 2000; Rosen and Galili, 2007; Galili *et al.*, 2009; Galili and Rosen, 2011, Galili and Rosen, forthcoming). These ingeniously designed artefacts were invented in Antiquity, by master-craftsmen, to solve the problem of maintaining a cooking-fire at sea. Cooked food and warm drinks are important in maintaining the health, stamina and morale of those aboard. But ships are exposed to fire-raising winds, and carry flammable materials such as wood, rope and sailcloth. Any accident involving a shipboard fire may end by destroying the ship and everything aboard. The inventors of the lead brazier aimed at mitigating such danger.

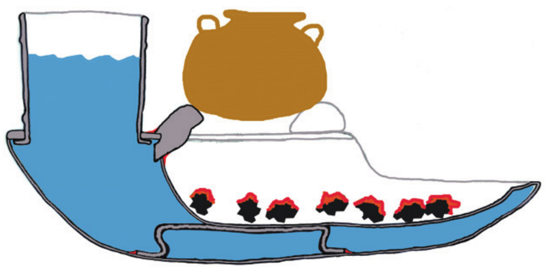

Figure 1. Cross-section of a nautical brazier in use. (E Galili)

These artefacts are not known, certainly not in such quantity and variety, from any other time and place in Antiquity. None has ever been found on land, where it could have been associated with a known cultural context. Consequently there are unanswered questions as to where, when and by whom these braziers were invented, designed and manufactured. This note describes a decorated lead brazier, how it was manufactured, and the exceptional decoration, which will be

Appendix 3: Description of Known Rams

Fifteen waterline rams have been found from antiquity- eleven from the Egadi Islands- as well as eight other bronze castings found in the sea that are potentially waterline rams or *proembolion*. *Proembolia* were auxiliary rams that fitted over wale joints in the bow (Casson 1995:85) as seen in Appendix 4, Figures 53 and 59. It appears that bronze was the preferred metal used for rams and though Pliny and Vitruvius mention iron rams, these accounts are confusing and are most likely describing other things (Casson 1995:85 n.40).[1]

Bronze was widely used in antiquity; however, it was expensive and it appears to be rare for ship fittings. Shipwreck finds indicate that bronze was highly common as a cargo, both as ingots and cast products. However, bronze used for shipbuilding is quite rare. Out of 1,785 published Mediterranean shipwrecks in the Oxford Roman Economy database (Strauss 2013) building on Parker's *Ancient Shipwrecks of the Mediterranean* (1992), only 38 sites have bronze related to ship construction, or 2% of the total, excluding warships (Strauss 2013). Of these, 27 used bronze or copper in shipbuilding only for fasteners. The remaining eleven shipwrecks (0.6%) used bronze for pulleys, bilge pump parts, anchor parts, fittings for furniture or the steering oar, sheathing, and a single unidentified rod (Strauss 2013). The Trier fitting and a boat fitting sold at Christies auction house are alone as examples of bronze decorative fittings (Göttlicher 1978:82; Christie's 2004a; Christie's 2004b), shown in Appendix 4, Figures 73 and 80. However, use of bronze on warships is widespread as the ram castings show. The high cost of bronze appears to have been prohibitive for most shipbuilders, but its non-corrosive qualities necessitate its use for warships that require castings at or below the waterline and survive impacts.

All of these bronze items found on shipwrecks are small objects, mostly fasteners or tools such as pulleys or pumps that are small solid cast objects. In contrast, the rams and *proembolia* were not simply the largest bronzes in shipbuilding, but they are the largest single cast objects in all antiquity since statues were cast in multiple pieces (Mattusch 1988:24). The eight unknown bronze fittings are likely from warships if one considers these casting in relation to the wider context of bronze use for shipbuilding, specifically how uncommon it was outside of warships.

The majority of the rams are without context or associated cultural material to date them. Being cast bronze, the only means to date them is either archaeological context or dating wood remains. However, some information can be gleaned from the bronze casting.

Casting of bronze objects developed early in Mediterranean societies, but the casting of object larger than figurines developed in the middle of the 6th century BC (Haynes 1992:11). Prior to this, large objects such as armour or statues were hammered bronze sheet (Haynes 1992:22;

[1] Pliny (Natural History 32.3) mentions "rams…[armed] with…bronze and iron" in a passage dealing with a mythical fish, while Vitruvius (10.15.6) writes "hard iron ram like warships" referring to terrestrial battering rams made of iron, likely not describing marine rams made of iron (Casson 1995: 85 n. 40).

Courbin 1957:340). Literary evidence points to hollow casting being brought from Egypt to Samos during the 6th century and archaeological evidence from Samos finds hollow cast Egyptian cats in 6th century contexts, as well as locally produced hollow-casting by the middle of the century (Mattusch 1988:50 nn.56, 52). While there are some earlier finds, such as two hollow-cast birds found at Delos in an 8th century context, these are rare and irregular (Mattusch 1988:51). It is in Samos during the 6th century that casting developed distinctly, before spreading to the mainland (Mattusch 1988:50). The two methods used in the ancient Mediterranean were direct and indirect lost wax casting (Mattusch 1988:24).

Early bronze alloys were composed of copper and tin with trace elements; however, various other alloys were developed rapidly to suit casting. Pure copper has a melting point of 1083˚ C and it absorbs gases (Haynes 1992:83). Since the molten metal begins to cool as the pour begins, higher melting point metals are more difficult to cast with, especially for larger castings. Copper does not flow as well as alloys for this reason and it weakens around casting holes. The addition of tin lowers the melting point to 1050˚ C at 7% concentration, or 1020˚ C at 10% concentration, which provides a better and longer flow into the casting, allowing for larger castings.[2] The copper-tin alloy also absorbs less gas for a higher quality cast and it possesses a higher tensile strength (Haynes 1992:83). Hardness increases with the addition of tin, but above 10% tin brittleness also increase; 15% tin is so brittle that statues could not be cast with it.

Tin was very costly, so early on bronze workers looked to other metals. Lead was cheap and it lowers the melting point even further, as well as increase fluidity and absorbs less gasses. Leaded bronze is also easier for cold working. However, lead does not form an alloy with copper and tin, instead it pools in its own clusters. In small percentages of lead this is not an issue, but if the level rises over a third of the total concentration then it is a threat to the "structural cohesion" of the casting (Haynes 1992:83). Lead added to bronze is seen in the 6th century BC, but in the 4th century heavily leaded bronze become standard. Lead appears to first be used in significant quantities (above 2%) by the Etruscans and Greeks in the west, not the mainland (Mattusch 1988:7, 71). By the Roman Period leaded bronze is the "rule" (Haynes 1992:88).

Analysis of ancient bronzes unfortunately has a few issues that do not currently allow for a chronology based on composition. First, analysis has only been done on a small sample per object, but elemental composition varies across the entire artefact (Mattusch 1988:14). Second, while many bronzes are known, only a selection have been analysed and several major pieces have not (Mattusch 1988:14). This means that it is not yet possible to draw strong conclusions about date or production location from elemental analysis (Mattusch 1988:15).

The early hollow cast objects were small, the largest statues from 550-500 BC were 2/3 the size of a human (Mattusch 1988:59). The Ugento God statue from the Greeks in the west dates to

[2] Iron's melting point is 1538˚ C, far exceeding copper and bronze alloys, and likely making it difficult to cast large rams using the technology of the day, to say nothing of its corrosive properties in saltwater.

Figure A3.1. The Berlin Foundry Cup, a Red Figure vase dating to 490-480 BC depicting bronze workers and their tools (Courtesy of the Altes Museum).

530-500 BC and it is 71 cm in height (Mattusch 1988:67), while the head of a youth dating to 550-525 BC in the Boston Museum of Fine at is 6.9 cm (Mattusch 1988:60). A late 6th and early 5th century bronze head of Zeus from Olympia is 17 cm, while the whole statue would have been approximately a meter in height (Mattusch 1988:64). There are two life size statues sometimes dated to 530-520 BC, a head of a warrior found on the Athenian Acropolis which would have been 1.7 m reconstructed and the Piraeus Apollo which is 1.91 m; however, some scholars argue it is not from this period at all (Mattusch 1988:60). These early castings already show great detail.

The Berlin Foundry Cup (Figure A3.1), an Attic Red Figure cup, depicts the casting process for two statues, one of which is the statue of a warrior twice life size (Mattusch 1988:102). Dating to 490-480 BC, the cup demonstrates the rapid development of hollow casting since 550 BC and the ability of bronze workers in the early decades of the 5th century to create larger castings. The Charioteer at Delphi demonstrates the abilities of these large casters, dating to 478 or 474 BC (Mattusch 1988:127).

The development of bronze casting relates four general conclusions about casting rams:

1) The iconography predating zoomorphic prows also predates hollow casting, meaning that- if sheathed- these bows would have been covered in hammered bronze sheet similar to the earliest statues (Haynes 1992:22). This would be ineffective at dispersing impact force (Mark 2008:264), but this fact does not mean it was not attempted. However, prows sheathed with bronze sheets is speculation based on attempting to explain iconography (cf. Casson 1995:64), but bronze

sheathing has not been found in a maritime context; only a single 2nd century BC Roman vessel uses copper sheathing (Strauss 2013). Lead sheathing did not appear until the 5th century BC after lead became widely and cheaply available, and it was only used until the 1st century BC when the price of lead once again increased (Hocker 1995a:199, 201); copper never became so affordable. The use of bronze sheathing for warships in the 6th century appears to be an archaeologist's construct to explain the possibility of early rams, though no warships have been found in the archaeological record to prove either way.

2) By the start of widespread ramming following the Battle of Alalia in 540-535 BC, casting was well developed in both Greece and its western colonies. For example, Samos developed hollow casting of the Greek style and the highly regarded bronze artist Pythagoras may have been Samian and fled to Zancle in the west with the exiles (Mattusch 1988:186). Phocaea likewise had a highly regarded artist named Telephanes (Mattusch 1988:188). Samos, Corinth, Athens, and Aegina all had highly regarded navies and advanced bronze casting by 540-535 BC. Therefore, at the advent of ramming as a tactic, the major players all had the ability to cast rams.

3) The earliest rams would most likely have been quite small. Statuary remained small until the early 5th century BC, and so it is possible to argue that the casting abilities of the time would have led to the first cast rams only covering the very end of the prow. Based on findings from statuary, the ability to manufacture large single-cast rams would have developed circa 490-480 BC.

4) High lead content (over 5%) in bronze casting relates to a post-4th century BC date.

1.1 Actium Fragment

Following the victory over Mark Antony and Cleopatra at Actium in 31 BC, Octavian Augustus founded the city of Nikopolis and built a monument (Murray and Petsas 1989). The monument was constructed with a façade fitted with captured rams of different magnitude (Appendix 4, Figure 72). While excavating the ram mounted in the façade, a large fragment of bronze was discovered (Varoufakis 2007).

Figure A3.2. Bronze fragment likely belonging to a ram from the Actium monument (Varoufakis 2007:344).

Though the fragment does little to reveal the design of the ram it was a part of, coinage and a marble ram from the Actium monument (Appendix 4, Figure 71), as well as iconographic depictions and historical accounts of the battle make it clear that the Actium rams were three-finned rams.

1.2 Actium Proembolion (British Museum)

This bronze casting was dredged up from the outer bay of Actium in 1839 and later donated to the British Museum (Leake 1843:246). The casting is designed to fit over two timbers coming together, such as the *proembolion* capping the wales in the Berenike mosaic (Appendix 4, Figure 59). It is decorated with a figure of Minerva, in a 2nd-1st century BC style (Göttlicher 1978:82).

Despite lacking context, this casting reveals quite a lot about ancient warships as the only known *proembolion*. An in depth study has never been undertaken and the museum assumes the fitting is from a small vessel (Walters 1899:no. 830); however, calculating its dimensions shows that it could have come from a sizeable vessel. The main wales on a Hellenistic merchant ship are generally two times the thickness of the strakes, such as the Kyrenia ship (Steffy 1985:79). The Athlit warship had a wale 2.4 times the thickness of its strakes (Steffy 2006:59). Warships are depicted as having several wales and upper wales decrease in size (Appendix 4, Figure 39). On the Kyrenia ship, the upper wale was 1.5 times the thickness of the strakes (Steffy 1985:79). Using these figures, a general idea of the possible dimensions of the Actium vessel emerges.

Conservative estimates can be generated by assuming the casting covers the entire wale, though if it did not then these dimensions would be larger. The Actium *proembolion* likely fitted to wales between 12-19.2 cm moulded with strakes from 5-12.8 cm (Table 4.8). The *proembolion*'s sided dimension is considerably smaller than the Kyrenia ship's wale dimension at amidships, but it is important to remember that dimensions can become constrained at the bow. If the Actium vessel's upper wales were the same dimensions as its waterline wale, then the vessel is likely the same class as the Egadi warships. If the wales decrease in size as the progress from the waterline wale, then the Actium vessel was larger. A ship model from Vulci and a coin of Darius III from the 4th century BC both show three upper wales that decrease in size as they progress upwards

Figure A3.3. The Actium proembolion in the British Museum (British Museum).

Wale Dimensions	*Sided (cm)*	*Moulded (cm)*		
Actium Wale Pockets	13.0	8.0		
Egadi 3 Wale Pockets	15.0	10.0		
Egadi 4 Wale Pockets	15.0	9.0		
Athlit Wale Pockets	24.0	10.0		
Athlit Wales	24.0	18.0		
Athlit Strakes	N/A	7.5		
Kyrenia Wale Dimensions				
Lower (amidships)	21.5	8.0		
Upper (amidships)	22.7	6.1		
Kyrenia Strakes	N/A	4		
Actium Estimated Wale Size				
High	13.0	19.2		
Middle	13.0	16.0		
Low	13.0	12.0		
Actium Estimate Strake Size		High	Middle	Low
High	N/A	12.8	9.6	8.0
Middle	N/A	10.7	8.0	6.7
Low	N/A	8.0	6.0	5.0

TABLE A3.1. DIMENSION OF POTENTIAL TIMBER SIZES BASED ON THE ACTIUM VESSEL'S WALES (AUTHOR).

(Appendix 4, Figure 39), as well as each wale having a chambered top edge which is also evident in the Actium casting. Though *proembolia* appear to have come in several different designs, the Actium casting's form appears to correspond with covering the upper wale on a warship, possibly on a trireme or larger.

1.3 Acqualadroni Ram

The Acqualadroni Ram was found in northern Sicily near the Strait of Messina. A swimmer spotted the ram and there were no associated artefacts are ship remains in the area. The ram fits the design of a three-finned ram similar to the Athlit Ram. It is 1.35m in length and weighs an estimated 300 kg (Buccellato and Tusa 2013:2). Radiocarbon dating revealed a date of the mid-2nd century BC. The ram is composed of a bronze alloy that is 69% copper, 20% lead, and 9.7% tin (Caruso et al. 2011:552). Lead isotope analysis revealed that the lead was likely either a Spanish or Cypriot source. Several publications have come out providing analysis of the ram (Caruso et al. 2011; Frank et al. 2012; Buccellato and Tusa 2013).

Figure A3.4. The Acqualadroni Ram during recovery (Soprintendenza del Mare 2009).

1.4 Athlit Ram

The Athlit Ram was discovered off the coast of Israel. It is the largest ram yet found, it has the best preserved wooden structure, and it is the most well-published (Casson and Steffy 1991; Oron 2001; Oron 2006). The ram is 2.26m in length and weighs 465kg (Steffy 1991:11). It dates to the 3rd century BC, scholars hypothesize the reign of Ptolemy V due to its decorations (Murray 1991:66). The ram is composed of a bronze alloy that is 90.4% copper and 9.78% tin with only trace amounts of lead (Oron 2006:72).

Figure A3.5. The Athlit Ram as it is currently on display (University of Haifa).

1.5 Belgammel Ram

The Belgammel Ram, formerly known as the Fitzwilliam Ram, was discovered off the coast of Libya. It is 64cm in length and weighs 19.7kg, making it a small casting (Adams et al. 2013:3). It features a three-finned design like the Athlit ram at its front, but the stern attachment is unlike any other ram known to date. Analysis shows that the ram dates to the first to centuries BC and is composed of a bronze alloy that is 87% copper, 7% tin, and 6% lead (Adams et al. 2013:14). The consensus is that the casting is a *proembolion* (Pridemore 1996:94; Adams et al. 2013:4), though it is a different design from the Actium *proembolion* and most iconography. It may have fitted on a volute bow, which could have accommodated the strange design of the casting (such as the volute bow in Appendix 4, Figure 69). It is possible that it is a decorative bow ornament for a small vessel, attached in the manner of Basch (1987:Fig. 867; Pridemore 1996:92).

Figure A3.6. The Belgammel Ram after its discovery in Libya (Adams et al. 2012: 2).

Figure A3.7. Basch's interpretation for attaching the Belgammel Ram (Pridemore 1996: 91 after Basch 1987).

1.6 Bremerhaven Ram

The Bremerhaven Ram was purchased from the Nefer Galley, a Swiss antiquities dealer (Pridemore 1996:63). The ram has an unknown find spot; however, the Nefer Gallery deals primarily in antiquities originating in Egypt (Pridemore 1996:63), though a representative of the gallery told Pridemore that it might have come from Levantine coast (1996:64). The ram is a three-finned design similar to the Athlit Ram, but it is small, 43.8cm in length and weighing 53 kg (Varoufakis 2007:458). Pridemore estimates the ram's date as the second half of the 2nd century BC to the 1st century BC based on iconography (1996:72). A study of the ram is soon to be published by the Bremerhaven Maritime Museum, but there is no publication currently available on the ram.

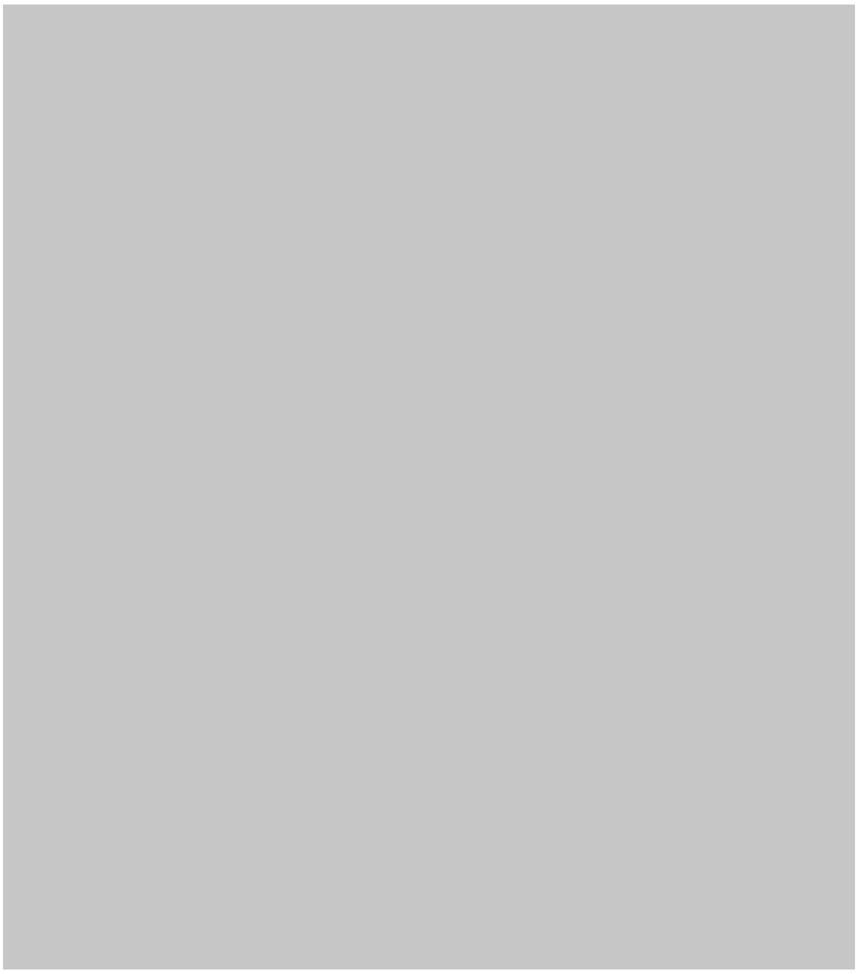

FIGURE A3.8. THE BREMERHAVEN RAM (BREMERHAVEN MARITIME MUSEUM).

1.7 Egadi Rams (1-11)

Eleven warship rams have been found off the Egadi Islands in Sicily, along with bronze helmets, amphoras, ballast stones, and other 3rd century artefacts (Tusa and Royal 2012). Spread over 250 square kilometres that is being surveyed and excavated annually, the artefacts constitute an assemblage from the Battle of the Egadi Islands. This was the decisive naval encounter of the First Punic War, which gave Rome victory at sea over the Carthaginians. This firmly dates the deposition of the Egadi Rams to 241 BC.

There are ten rams with Roman inscriptions and one with a Punic inscription (Tusa and Royal 2012). All have the same design, following the Athlit-type. Two rams have wooden remains of bow structure on their interiors, while four rams have wood from enemy vessels stuck in their fin pockets. Two of the rams are split into fragments and all eleven show damage from head to head ramming.

The Rhodes Archaeological Museum contains a fragment from a marble statue that is slightly smaller to the Egadi Rams. Though missing 5-10 cm due to damage, 55 cm survives of the driving centre, which undamaged would have been slightly larger (Göttlicher 1978:69; Appendix 4, Figure 61). This compares to 58.8 cm driving centre the on Egadi 1 ram or 59.5 cm on the Egadi 5 ram. The Rhodes fragment is 26 cm wide, which compares to Egadi 1's 39.7 cm width and Egadi 5's 31.5 cm width. The marble fragment most likely depicts a *trihemiola*, which was the Rhodian vessel of choice in the 3rd century BC (Morrison 1995:122). This suggests the Egadi Rams are triremes due to their dimensions close proximity to the *trihemiola*, a slightly smaller version of the trireme.

Figure A3.9. The Egadi 9 ram (Courtesy of William Murray).

1.8 Follonica Ram

A recent article mentions an unpublished ram recently found at Follonica, Tuscany, in Italy (Buccellato and Tusa 2013). At this time there are no photographs or drawings, only a description stating, "Although this ram is similar in form to the other [sic], given its modest size and its crude manufacture, it would seem to be one of the first three-finned rams, belonging to a *pentecontor*" (Buccellato and Tusa 2013:10 n. 3). As this chapter will explore later, it is highly unlikely to have come from a pentecontor.

1.9 Kanellopoulos Ram

The Kanellopoulos Ram is bronze casting for a ships' bow. Found at Drepena in the Gulf of Corinth by a collector, the ram has no context and has been dated solely through relative means (Varoufakis 2007:455). The ram is zoomorphic, though the creature it is depicting is unclear. At 35 cm in length and weighing 4.165 kg (Calligas 1996:136), the casting has traditionally been thought to be too small to be a waterline ram and therefore supposed to be a late Hellenistic *proembolion* (Murray and Petsas 1989:103; Pridemore 1996:101). There are a few issues with this hypothesis and the author argues that it is more likely a waterline ram.

Figure A3.10. The Kanellopoulos Ram, whose design suits covering a keel and stem, a different design from the Actium proembolion (Figure 4.12), which is designed to cover the wales (Author).

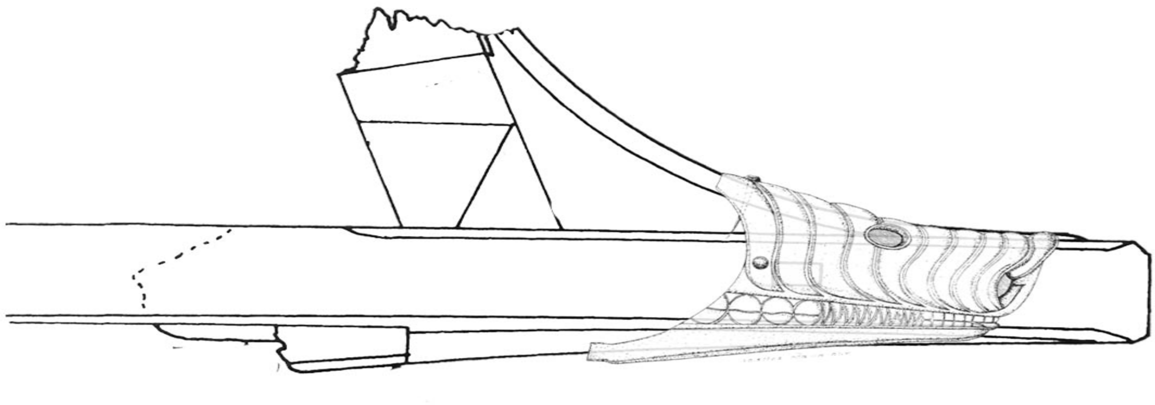

Figure A3.11. The angle exiting the Kanellopoulos Ram fits the Athlit Ram's bow structure, though the Athlit bow is constructed on a far larger scale and extended much further, as shown in the figure (Author).

Dating of the casting is complex since no wood survives for radiocarbon dating. Brouskari argues that it dates to the early Classical period (1985:46)- a period variously dated as starting 510 BC or 479 BC- while the others argue for the Hellenistic period (Murray and Petsas 1989:103; Pridemore 1996:101; Calligas 1996:136; Varoufakis 2007:458). Without archaeological context or dateable organics, dating of the Kanellopoulos Ram falls to other evidence.

Stylistically, the Kanellopoulos Ram depicts a creature with incisors, canines, and molars, a uniquely mammalian set of teeth, as well as a tongue with the ability to extend, that discounts a crocodile (Pridemore 1996:104) or a shark (Calligas 1996:136). It could be a sea creature- mythical or real- though the casting's eyes fit with Greek depictions of mammals rather the perfectly round eyes of sea creatures (Carlson 2009:357). While it is not clear what the casting is meant to depict, its features indicate terrestrial mammals such as a boar, lion, bear, horse, or dog. Both lions and horses are commonly portrayed in Greek sculpture from the Archaic Period onwards with furrowed snouts and their tongues extended (Boardman 2011:69).[3]

The ram is composed of a bronze alloy of 85.5% copper, 10.5% tin, and 3.6% lead (Varoufakis 2007:454). Heavily leaded bronzes appear in the late 4th century BC (Haynes 1992:87–88), such as the British Museum Actium *proembolion* dating to 31 BC, which has a composition of 79% copper, 16.8% lead, and 1.78% tin (Craddock 1986:59). The Kanellopoulos casting's elemental content fit closer to a 6th to 5th century date when ~3% lead was used by western Greek colonies in the 6th century and the mainland in the 5th (Mattusch 1988:7). 530-490 BC is also the period where zoomorphic waterline rams are seen found in iconography (i.e. Appendix 4, Figures 26 and 30).

[3] Early coins issued by cities such as Miletus and Knidos among the Ionian city-states that developed ramming feature snarling lions. While the symbol of Samos was a boar and their rams are said to feature boars' heads, perhaps other city-states had vessels with rams depicting other creatures. The only historical description of rams from the zoomorphic ram period describes those from Samos, leaving a gap as to whether other cities states depicted boars or other creatures.

FIGURE A3.12. PROFILE OF THE KANELLOPOULOS RAM (CALLIGAS 1996:139).

Due to its size, could it be a 6th or 5th century *proembolion*? This is unlikely, as the *proembolion* appears to be a Hellenistic invention. If one accepts that Kanellopoulos Ram is designed to accept a keel and stem, then it predates 398 BC and the arrival of head to head ramming. The *proembolion* does not appear in direct or indirect evidence until the 4th century BC and its functionality comes as support for the new acute angle attacks. The first reference to *proembolia* is IG II 1614.27-30, dating to 353/2 BC (Casson 1995:85). It requires at least a two-decked vessel, as it protects the wale that supports the deck on which the second set of rowers sit during head to head attacks. This explains why it is not seen on the single decked aphracts of the 6th century BC (Appendix 4, Figure 26). If we accept *proembolia* as a functional technology to protect the wale during ramming, then it does appear until after the advent of head to head ramming and indeed it does not appear in archaeological and historical evidence until c. 350 BC (Appendix 4, Figure 49).

Murray and Pridemore argue that the Kanellopoulos Ram is too small to be functional as a waterline ram and it is therefore a Hellenistic *proembolion* (Murray and Petsas 1989:103; Pridemore 1996:104). Varoufakis likewise argues for the Hellenistic period, but he is cautious not to exclude the possibility that it could be a functional ram for a small vessel (Varoufakis 2007:458). The Roman *proembolion* hypothesis argues that a 1st century relief in the Vatican Museum showing a crocodile *proembolion*, which authors see as parallel to the Kanellopoulos casting (Pridemore 1996:104; Appendix 4, Figure 69). However, it does not have the design of a *proembolion*. Upper rams covered the seam of the wales where they met in the bow, meaning a *proembolion* must have wide troughs on the sides, as well as having little or no protrusions on the top and bottom to interfere with the stem. The British Museum Actium fitting is an excellent example of how a *proembolion* was designed to attach to the wales (Figure 4.12). Instead, the Kanellopoulos Ram flares at the bottom and top (Figure 4.21), where a keel and stem would enter. The sides are completely missing any attachment or protection for wales. In fact, super-imposing the Kanellopoulos Ram on the Athlit ram's bow assembly reveals that the ram matches the angle of entry of the keel and stem, though the two ships are built on very different scales (Figure

Figure A3.13. Schematic of the Kanellopoulos Ram (Calligas 1996: 138, 141).

4.20). Due to the attachment of wooden elements, the Kanellopoulos Ram is unlikely to be a *proembolion*, but a waterline ram.

The bronze composition is not a conclusive indicator, but it points toward a date prior to the 4th century BC. It is also important to remember that hollow casting began during the mid-6th century BC and these castings were quite small for the first fifty to seventy-five years (Mattusch 1988:59), so warship ram would not likely have been able to be cast very large. While overall the Kanellopoulos casting is small in length, it is a strong bronze alloy (Varoufakis 2007:458) and with 4 mm thickness in certain areas (Calligas 1996:136), the casting is heavier built than statuary.

Interpretations of the Kanellopoulous Ram have largely been driven by the preconceived notion that it is too small to be a waterline ram, so it must be a Hellenistic period zoomorphic *proembolion* (Pridemore 1996:101; Murray and Petsas 1989:103). But notions of ram size may be biased based on the large Hellenistic period warships found in the archaeological record, such as the Athlit Ram. Archaic and Classical period rams may have been quite small, only covering the tip of the ship's prow, due to the casting abilities of the time and the price of bronze. The lead content of the Kanellopoulous casting does not fit the Hellenistic period, at least if it was a *proembolion*, but there is little other evidence that may provide a date.

How large might the Kanellopoulos vessel have been? At 10-15 cm, the keel of the Kanellopoulos vessel would have been comparable to the fifteen meter long Kyrenia vessel, which had a keel of 10-13 cm (Steffy 2006:43). In fact, the narrowing Athlit ram keel was 6-8 cm where it fitted the baseplate, though obvious it tapered outward significantly (Steffy 1991:17). Indeed, size is not a functional hindrance when ramming, as a smaller point more effectively transfers force. Though relatively small, the Kanellopoulos Ram has the features of a waterline ram that accepted keel and stem timbers. It was a strong alloy and, if it dates to the 6^{th}-5^{th} centuries BC, then its size matches the casting capabilities of the time. This casting may represent a zoomorphic ram early in development, even if not designed for a larger warship from the period such as a bireme or *samaina*.

1.10 Koln Casting

Almost nothing is known of this bronze casting. It was sold by Christies Auction House in 2004 on behalf of the Axel Guttmann Collection of Ancient Arms and Armour, purportedly acquired by Guttmann in 1992 (Christie's 2004a). The bronze casting is 43.5 cm long and 35 cm in height. The casting had wood remaining on the interior, which was studied and said to be carob (*ceratonia siliqua*), which grows primarily in the Mediterranean region (Brather 1994).

The casting has two decorations, a hoop in the form of a dolphin and a phallus. The hoop is similar to one on the Belgammel Ram (Figure 4.15), though the Belgammel hoop is interpreted as a bird. The function on both rams is unclear. The phallus decoration is unique among the known rams, though there are many explicit analogies to rams and phalluses in ancient sources (i.e. Aristophanes 2003:line 1224). The presence of the phallus also belies the penetrating nature of this casting and implies that it is in fact a ram, though quite different from the Athlit-type three-finned rams found elsewhere.

Christies dated the casting to the 1^{st} to 2^{nd} centuries AD based on iconography. If the casting is in fact a ram, then the design would fit *liburnian* type rams, which were used from the 3^{rd} century

Figure A3.14. The Koln casting (Christie's 2004a).

BC through 2nd century AD. The most famous depiction of this type of ram is Trajan's Column (Appendix 4, Figure 83), but also found on models and other iconography (Appendix 4, Figures 64, 77, 81). While its design is different, the Koln casting has similar ramming properties as the Phanagoria casting (Figure 4.24). The Koln casting is most likely a *liburnian*-type ram from the 2nd century BC to 2nd century AD.

1.11 Phanagoria Casting

A vessel was found in shallow water off the ancient Black Sea city of Phanagoria. It has not been published yet, though archaeologists have revealed quite a bit of information through media outlets. The vessel measures 16 m in length and 3 m beam, as well as has a bronze casting in the bow of the vessel (Figure 4.24) (Popular-Archaeology 2014). Though the casting was not found attached the vessel's bow timbers, communications with the excavating archaeologists indicates it was excavated directly in front of the vessel, oriented correctly, and it was located on a strata matching the vessel, meaning the casting does match fit this vessel. The site can be dated to 89-60 BC based on pottery and dendrochronology (Popular-Archaeology 2014). Researchers suggest it fits the reign of Mithradates VI, who sent a fleet to Phanagoria when it revolted in 63 BC.

The design of the Phanagoria casting is different from the Athlit-type rams. Could the Phanagoria casting be a ram or is it a cutwater? Cutwaters were very common on merchant ships, as shown

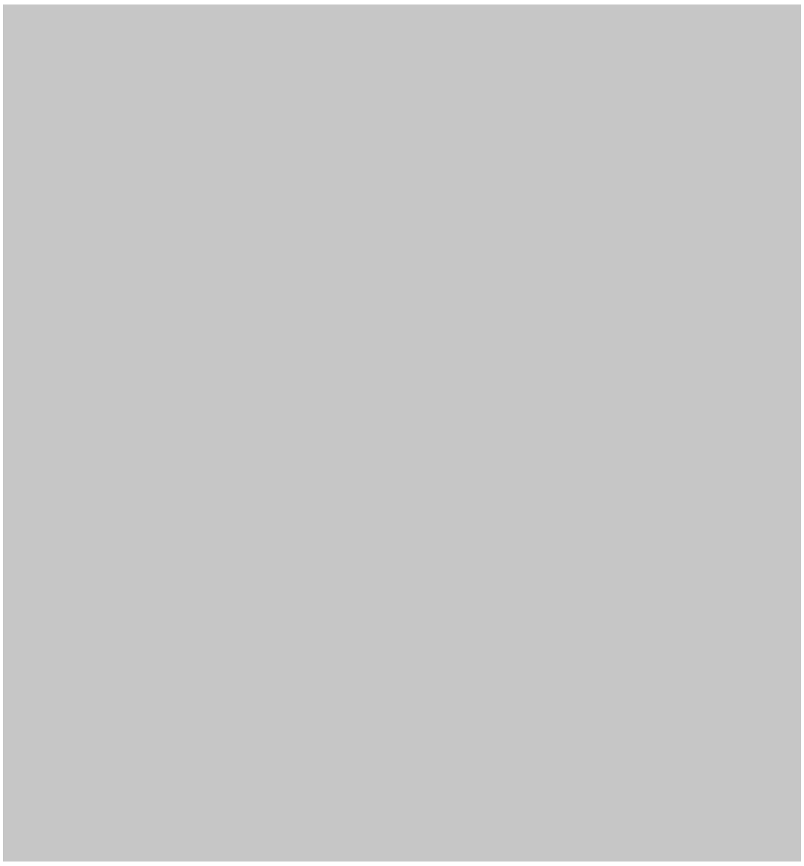

Figure A3.15. Bronze bow fitting from Phanagoria; it is on its side, the keel is on the right and the stem would have entered on the left (Popular-Archaeology 2014).

Figure A3.16. Image of the Phanagoria shipwreck (Popular-Archaeology 2014).

by over half of the merchant ships on the Althiburus Mosaic having cutwater bows (Appendix 4, Figure 84), as well as archaeological remains like the Madrague de Giens shipwreck (Pomey 1982). However, bronze was expensive and castings for cutwaters are not known in either the archaeological or historical record; the well-funded Madrague de Giens vessel did not have a casting (Pomey 1982). As mentioned earlier, out of 1,785 published shipwrecks, only warships had large bronze castings (Strauss 2013a). This does not exclude the possibility that the Phanagoria artefact is a bronze cutwater; however, it would be the first known in the archaeological and historical record.

Notably, the casting displays the sunburst and crescent symbols (Figure 4.26). Mithradates VI of Pontus issued coins featuring these two symbols together (Appendix 4, Figure 68). The starburst is the symbol of kingship. It is also found on the sides of the Athlit Ram's cowling (Figure 4.49). A coin from the Black Sea region offers intriguing questions (Appendix 4, Figure 82). It was struck by Asander, archon and later king of Bosporus, in 47-43 BC (CNG 2014). The coin clearly shows a three-finned ram; however the coin is an overstrike of a coin issued by Mithradates VI with a starburst symbol- the same symbol as on the Phanagoria casting. Of further interest, Asander's ram depicted on the coin has the starburst symbol on its wale pocket. The starburst was the mark of kingship by the Mithradates, Asander, and the Ptolemies and all put it on their rams. This suggests that when the starburst appears on the Phanagoria Ram that it is a royal vessel such as a warship, not a merchant vessel with a bronze cutwater.

Mithradates sent vessels to quell an uprising at Phanagoria in 63 BC (Abramzon and Kuznetsov 2011). The vessel excavated at Phanagoria fits well with what is known of Mithradates VI's navy. Appian states that it was composed of "300 cataphracts and 100 biremes" largely supplied by

FIGURE A3.17. CLOSE UP OF THE DECORATION ON THE PHANAGORIA FITTING (LIVE SCIENCE 2013).

pirates (Casson 1995:124; Appian, Mithradates 17) while Memnon states Mithradates was using "no small number" of penteconters in 74 BC (Casson 1995:124 n. 98). The terms penteconter and *lembos* are used interchangeably by at least one ancient author and Casson argues it would be more understandable if Mithradates had *lembos* in the 1st century BC rather than penteconters (1995:124 n. 98).

Since bronze cutwaters are not known on merchant ships in the archaeological, historical, or iconographic evidence, the vessel likely represents a small warship such as a *liburnian*, *lembos*, or *pristis*. The warships were not fitted with three-finned Athlit-type rams, but elongated rams of a later design, which can be seen on Trajan's Column (Appendix 4, Figure 101). Džino argues that the *pristis* was fitted with a bronze covered cutwater and the *lembos* was the same type of vessel without a bronze cutwater (2003: 24). These vessels were used interchangeably for war and transport of goods. They held up to 30 rowers and were approximately 15 m in length according to estimates (Džino 2003: 35), which fits the dimensions of the Phanagoria vessel. Since the Phanagoria vessel is unpublished, it is necessary to wait the researchers findings, but the vessel appears to offer insight into a later design of rams that was introduced after the three-finned ram.

1.12 Piraeus Ram

The Piraeus Ram was found by a fisherman off Cape Artemision northern Euboea and sold to a businessman, Vassilis Kallios, who recognized its archaeological value and donated it to the Piraeus Archaeological Museum (Steinhauer 1994: 39). The Piraeus Ram follows the design of the Athlit Ram, but it has been split in half, likely due to a ram-to-ram strike. The fragment weighs 36.7 kg (Varoufakis 2007: 453). The ram is composed of a bronze alloy that is 86.5% copper and 11.72% tin (Varoufakis 2007: 454). It has been variously dated from Classical (Steinhauer 1994: 39) through the beginning of the Hellenistic era (Steinhauer quoted in Varoufakis 2007: 453). The lack of archaeological context or wood remains for radiocarbon dating means that dating relies on comparison. A full study of this ram has not been conducted or published.

Figure A3.18. The ram found off Artemision and currently in the Piraeus Museum (Steinhauer 2001).

1.13 Turin Ram

The Turin Ram was dredged from Genoa harbour and is current on display in the Turin Armoury. It measures 55cm in length and for this reason it is generally considered to be a *proembolion* (Torr 1894:65; Murray and Petsas 1989:103; Pridemore 1996:99). It is in the form of a boar's head with a plain sheathed stern section that connected to a wooden beam.

Figure A3.19. The Turin Ram (Turin Armoury 2014).

The Turin Ram is difficult to date. No wood remains for radiocarbon dating and the bronze has not been analysed. Torr estimates a date of 50 BC based on zoomorphic *proembolion* during the Hellenistic Period (Torr 1894:65). Pridemore is more cautious and simply estimates the 3rd century BC through 1st century AD (Pridemore 1996:99). Were the ram not found in a maritime context then it would be easy to suggest it is a battering ram, as the attachment for its wooden elements is closer to the Olympia *krios* than the British Museum Actium *proembolion*.

1.14 Silifke Ram

Figure A3.20. Divers recording the ram, which lies on its side with the forward end facing the divers (Current World Archaeology).

A ram was discovered off Silifke, Turkey, in 2015, but little has been reported outside of the media (Current World Archaeology 2015). Until an academic report is published, it is difficult to gauge the information about the ram, since it is reported as iron. The article speculates that the ram was fitted to a bireme and could date between the 8th to 4th centuries BC. The ram is damaged, but the condition is not what one would expect from iron, suggesting it may be a low quality bronze alloy. It appears to be quite different from the Athlit-type rams with the attachment most closely resembling the Phanagoria Ram.

1.15 Non-Naval Battering Rams

A bronze ram was found at Olympia, Greece, during archaeological excavations in the 1950s. The ram is a battering ram for attacking cities under siege, though many researchers have speculated about the connection between terrestrial *krios* and maritime *embolos* (Pridemore 1996). It was found in a trench near the stadium and may have been a dedication. Currently located in the Olympia Archaeological Museum, the ram is relatively dated by its decoration, thought to correspond to the first half of the 5th century BC (Sekunda 1994:187).

It is cast bronze, measuring 24.2 cm high and 25.2 cm wide. The opening in the back would have fit a straight timber approximately 22 cm by 8 cm (Campbell 2006:41). The ram has a central blade similar to naval rams, but also five points on each side. Campbell posits that the triangular points may have been designed with the intent to break through mud brick (Campbell 2006:41). On its side it is decorated with a ram head motif.

Figure A3.21. The battering ram (krios) from Olympia (Richard Mortel).

The Olympia ram is an excellent example of a Greek *krios* and the conceptual approach of battering, compared to the warship rams we will examine in the discussion. Similar to the Turin Ram, the Olympia *krios* does not flare at the back to accept wales, but instead has a straight run aft to fit a single straight timber.

Was the development of terrestrial *krios* connected to maritime *embolos*? Diodorus Siculus (12.28.3) writes in the 1st century BC that Pericles and his engineer Artemon of Clazomenae was the first Greek to use a battering ram against a city when he attacked Samos in 440 BC; however Plutarch casts some doubt on this story when he likewise told it based on papers from Greek historian Ephorus (Plutarch *Pericles* 27). Ascribing innovations to great men was commonplace, as seen in Chapter 3. Another problem was later authors projecting the technology of their day back to the 5th century BC, including Pausanias and Cornelius Nepos (Campbell 2006:41–42). Egyptians may have used rams as early as the 12th century BC (Whitehead and Blyth 2004:79), the Assyrians and Persians had been using rams for sieges since 850 BC (Campbell 2006:47), and the Carthaginian are purported to have "invented"- read used- battering ram at the siege of Gades (modern Cádiz) circa 500 BC (Whitehead and Blyth 2004:79), so it would be a surprise if the Greek were not cognizant of them prior to 440 BC. This means that the *krios* appears many decades after the maritime ram.

It appears that it was convention to shape the head or fit a casting in the shape of a ram's head, such as the battering ram depicted on Trajan's column (Campbell 2006:42). Both the name *krios* and this imagery suggest a specific functional use as battering in the manner of the animal. Though writing much later in 209 AD, Tertullian writes, "the ram…the timber machine which serves to break walls…appreciated the power of the machine like the anger of the beast that asserts itself with its head" (Tertullian De Pallio 1.3; Campbell 2006: 46). This contrasts linguistically to the *embolos* and *rostra*. There appears to be a connection between linguistics, imagery, and functional technology. Honor Frost noted this, stating, "The boar's tusks attack the soft underbelly of his prey; so do rams that curve upwards from the keel. Lion's heads and trident-daggers adorn the rams that spring from the wales" (Frost 1975:227). It must be noted that Thucydides uses the word *embolos* to describe Spartan battering rams at Plataea in 429 BC, though his preferred word appears to be *mēchanai* or machine[4] (Campbell 2006:42), and the Olympia battering ram without the points bears a striking resemblance to the naval rams depicted in iconography from the same period.

[4] Machine in Greek meant "stratagems, devices, artificial means by which man was able to infringe the laws of nature" (Garlan 1994:682).

Appendix 4. Analysis of the Egadi Rams

As survey and excavation has been continuous on the Egadi site, from 2011 to present shore-based research has focused on analysing the battle site artifacts (Tusa and Royal 2012). Under the auspices of the project directors, Peter Campbell has coordinated analysis providing basic quantitative measurements of the warship rams such as weight and dimensions, metal analysis, and provenience data.

The approach to this analysis was adopted from the University of Southampton, which developed a methodology for analysing ancient bronze castings during the study of the Belgammel Ram (Adams *et al.* 2012). A series of tests were tried so that best practice could be identified. This practice was followed for the Egadi Rams using several of the same team members (Ian Croudace and consultation by Nic Flemming and Jon Adams).

The results of the analysis will be published in an upcoming article in *Analytical Chemistry.*

3D Recording

Structured light was chosen a 3D scanning method to provide high-resolution models. In 2011 a team from University of Kentucky scanned the Egadi 3 ram (Tusa and Royal 2013: 17). In 2013 Breuckmann GmbH provided an academic loan grant of a SmartSCAN structured light scanner. This partnership with industry provided one the highest accuracy 3D scanner currently available on the market. The scanner was high resolution and the author settled on a rapid setting that offered an average accuracy of 25 microns. Eight of the Egadi rams were scanned using this system.

Figure A4.1. A structured light scan in progress on the Egadi 5 ram (Author).

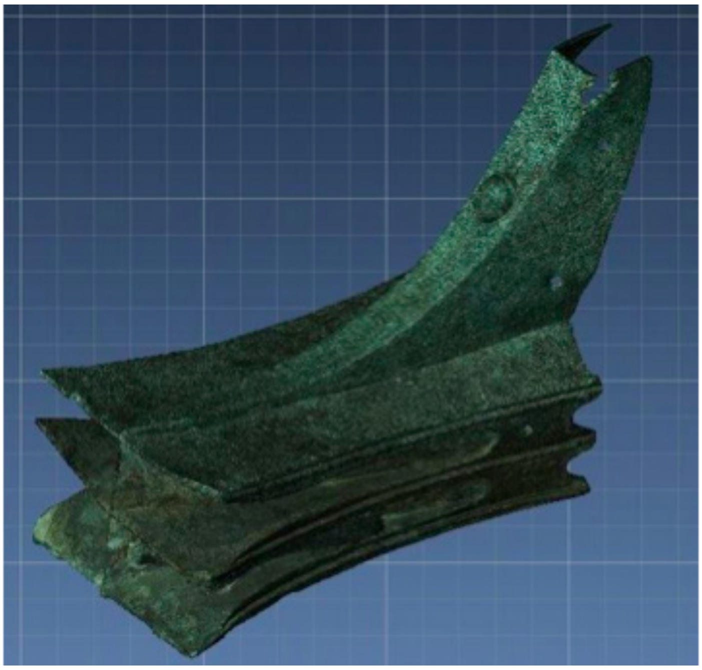

Figure A4.2. The 3D model of the Egadi 8 ram (Author).

Reflectance Transformation Imaging (RTI) was conducted on four rams that have incised inscriptions. RTI uses polynomial texture mapping to create surface renders accurate to a few microns, allow for the reading of weathered or damaged surfaces. The rams' inscriptions are an important source of information and the RTI data was shared with the project's epigraphy specialists.

Weights

Each of the rams was weighed with a digital scale, the first time that accurate weights were recorded for the rams. Note that Egadi 3, the single Carthaginian ram, weighs more than all the Roman examples. The weights are as follows.

Egadi Rams	*Weight in kg*
1	167.8
2	75.5
3	184.5
4	130.5
5	57.4
6	154.0
7	141.4
8	164.1

Table A4.1. Weights of the Egadi Rams (Author).

Metal Analysis

The castings were then examined for their metallurgical properties. Each ram was weighed with the complete rams weighing between approximately 130 and 190 kg. Metal sampling was overseen by Professor Ian Croudace on nine of the rams. This consisted of delicate sampling using a jeweller's saw or small drills. These samples were analysed at the National Oceanography Centre (UK) using a range of analytical procedures including an EAGLE III micro X-ray fluorescence

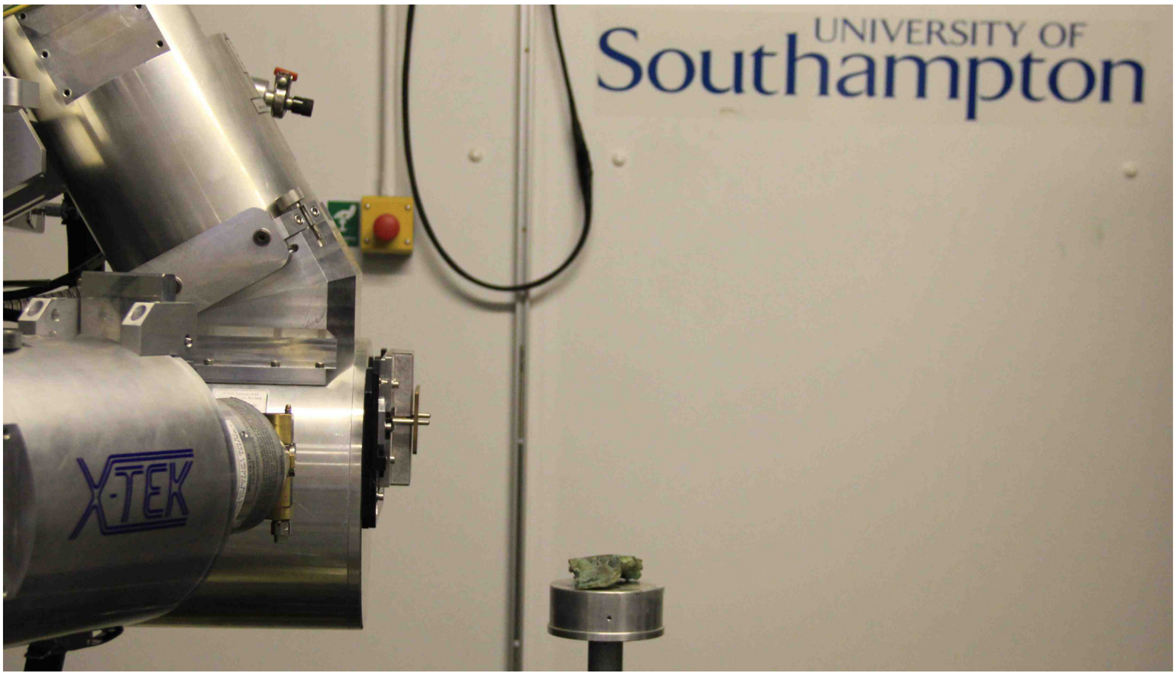

FIGURE A4.3. CONDUCTING 3D COMPUTED CT TOMOGRAPHY OF A FRAGMENT OF THE EGADI 2 RAM (AUTHOR).

spectrometer and a LEO scanning electron microscope to investigate elemental and metallurgical textures. A Thermo NEPTUNE MC-ICPMS was used for high precision lead isotope analysis. Micro-XRF analysis revealed the Egadi rams to be a leaded bronze mixture not dissimilar to the Belgammel Ram, which had a nominal composition of ~85 Cu, ~6 Sn, and ~6 Pb (Adams *et al.* 2012: 12), but different from the Athlit Ram, which had a composition of ~90 Cu, ~9.8 Sn, and less than 1% Pb (Oron 2001: 107). Lead isotope analysis should provide constraints on the provenance of the lead used. This analysis is still being conducted at the time of writing.

Summary

Analysis of the Battle of the Egadi Islands artifacts is revealing a considerable amount regarding the manufacture of large single cast objects in Antiquities, as well as the function of rams. On the basis of an admittedly limited collection of naval rams from the central Mediterranean (Belgammel and Egadi warship rams) it may be that the Athlit's high bronze and low lead content is unusual. Following completing of the current studies on metallurgy and 3D image analysis, the findings will be published in one or more articles. The authors would like to acknowledge the support of the Honor Frost Foundation, Southampton Marine and Maritime Institute, Breuckmann GmbH, Explorers Club, and Historical Metallurgy Society.

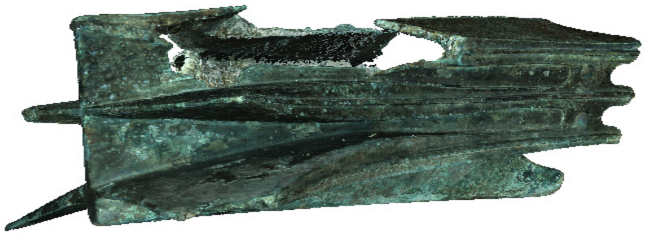

Figure A4.4. Three-dimensional model of the Egadi 2 ram made using structured light scanning (Author).

Figure A4.5. Three-dimensional model of the Egadi 5 ram made using structured light scanning (Author).

In addition to the Egadi rams, the author created 3D models of the Piraeus Ram, Actium proembolion, and the Kanellopoulous Ram for impact testing.

Figure A4.6. Three-dimensional model of the Actium proembolion created using photogrammetry (Author).

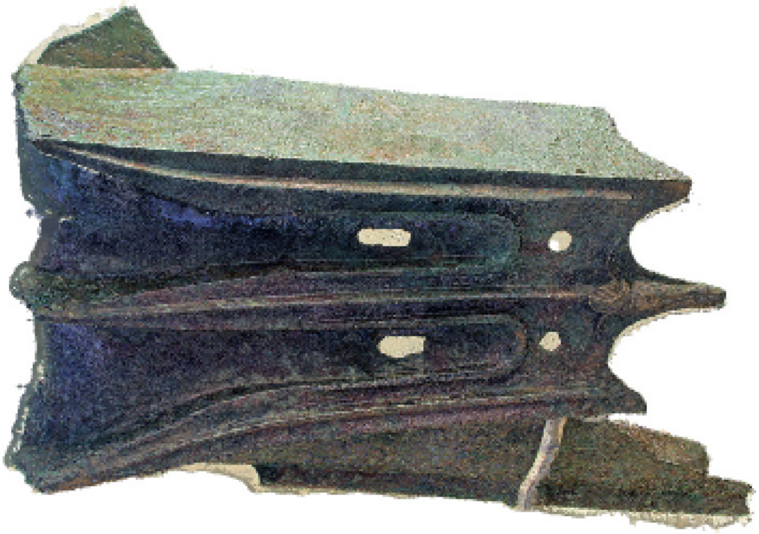

Figure A4.7. Three-dimensional model of the Piraeus ram created using photogrammetry (Author).

Appendix 5. Chronological Evidence for Warship Rams

Note: Each image description contains A) date B) title of the artefact C) method used to date the artefact D) Citation

Unknown Dates

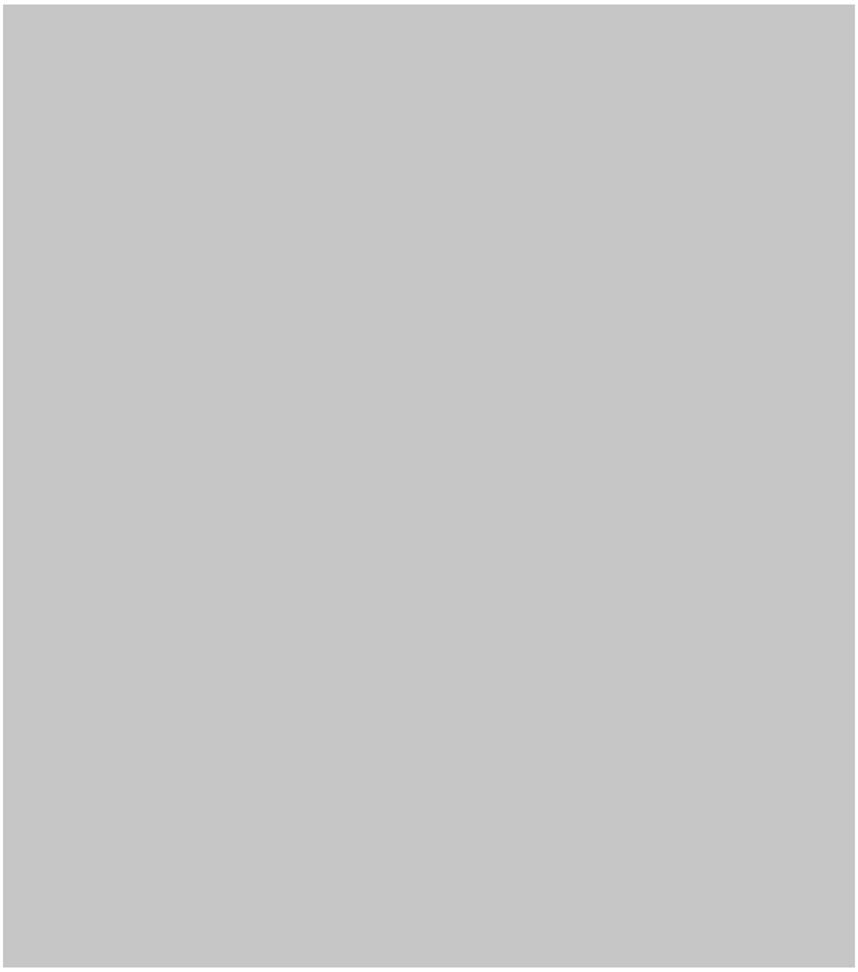

Figure A5.1. Estimated variously as 4th to 1st centuries BC. Bremerhaven Ram. Dated relatively based on iconography; looted and sold at auction by the Nefer Galley to the Bremerhaven Maritime Museum (Courtesy of Bremerhaven Maritime Museum).

Figure A5.2. Estimated variously as 5th to 1st centuries BC. Kanellopoulos Ram. Dated relatively based on iconography; found by a collector at Drepana in the Gulf of Corinth (Courtesy of Kanellopoulos Museum).

Figure A5.3. Estimated as 50 BC. Turin Ram. Dated relatively based on iconography; dredged from Genoa harbour in the 19th century (Courtesy of the Turin Armoury).

Figure A5.4. Estimated as 5th to 3rd centuries BC. Piraeus Ram. Dated relatively; found by fisherman off Cape Artemision (Steinhauer 2001).

Figure A5.5. Estimated as 1st to 2nd centuries AD based on iconography; sold at auction with no provenience. Dated relatively based on iconography; looted prior to 1992 and sold at auction by Christie's (Christie's 2004a).

Prior to the 10th century BC

Figure A5.6. ~2600 BC. Mochlos boat model. Dated from archaeological context. (Göttlicher 1978: 61 n. 313, plate 24).

Figure A5.7. ~2400 BC. Palaikastro boat model. Dated from archaeological context (Göttlicher 1978: 61 n. 324, plate 24).

Figure A5.8. 1200-1100 BC. Asine vase. Dated from archaeological context (Basch 1975: 202; Frödin and Persson 1938: 207).

Figure A5.9. 1178-1175 BC. Medinet Habu Relief depicting a naval battle between Egyptian naval forces and the Sea Peoples. Dated from in situ archaeological context (Wachsmann 1995:29).

Figure A5.10. c .1,000 BC. The Gurob Ship-Cart. Dated from in situ archaeological context of a tomb (Wachsmann 2013).

10th century BC

Figure A5.10. 900-700 BC. Geometric proto-Corinthian vase from Thebes depicting a galley with a bow projection. Dated stylistically (Basch 1975: 202; Berlin 3143).

899-750 BC

Figure A5.11. 850-800 BC. A cup from Eleusis depicting a galley. Dated from archaeological context (Casson 1995: Figure 30).

Circa mid-8th century BC, the poet Homer composes the *Iliad* and *Odyssey* without any mention of rams (Basch 1975; Morrison 1995; Mark 2006).

Figure A5.12. 8th century BC. Funerary etching from Athens. Dated from archaeological context (Casson 1994).

Figure A5.13. 799-750 BC. Warships attacking land forces from a black figure vase. Dated stylistically (Casson 1996: Figures 65 and 66).

750-700 BC

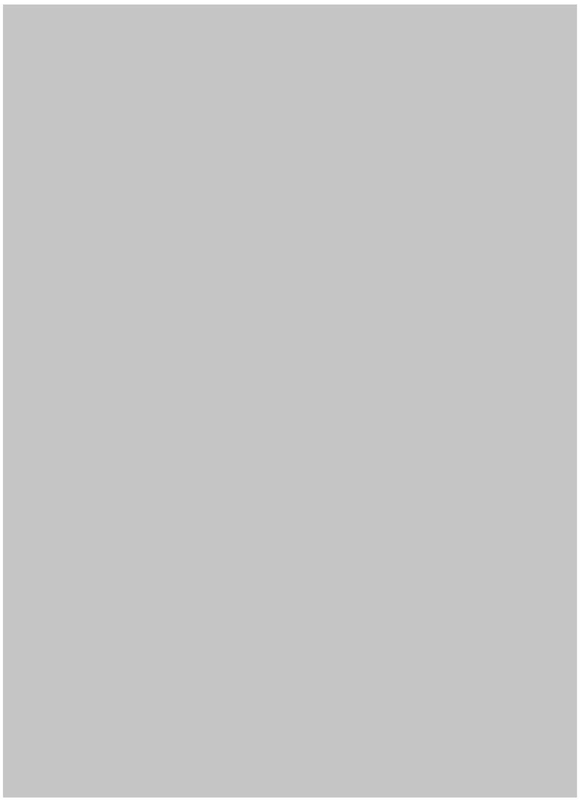

Figure A5.14. 745-727 BC. Relief from Til Barsip, Assyria. Dated from archaeological context (Mark 2006).

700-600 BC

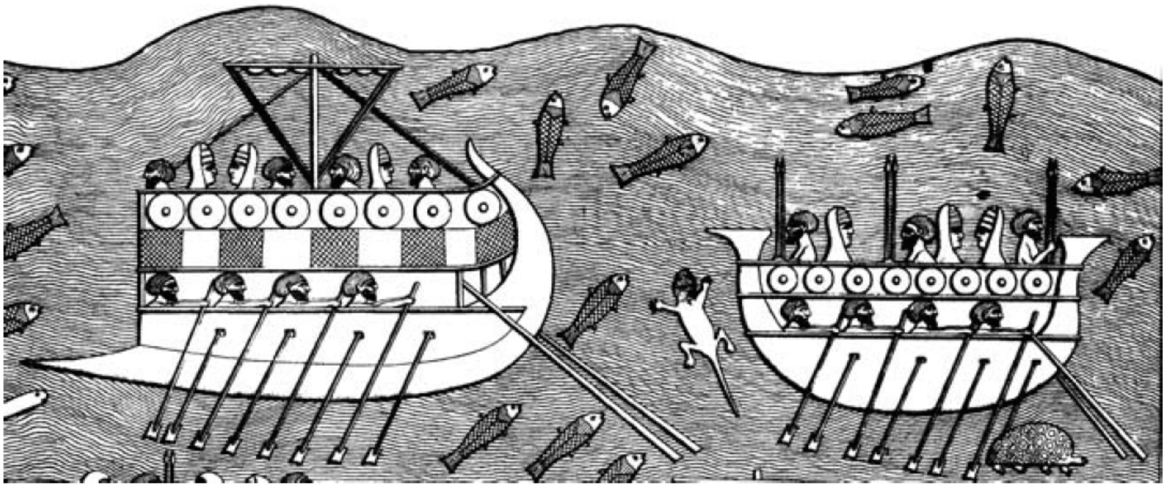

Figure A5.15. 704-681 BC. Relief carved for the Southwest palace of Sennacherib at Nineveh, Assyria. Dated from archaeological context (British Museum).

660 BC. First naval battle according to Thucydides, no mention of ramming (Thucydides 1.13).

Figure A5.16. 625-575 BC. The Novilara Stele from Pesaro in the Oliveriani Museum. Dated stylistically (Casson 1994).

Figure A5.17. ~600 BC. Ship model from Cyprus. Dated stylistically (British Museum).

Figure A5.18. ~600 BC. Geometric spouted vessel from Boeotia in the shape of a warship. Dated stylistically (Göttlicher 1978: 66 n. 351, plate 26; Boston Museum of Fine Art 99.915).

Figure A5.19. ~600 BC. Wooden ship model from the Heraion at Samos. Dated from archaeological context (Göttlicher 1978: 66 n. 352, plate 26).

600-550 BC

Figure A5.20. 570-560 BC. The François Vase, painted by Kleitias in the Attic black figure style and found in an Etruscan tomb. Dated based on the years Kleitias was operating (Boardman 1974).

Figure A5.21. 575-550 BC. Kantharos or kyathos with a warship with Boeotian characteristics. Dated stylistically (Johnston 1985: 67-68; Louvre CA577).

Figure A5.22. ~560 BC. Bas-relief of the ship Argo from a metopes of the Treasury of the Sicyonians at Delphi. Dated based on archaeological context. (Basch 1975: 203; GOS: 86, pl. 12).

550-500 BC

Figure A5.23. 6th-5th centuries BC. Model of an oared ship with a zoomorphic prow. Unknown provenience, dated based relatively based on iconography (Göttlicher 2004).

Figure A5.24. 545-530 B.C. Black figure dinos by the Exekias painter, currently in Museum of the Villa Giulia, Rome. Dated based on the Exekias painter (Boardman 1974: 56).

~540 BC. Hipponax poem is the earliest surviving mention of the word *embolos* (Morrison et al. 2000: 34).

540-535 BC: Battle of the Straits of Sardinia, aka Battle of Alalia (Herodotus 1.163).

Figure A5.25. 530-500 BC. Silver stater from Phaselis in Lycia, Asia Minor, depicting a zoomorphic warship prow. Dated based on this coin series' minting period (Heipp-Tamer 1993).

Figure A5.26. 525 BC. Painting in tomb from Elmali, Turkey. Dated based on archaeological context (Toby 1979: 7).

Figure A5.27. 520-500 BC. Kylix depicting a merchant ship, an oared vessel with a zoomorphic prow, and a third vessel with a penetrating prow. Dated based on the style of the black figure pottery (British Museum 1867.0508.963)

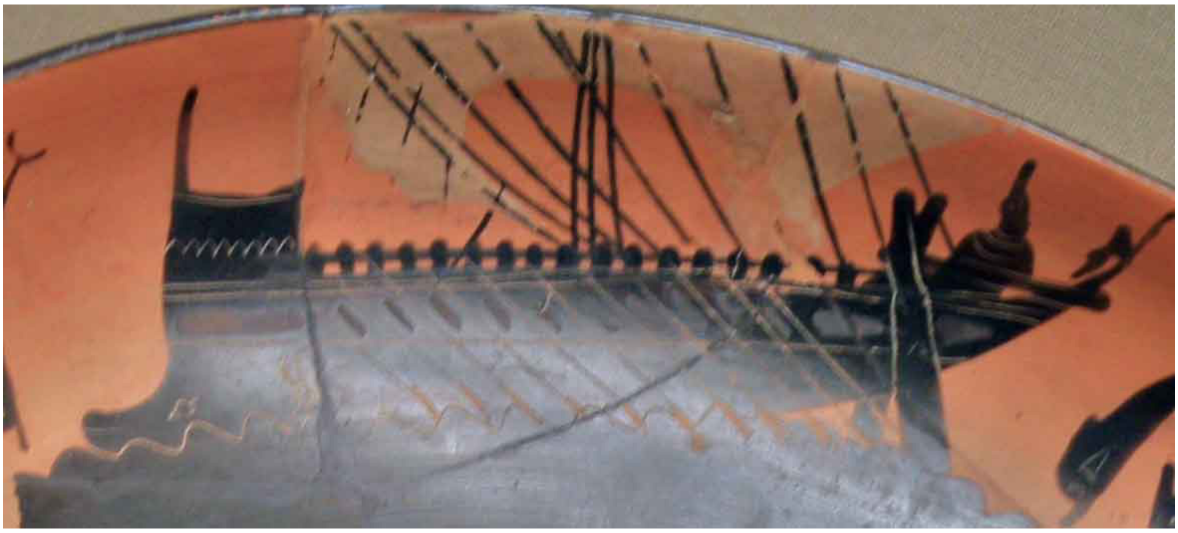

Figure A5.28. 510-500 BC. Red and black figure kylix *made in Athens. Dated based on red and black figure pottery (British Museum).*

Figure A5.29. 500 BC. Vase of Achilles jumping from a ship's bow. Dated stylistically (British Museum).

Figure A5.30. 525-500 BC. Seal depicting a decked warship with a zoomorphic prow. Dated stylistically (Casson 1995: Figure 84).

500-450 BC

Figure A5.31. 500-450 BC. Attic skyphos depicting a Dionysian ship cart. Dated stylistically based on Black Figure pottery (Waschsmann 2012: 49)

Figure A5.32. 500-475 BC. Oinochoe by the Keyside Class depicting Odysseus and the Sirens. Dated based on the operating years of the Keyside Class style (Boardman 1974: 150).

494 BC. Battle of Lade, Ionian Greeks versus Persia (Herodotus 6.6-17).

492-449 BC. Greco-Persian Wars (Herodotus 8.4-96).

Figure A5.33. 494-489 BC. Samian warship depicted on a coin struck at Zancle in Messina, Sicily. Precisely dated by the mint each year from 494-489 (Basch 1975: 203).

480 BC. Battle of Salamis, Greeks versus Persia (Herodotus 8.4-96).

Figure A5.34. 480-470 BC. Red figure Attic Siren Vase. Dated based on red figure pottery (British Museum).

Figure A5.34. 500-450 BC. Non-naval battering ram from Olympia, found in a mixed deposit during an archaeological excavation in 1952. Dated based on the style of the ram-head decoration (Cook 1965: 119).

450-400 BC

440 BC. Herodotus completes his History (lived circa 484-425 BC).

431-404 BC. Peloponnesian War (Thucydides).

415-413 BC. The Sicilian Expedition (Thucydides 6.1).

Figure A5.35. 411-350 BC. Silver obol struck at Phaselis Lycia. Dated based on the minting of this series (Heipp-Tamer 1993).

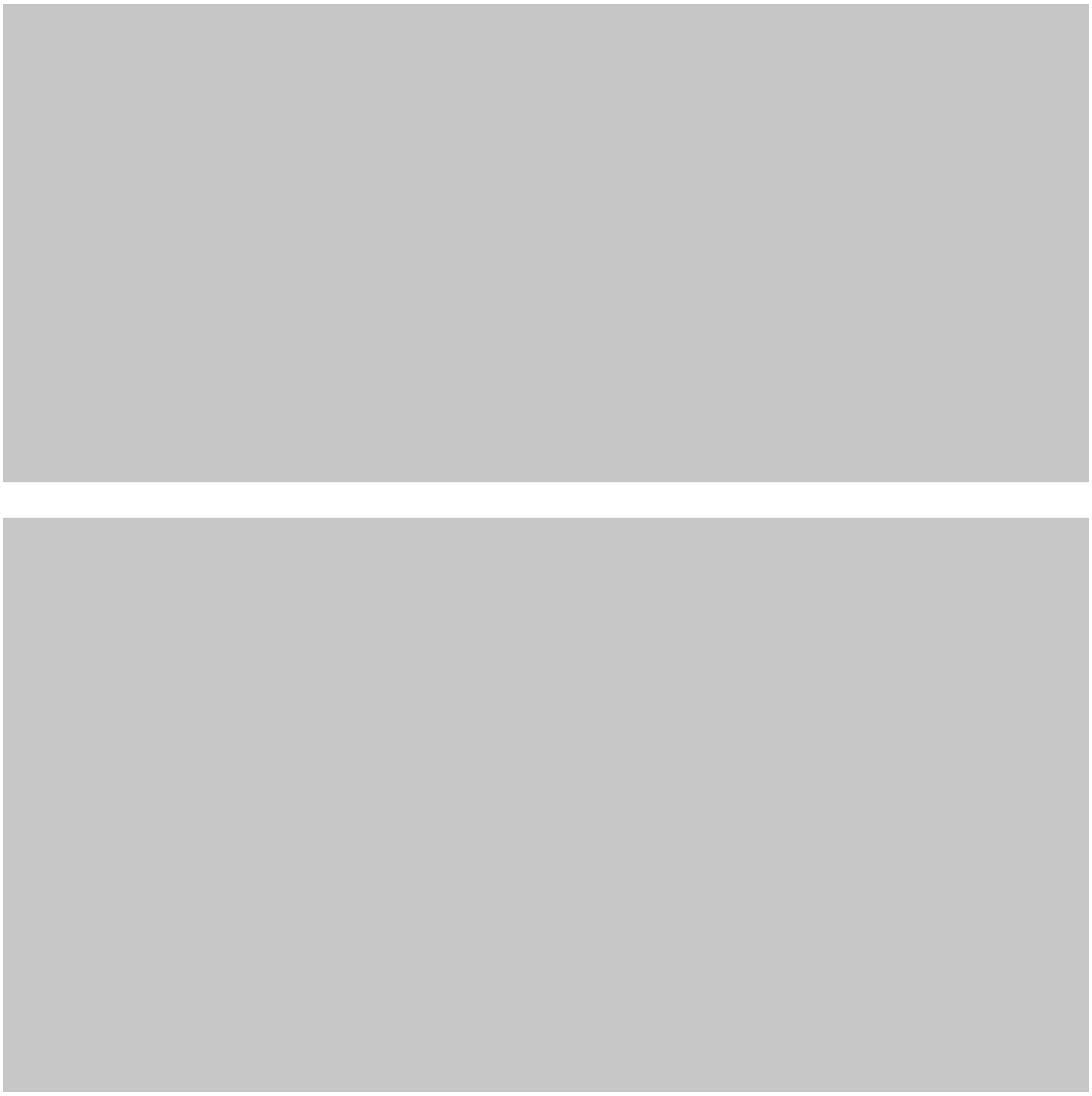

Figure A5.36. 415-400 BC. Lamp in the shape of a ship found in the Erechtheion on the Athenian acropolis. Dated based on archaeological context and style (Göttlicher 1978; Johnston 1985).

405 BC. Battle of Aegospotami, Spartan victory and the decisive naval engagement of the Peloponnesian War (Xenophon 2.2.3).

404 BC. Athens capitulates to Sparta, ending the Peloponnesian War (Xenophon 2.3).

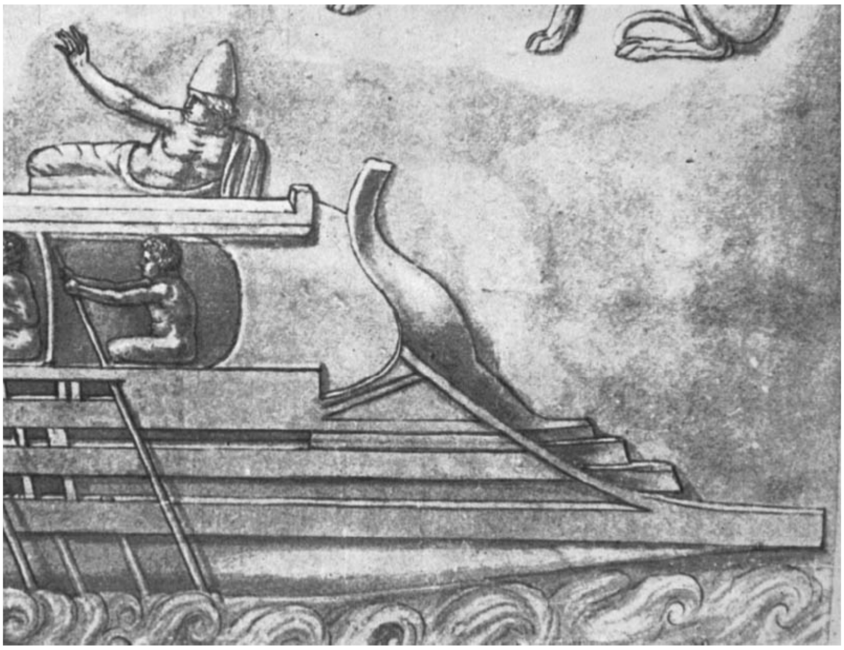

Figure A5.37. Circa 400 BC. Cavaliere dal Pozzo drawing from 17th century based on unknown original. Dated to approximately 400 BC based on similarity to the Lenormant Relief (British Museum).

Figure A5.38. Circa 400 BC. An Apulian rhyton currently in the Petit Palais, Paris. Dated relatively based on iconography (Petit Palais, Musée des Beaux-Arts de la Ville de Paris, Collection Dutuit).

Figure A5.39. Circa 400 BC. Rhyton found at Vulci. Dated relatively based on iconography, such as ~400 BC by Göttlicher (1978: 67 n. 360, plate 27), Hellenistic by Basch (1969b: 432), and late 4th to early 3rd century BC by Johnston (1986: 96) (British Museum).

400-350 BC

Figure A5.40. 400-380 BC. A silver obol from the Phoenician city of Arados. Dated based on the issues minted by the king of Arados (Wildwinds 2015).

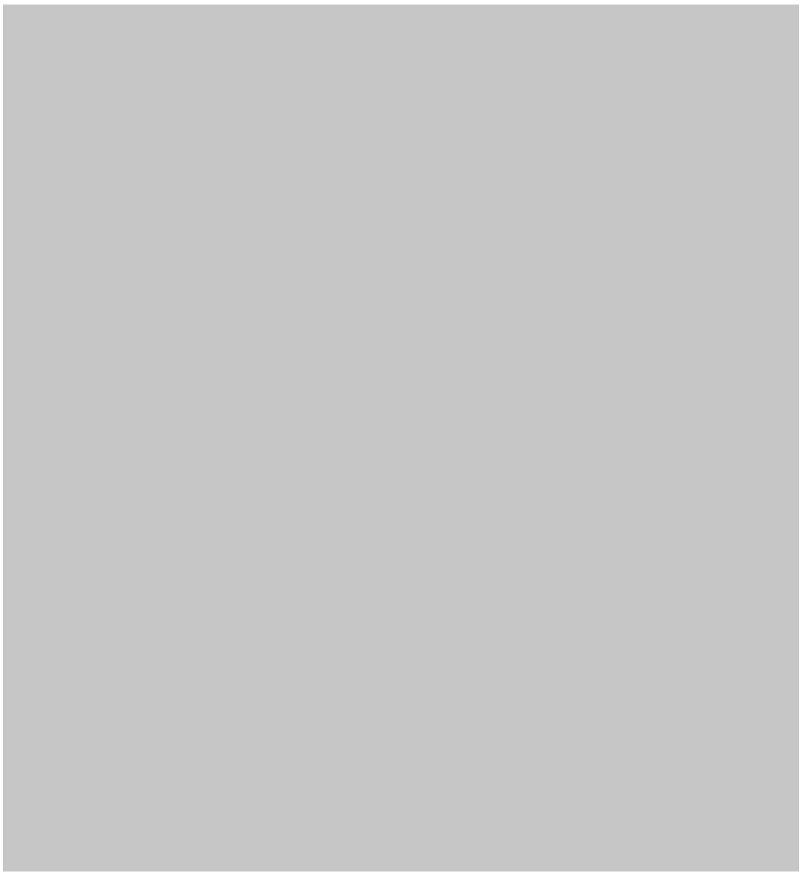

Figure A5.41. 400-384 BC. A silver coin of Sidon. Dated based on the minting issues by the king of Sidon (Wildwinds 2015).

399-397 BC. Quinquereme invented by Syracuse.

397 BC. Siege of Syracuse, Syracuse versus Carthage. 40 quinqueremes present.

Figure A5.42. 398-395 BC. Silver tetradrachm struck at Mysia by Persian satrap Pharnabazus. Dated based on evidence of the Persian king providing Pharnabazus with silver to mint coins for a fleet and the fleet's construction (British Museum).

Figure A5.43. 399-375 BC. Democleides Stele early 4th century BC from Kerameikos cemetery in Athens. Dated stylistically (National Museum in Athens 752).

Figure A5.44. 401-366 BC. Phoenicia Sidon silver dishekel. Dated based on the mint's issues of the king of Sidon (Rouvier catalog #1096).

Figure A5.45. 373 BC. Coin from Sidon, first Phoenician depiction of a three-finned ram and traced by Basch. Dated based on the mint's issues by the king of Sidon (Basch 1969: 233, fig. 25).

Figure A5.46. 350-300 BC. Phoenician warship model found at Erment in Egypt. Dated stylistically (Morrison et al. 2000: 37).

Figure A5.47. 356 BC (upper) and 359-336 BC (lower). Coins minted by Philip of Macedonia depicting a penetrating-type prow. Dated based on Philip II's coin issues from each mint (British Museum).

350-300 BC

Figure A5.48. 350-300 BC. Apulian rhyton in the shape of warship bow, from a private collection (n. 49 Malaguzzi Valeri, Bari, Italy). Unknown context, likely looted from a tomb, and relatively dated based on style and Apulian pottery dates (Trendall and Cambitoglou 1982:617 nn. 96, 5-7).

Figure A5.49. 350-300 BC. Silver hemidrachm from Bithynia Kios. Dated generally based on the mint's issues (British Museum Catalog, Pontus 131, 13).

Figure A5.50. 350-275 BC. Bronze dichalkon from Megara depicting a warship prow. Dated based on the Megara mint's issues of coinage (Kroll catalog #643; Copenhagen catalog #482).

304 BC. First mention of trihemiolia, likely invented by the Rhodian Navy (Diodrous XX.93.3).

Figure A5.51. 306-139 BC. The Acqualadroni Ram. Dated based on radiocarbon dating (Buccellato and Tusa 2012).

300-250 BC

Figure A5.52. 270-250 BC. Clay model of warship from Ardea. Dated stylistically (Courtesy of the Louvre).

Figure A5.53. 270-240 BC. Samos silver tetrobol. Dated based on the Samos mint's issues after the Delian League's collapse (Egger catalog 11/1909).

Figure A5.54. Circa 260 BC. The Acropolis of Lindos monument. Dated relatively based on the Hellenistic naval victories that it could have been built following (Göttlicher 1978: 68 n. 367, plate 28).

Figure A5.55. 3rd to 2nd centuries BC. Bronze head with a warship headdress from the Tomb of Bruschi at Tarquinia in Eturia, Italy. Dated stylistically (Friedman 2011: 18).

250-200 BC

Figure A5.56. 241 BC. The Egadi 8 Ram. Dated based on archaeological context and historical data (Author).

Figure A5.57. 215-175 BC. The Athlit Ram. Dated based on radiocarbon dating and stylistic components (Courtesy of University of Haifa).

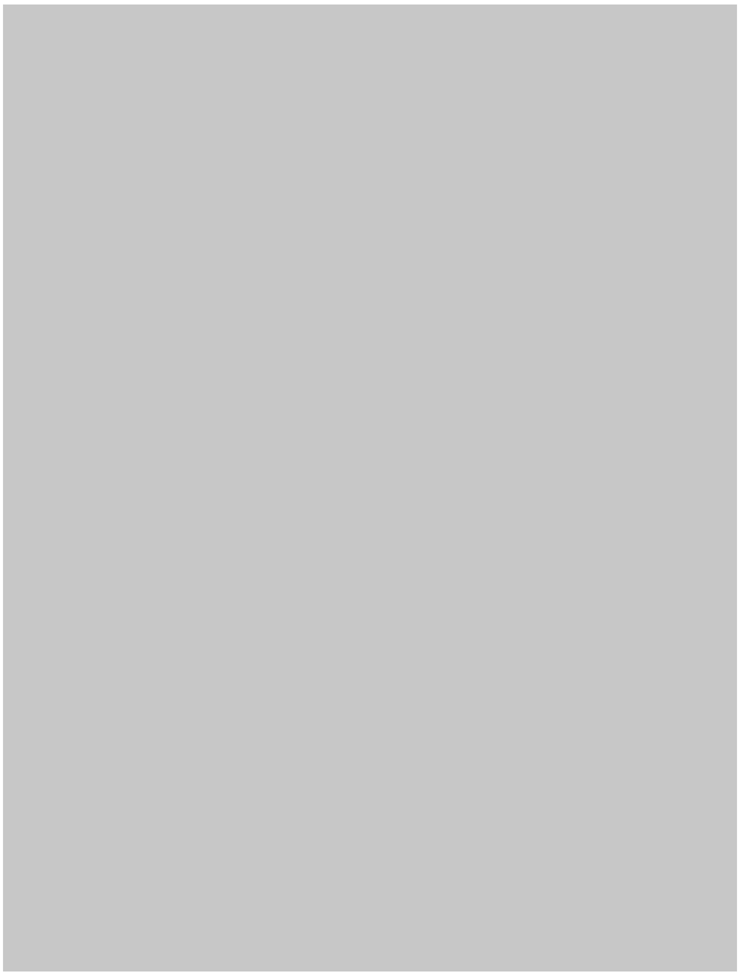

Figure A5.58. 206 BC. The Epidauros monument. Dated stylistically (Göttlicher 1978: 68 n. 368, plate 28).

200-150 BC

Figure A5.59. 200 BC. The Berenike mosaic. Dated stylistically (Friedman 2011: 7).

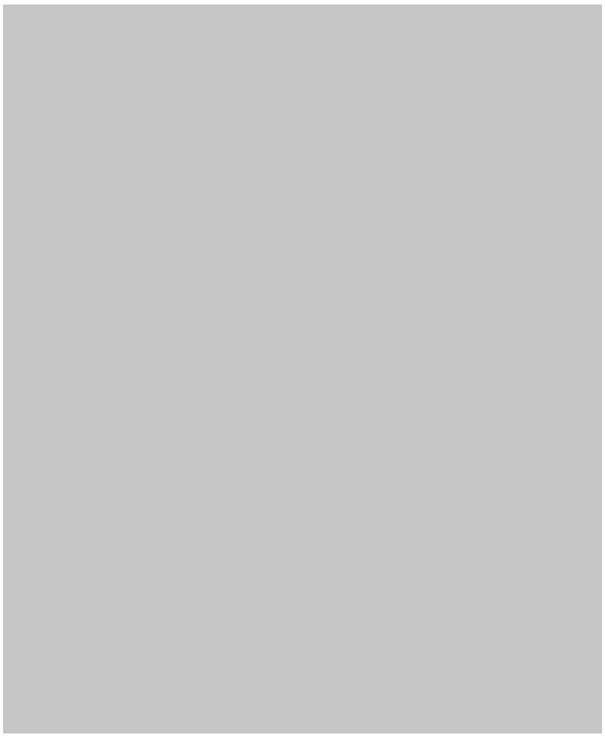

Figure A5.60. 190 BC. Winged Victory of Samothrace. Dated based on contextual information and style (Courtesy of the Louvre).

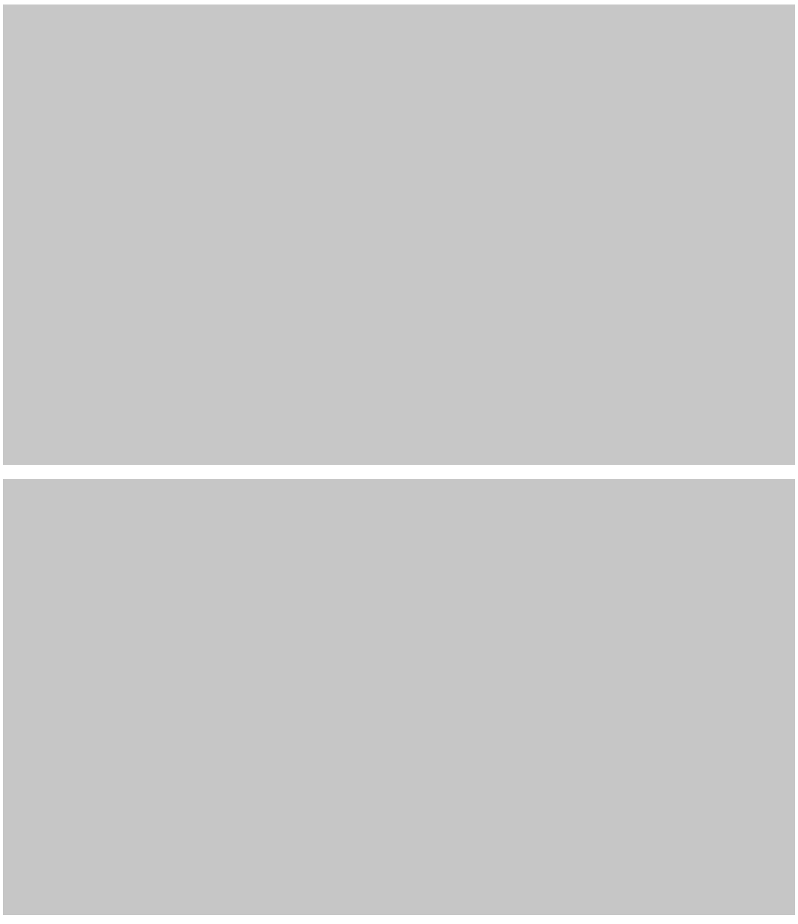

Figure A5.61. 2nd century BC. A marble ram from Rhodes. Dated stylistically (Göttlicher 1978: 69. 368c, plate 29).

Figure A5.62. 2nd century BC. The Belgammel/Fitzwilliam Ram. Dated based on radiocarbon dating of wood remains fits the 4-3 centuries BC and the articles authors state this make the ram date to "in or just after the last two centuries BC (Adams et al. 2011).

100-50 BC

Figure A5.63. 100-50 BC. The Tiber Island Monument in Rome, Italy. Dated based on historical information and style (Piranesi 1774).

Figure A5.64. Circa 100 BC. Relief of a bireme, potentially a liburnian. Dated stylistically (Courtesy of the British Museum).

Figure A5.65. Circa 100 BC. The Cyrene Monument. Dated based on archaeological context (Göttlicher 1978: 81 n. 485, plate 37).

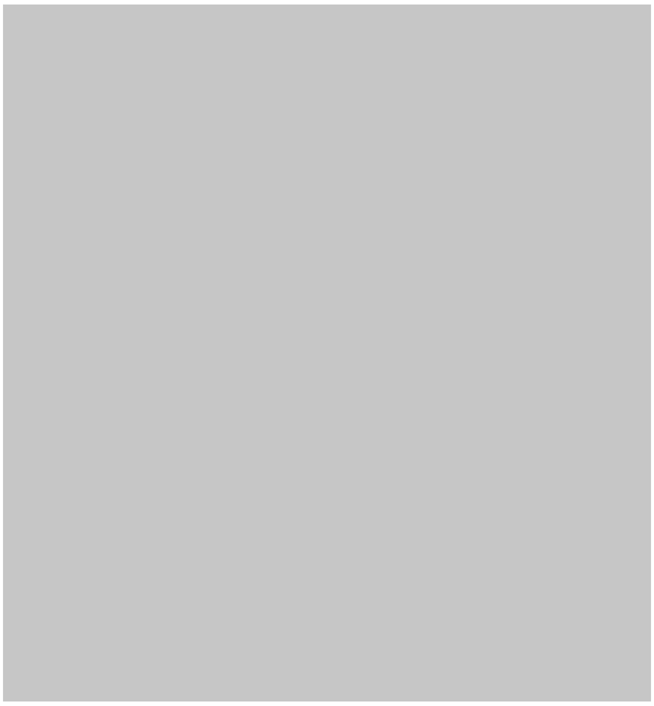

Figure A5.66. 89-60 BC. Bronze bow fitting from Phanagoria. Dated based on archaeological context (PopularArchaeology 2014).

Figure A5.67. 47-43 BC. Coin issued by the king of Bosporus. Dated based on the mint's issuance of the king's coins (Wildwinds 2015).

Figure A5.68. 100-63 BC. Coin of Mithradates VI. Dated based on the mint issuing coins under the king (WildWinds 2015).

Figure A5.69. 100-50 BC. Relief from Palestrina currently in the Vatican Museum. Dated stylistically (Torr 1895).

50-0 BC

Figure A5.70. 31 BC. Preveza boat-fitting, a Roman proembolion found off Actium during the 19th century. Dated based on the likelihood that it dates to the battle (Courtesy of the British Museum).

Figure A5.71. After 31 BC. Marble fragment from the Actium monument. Dated based on archaeological context (Varoufakis 2007).

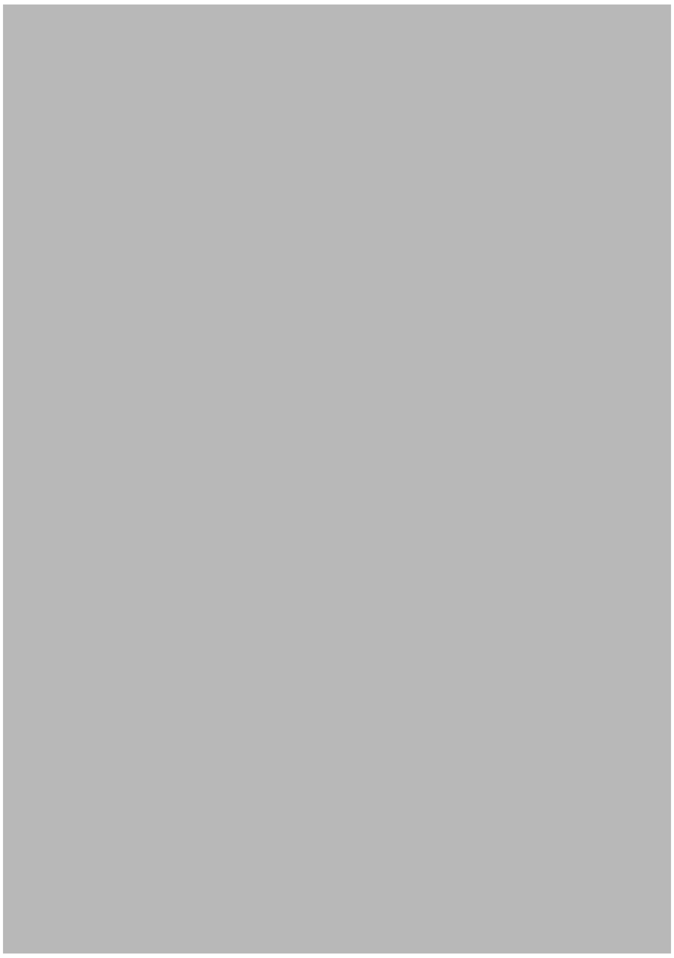

Figure A5.72. After 31 BC. Artistic rendering of the Actium monument. Reconstructed and dated based on archaeological evidence (Murray 2012).

Figure A5.73. After 31 BC. Medinaceli Relief depicting the Battle of Actium. Dated stylistically (Anderson 2013).

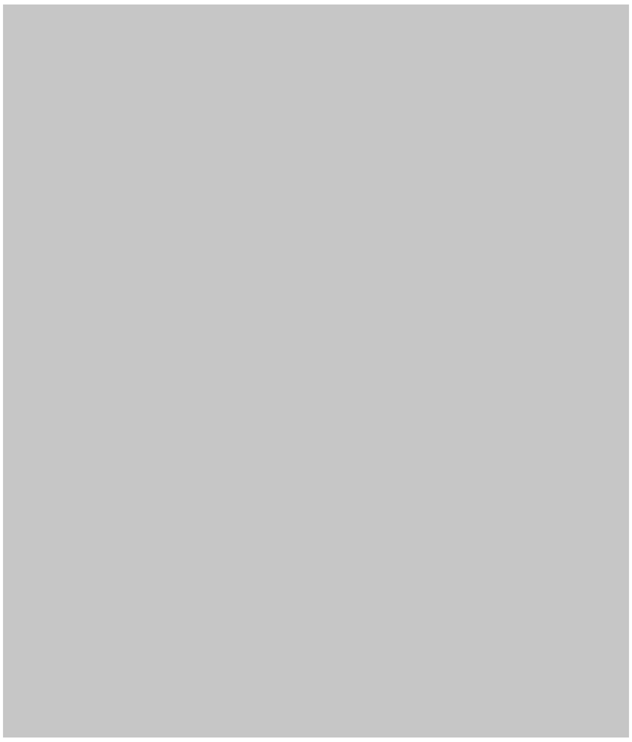

Figure A5.73. Estimated as 1st century BC. Bronze bow fitting. Dated stylistically (Christie's 2004b).

0-100 AD

Figure A5.74. 30 AD. New Capitoline Museum, Rome. Dated stylistically (Göttlicher 1978: 82 n. 492, plate 39).

Figure A5.75. 1st century AD. Ship model found at Aquileia. Dated stylistically (Göttlicher 1978: 83 n. 497, plate 39).

Figure A5.76. 1st century AD. Aquileia Museum Qintus Caelius monument. Dated stylistically (Göttlicher 1978: 81 n. 482, plate 36).

Figure A5.77. 120 AD. Cup from Beth-Marē, Syria. Dated based on archaeological context (Göttlicher 1978: 84 n. 505, plate 40).

Figure A5.78. 2nd century AD. Votive model in the British Museum 56.7-1.29. Dated stylistically (Göttlicher 1978: 85 n. 507, plate 40).

Figure A5.79. 161 AD. Darstellung Relief. Dated based on its inscription (Göttlicher 1978: 85 n. 510, plate 40).

Figure A5.80. 180 AD. Bow fitting in the Trier Museum. Dated based on its inscription (Göttlicher 1978: 82, n. 491, plate 38; Landesmuseum Trier Nr. 62.8).

Figure A5.81. 2nd century AD. Bronze lamp in the form of a ship from Crete. Dated stylistically (Göttlicher 1978: 88 n. 523, plate 42).

Figure A5.82. 2nd century. Fresco of fishermen. Dated based on archaeological context (Casson 1996: 86).

Figure A5.83. 113 AD. Ship scene from Trajan column showing an aphract trireme in the background and a liburnian in the foreground. In situ archaeological context (Morrison 1995: 72).

Figure A5.84. 3rd or 4th century AD. Althiburus mosaic. Dated stylistically (Casson 1995: 135, ill. 137).

324 AD. First pitched battle since Actium fought at Propontis. Ramming becomes secondary or non-existent compared to boarding action, projectiles, and Greek fire (Emanuele 1974: 37-38).

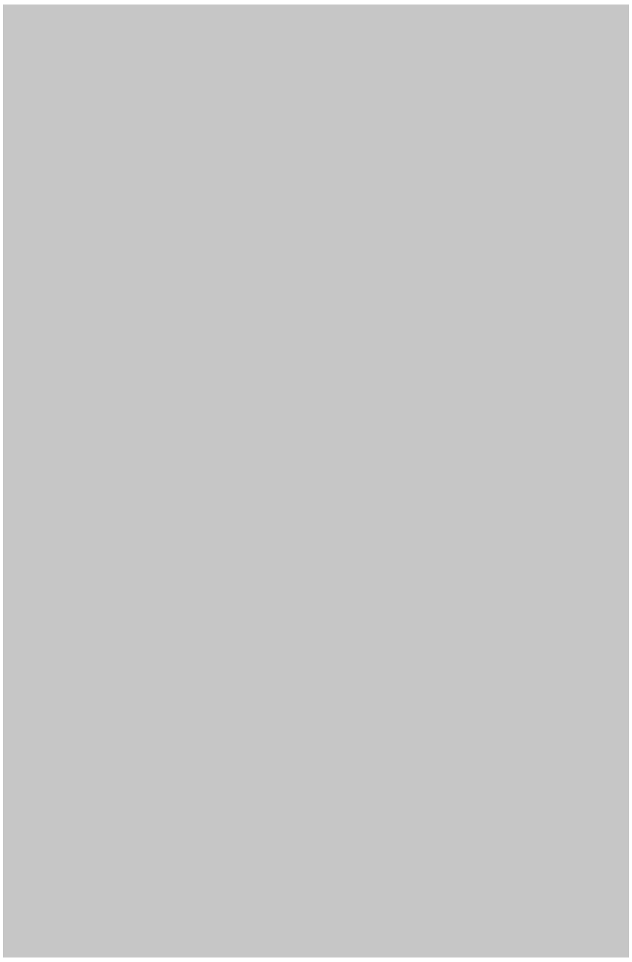

Figure A5.85. 600-1000 AD. Four Yenikapi galleys. Dated based on archaeological context (Pulak 2007a, 2007b; Kocabas 2008).

Appendix 6: Hull Analysis

$$Coefficient\,of\,fineness(C_w) = \frac{Area\,of\,water-plane}{Area\,of\,rectangle\,ABCD}$$

$$= \frac{Area\,of\,water-plane}{L \times B}$$

$$\therefore Area\,of\,water-plane = L \times B \times C_w$$

Figures showing the method of calculating the Coefficient of fineness (Cw) (Tupper and Rawson 2001:12). The following calculation were made using the software RhinoMarine by inputting 3D models of ships build in Rhinoceros NURBS using published lines plans.

Kyrenia

The lines plans used for the Kyrenia analysis were taken from Steffy (1985:100).

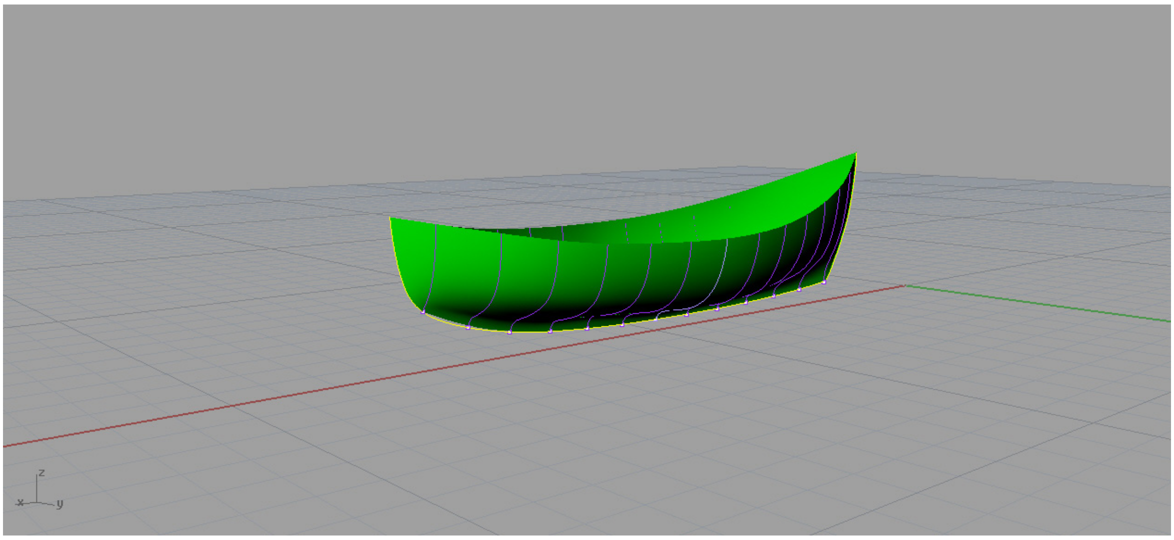

Condition Summary

Load Condition Parameters

Condition	Weight / Sinkage	LCG / Trim	TCG / Heel	VCG (m)
Condition 1	0.500 m	0.000 deg	0.000 deg	None available
Condition 2	0.750 m	0.000 deg	0.000 deg	None available
Condition 3	1.000 m	0.000 deg	0.000 deg	None available
Condition 4	1.250 m	0.000 deg	0.000 deg	None available
Condition 5	1.500 m	0.000 deg	0.000 deg	None available
Condition 6	2.000 m	0.000 deg	0.000 deg	None available

Resulting Model Attitude and Hydrostatic Properties

Condition	Sinkage (m)	Trim(deg)	Heel(deg)	Ax(m^2)
Condition 1	0.500	0.000	0.000	0.00
Condition 2	0.750	0.000	0.000	0.00
Condition 3	1.000	0.000	0.000	0.00
Condition 4	1.250	0.000	0.000	0.00
Condition 5	1.500	0.000	0.000	0.00
Condition 6	2.000	0.000	0.000	0.00

Condition	Displacement Weight (kgf)	LCB(m)	TCB(m)	VCB(m)	Wet Area (m^2)
Condition 1	2516.603	9.600	-0.013	0.388	19.548
Condition 2	7813.880	9.767	-0.008	0.555	31.130
Condition 3	15096.341	9.853	-0.006	0.712	40.386
Condition 4	23685.787	9.903	-0.005	0.862	48.508
Condition 5	33136.508	9.929	-0.005	1.009	56.172
Condition 6	53585.846	9.943	-0.004	1.293	71.165

Condition	Awp(m^2)	LCF(m)	TCF(m)	VCF(m)
Condition 1	15.603	9.750	-0.009	0.500
Condition 2	25.063	9.901	-0.005	0.750
Condition 3	31.307	9.974	-0.004	1.000
Condition 4	35.397	9.995	-0.003	1.250
Condition 5	38.130	9.987	-0.003	1.500
Condition 6	41.155	9.946	-0.003	2.000

Condition	BMt(m)	BMl(m)	GMt(m)	GMl(m)
Condition 1	2.338	29.266	None Available	None Available
Condition 2	2.007	22.135	None Available	None Available
Condition 3	1.648	17.357	None Available	None Available
Condition 4	1.372	13.773	None Available	None Available

Condition 5	1.159	11.194	None Available	None Available
Condition 6	0.847	7.934	None Available	None Available

Condition	Cb	Cp	Cwp	Cx	Cws	Cvp
Condition 1	0.160	0.000	0.508	0.000	3.669	0.314
Condition 2	0.248	0.000	0.612	0.000	3.202	0.405
Condition 3	0.306	0.000	0.652	0.000	2.914	0.470
Condition 4	0.351	0.000	0.672	0.000	2.761	0.522
Condition 5	0.385	0.000	0.682	0.000	2.680	0.565
Condition 6	0.436	0.000	0.687	0.000	2.638	0.635

Notes

1. Locations such as the center of buoyancy and center of flotation are measured from the origin in the Rhinoceros world coordinate system.

2. The orientation of the model for an Orca3D hydrostatics solution is defined in terms of “sinkage,” “trim,” and “heel.” The sinkage value represents the depth of the body origin (i.e. the Rhino world origin) below the resultant flotation plane, and is sometimes referred to as "origin depth." Heel and trim represent angular rotations about the Rhino longitudinal and transverse axes, respectively, and are taken in that order. For a more detailed description of these terms see the Orca3D documentation.

3. Hull form coefficients are non-dimensionalized by the waterline length.

4. Calculation of Cp and Cx use Orca sections to determine Ax. If no Orca sections are defined, these values will be reported as zero.

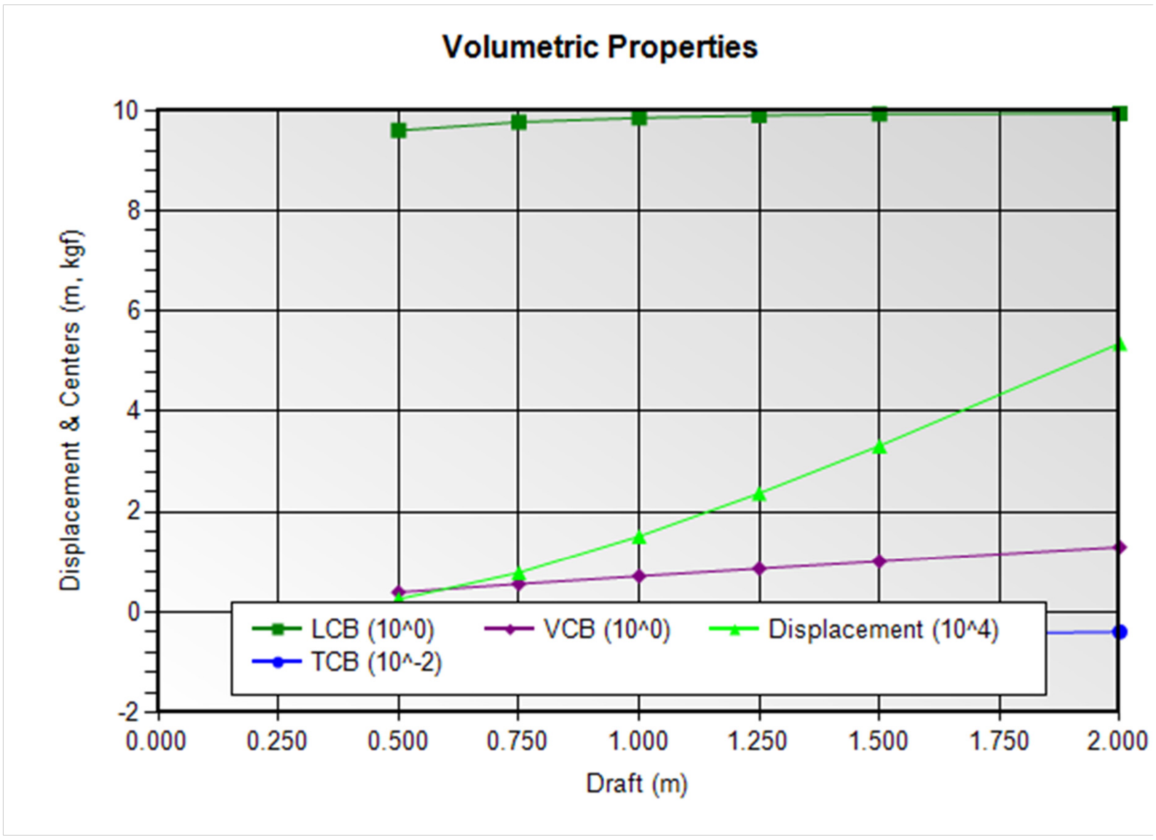
Volumetric Properties
Displacement & Centers (m, kgf)
Draft (m)
LCB (10^0)
VCB (10^0)
Displacement (10^4)
TCB (10^-2)
10
8
6
4
2
0
-2
0.000
0.250
0.500
0.750
1.000
1.250
1.500
1.750
2.000

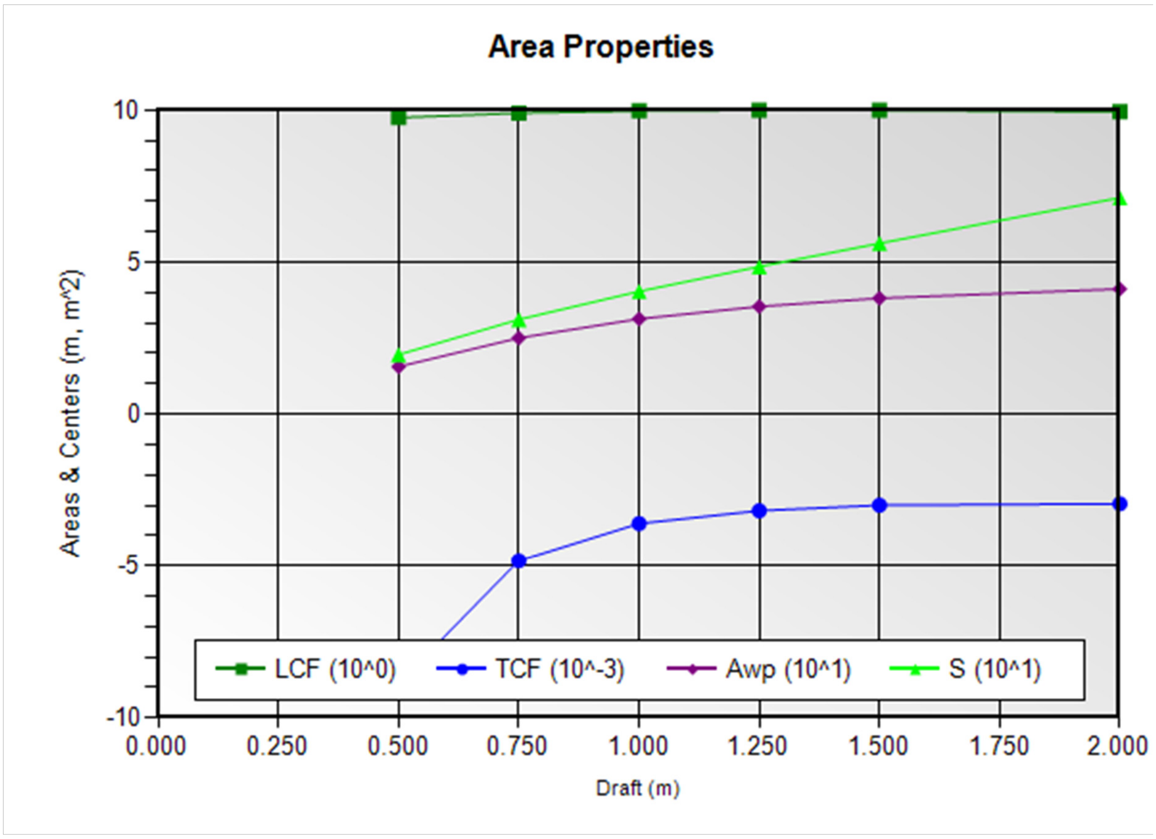
Area Properties
Areas & Centers (m, m^2)
Draft (m)
LCF (10^0)
TCF (10^-3)
Awp (10^1)
S (10^1)
10
5
0
-5
-10
0.000
0.250
0.500
0.750
1.000
1.250
1.500
1.750
2.000

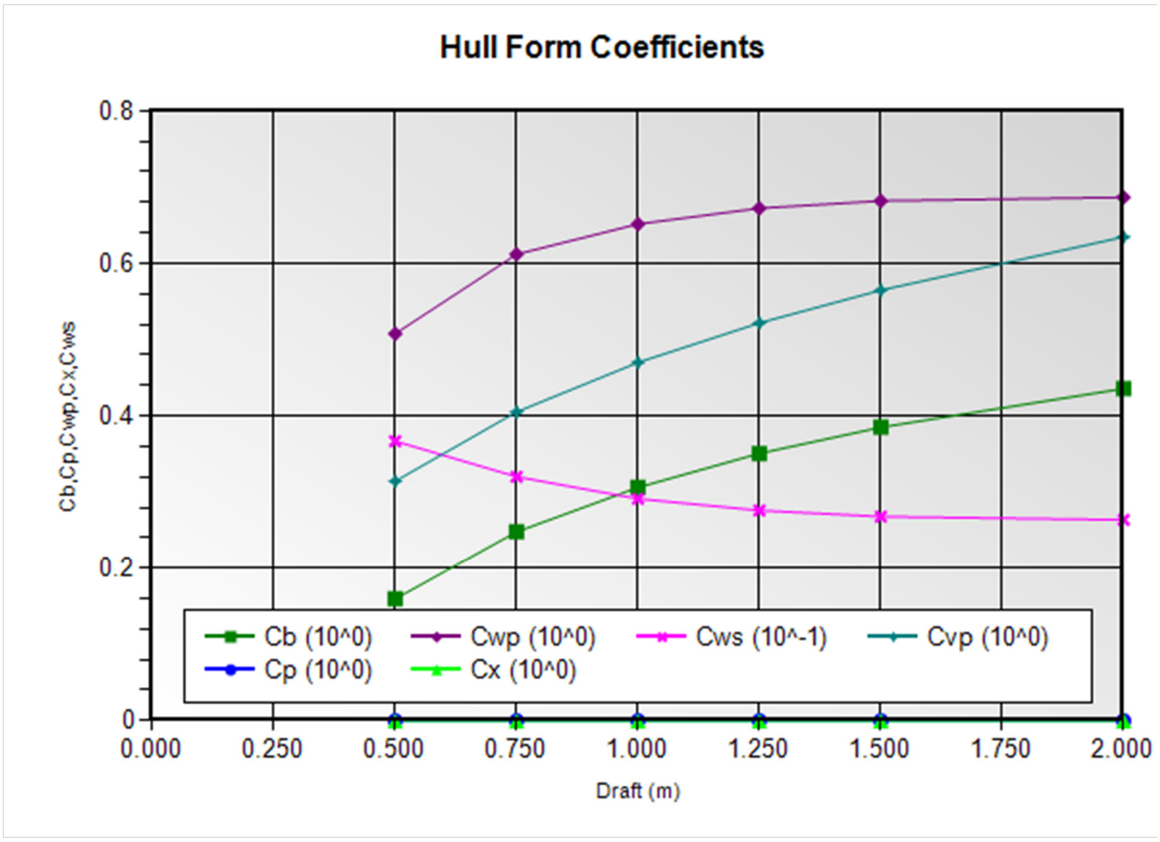
Hull Form Coefficients
0.8
0.6
0.4
0.2
0
Cb,Cp,Cwp,Cx,Cws
Cb (10^0)
Cwp (10^0)
Cws (10^-1)
Cvp (10^0)
Cp (10^0)
Cx (10^0)
0.000
0.250
0.500
0.750
1.000
1.250
1.500
1.750
2.000
Draft (m)

Condition Name=Condition 1,Model Sinkage=0.50,Model Trim=0.00,Model Heel=0.00

General Info

Analysis Type	FixedFlotationPlane	Up Direction = Positive_Z
		Fwd Direction = Negative_X

Surface Meshing Parameters

Density	1	Minimum edge length	0.0001 m
Maximum angle	0	Maximum edge length	0 m
Maximum aspect ratio	0	Max distance, edge to surf.	0 m
Minimum initial grid quads	0	Jagged seams	False
Refine mesh	True	Simple planes	True

Load Condition Parameters

Model Sinkage	0.500 m
Model Trim	0.000 deg
Model Heel	0.000 deg
VCG	None available m
Fluid Type	Seawater
Fluid Density	1025.900 kg/m^3
Mirror Geometry	False

Resultant Model Attitude

Heel Angle	0.000 deg	Sinkage	0.500 m
Trim Angle	0.000 deg		

Overall Dimensions

Length Overall, LOA	14.286 m	Loa / Boa	3.315
Beam Overall, Boa	4.309 m	Boa / D	1.198
Depth Overall, D	3.596 m		

Waterline Dimensions

Waterline Length, Lwl	11.574 m	Lwl / Bwl	4.359
Waterline Beam, Bwl	2.655 m	Bwl / T	5.310
Navigational Draft, T	0.500 m	D / T	7.193

Volumetric Values

Displacement Weight	2516.603 kgf	Displ-Length Ratio			45.233
Volume	2.453 m^3				
LCB	9.600 m	FB/Lwl	0.523	AB/Lwl	0.477
TCB	-0.013 m	TCB / Bwl			-0.005
VCB	0.388 m				
Wetted Surface Area	19.548 m^2				
Moment To Trim	63.632 kgf-m/cm				

Waterplane Values

Waterplane Area, Awp	15.603	m^2				
LCF	9.750	m	FF/Lwl	0.536	AF/Lwl	0.464
TCF	-0.009	m	TCF / Lwl			-0.001
Weight To Immerse	160.071	kgf/cm				

Sectional Parameters

Ax	0.000	m^2		
Ax Location	0.000	m	Ax Location / Lwl	0.000

Hull Form Coefficients

Cb	0.160	Cx	0.000
Cp	0.000	Cwp	0.508
Cvp	0.314	Cws	3.669

Static Stability Parameters

I(transverse)	5.736	m^4	I(longitudinal)	71.791	m^4
BMt	2.338	m	BMl	29.266	m
GMt	None Available	m	GMl	None Available	m
Mt	2.226	m	Ml	29.154	m

Saint Gervais 3

The Saint Gervais 3 lines plans drawn by Robert Roman and published in Liou and Gassend 1990:262).

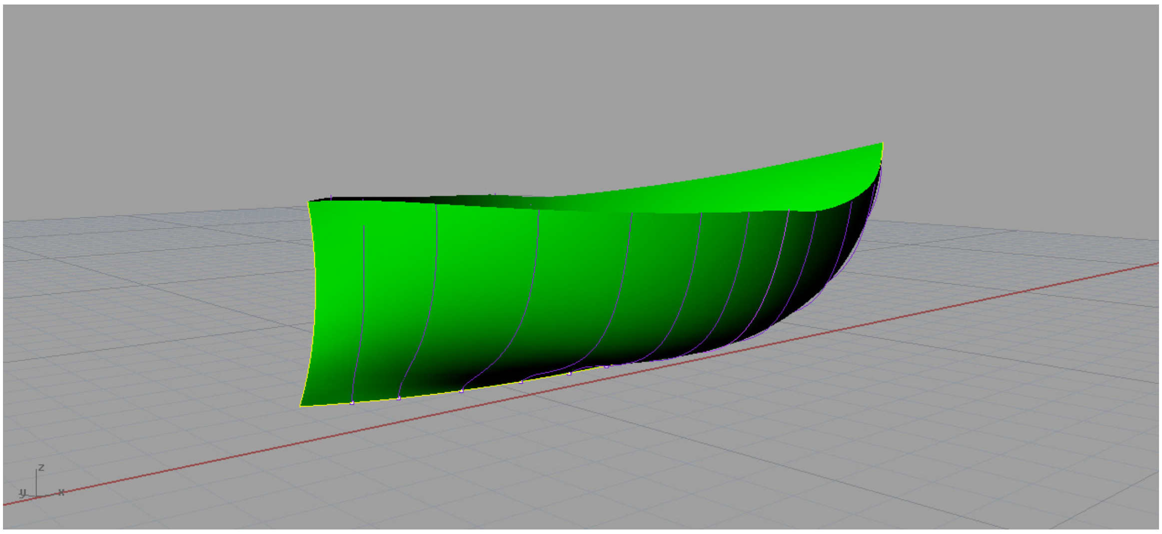

Condition Summary

Load Condition Parameters

Condition	Weight / Sinkage	LCG / Trim	TCG / Heel	VCG (m)
Condition 6	3.000 m	0.000 deg	0.000 deg	None available
Condition 5	2.600 m	0.000 deg	0.000 deg	None available
Condition 4	2.200 m	0.000 deg	0.000 deg	None available
Condition 3	1.750 m	0.000 deg	0.000 deg	None available
Condition 2	1.300 m	0.000 deg	0.000 deg	None available
Condition 1	1.000 m	0.000 deg	0.000 deg	None available

Resulting Model Attitude and Hydrostatic Properties

Condition	Sinkage (m)	Trim(deg)	Heel(deg)	Ax(m^2)
Condition 6	3.000	0.000	0.000	0.00
Condition 5	2.600	0.000	0.000	0.00
Condition 4	2.200	0.000	0.000	0.00
Condition 3	1.750	0.000	0.000	0.00
Condition 2	1.300	0.000	0.000	0.00
Condition 1	1.000	0.000	0.000	0.00

Condition	Displacement Weight (kgf)	LCB(m)	TCB(m)	VCB(m)	Wet Area (m^2)
Condition 6	-151474.958	12.864	0.000	1.872	127.256
Condition 5	-121487.782	12.775	0.000	1.643	112.653
Condition 4	-92988.674	12.670	0.000	1.410	98.007
Condition 3	-63347.824	12.527	0.001	1.144	81.302
Condition 2	-37214.847	12.351	0.002	0.872	63.912
Condition 1	-22451.217	12.204	0.003	0.686	51.366

Condition	Awp(m^2)	LCF(m)	TCF(m)	VCF(m)
Condition 6	-74.541	13.267	-0.001	3.000
Condition 5	-71.449	13.176	-0.001	2.600
Condition 4	-67.252	13.056	-0.001	2.200
Condition 3	-60.831	12.880	-0.001	1.750
Condition 2	-51.888	12.658	0.000	1.300
Condition 1	-43.715	12.472	0.000	1.000

Condition	BMt(m)	BMl(m)	GMt(m)	GMl(m)
Condition 6	1.484	6.196	None Available	None Available
Condition 5	1.688	7.139	None Available	None Available
Condition 4	1.941	8.313	None Available	None Available
Condition 3	2.321	10.045	None Available	None Available

Condition 2	2.872	12.546	None Available	None Available
Condition 1	3.379	14.951	None Available	None Available

Condition	Cb	Cp	Cwp	Cx	Cws	Cvp
Condition 6	-0.421	0.000	-0.637	0.000	NaN	0.660
Condition 5	-0.406	0.000	-0.637	0.000	NaN	0.638
Condition 4	-0.389	0.000	-0.635	0.000	NaN	0.613
Condition 3	-0.363	0.000	-0.626	0.000	NaN	0.580
Condition 2	-0.326	0.000	-0.606	0.000	NaN	0.538
Condition 1	-0.292	0.000	-0.583	0.000	NaN	0.501

Notes

1. Locations such as the center of buoyancy and center of flotation are measured from the origin in the Rhinoceros world coordinate system.

2. The orientation of the model for an Orca3D hydrostatics solution is defined in terms of “sinkage,” “trim,” and “heel.” The sinkage value represents the depth of the body origin (i.e. the Rhino world origin) below the resultant flotation plane, and is sometimes referred to as "origin depth." Heel and trim represent angular rotations about the Rhino longitudinal and transverse axes, respectively, and are taken in that order. For a more detailed description of these terms see the Orca3D documentation.

3. Hull form coefficients are non-dimensionalized by the waterline length.

4. Calculation of Cp and Cx use Orca sections to determine Ax. If no Orca sections are defined, these values will be reported as zero.

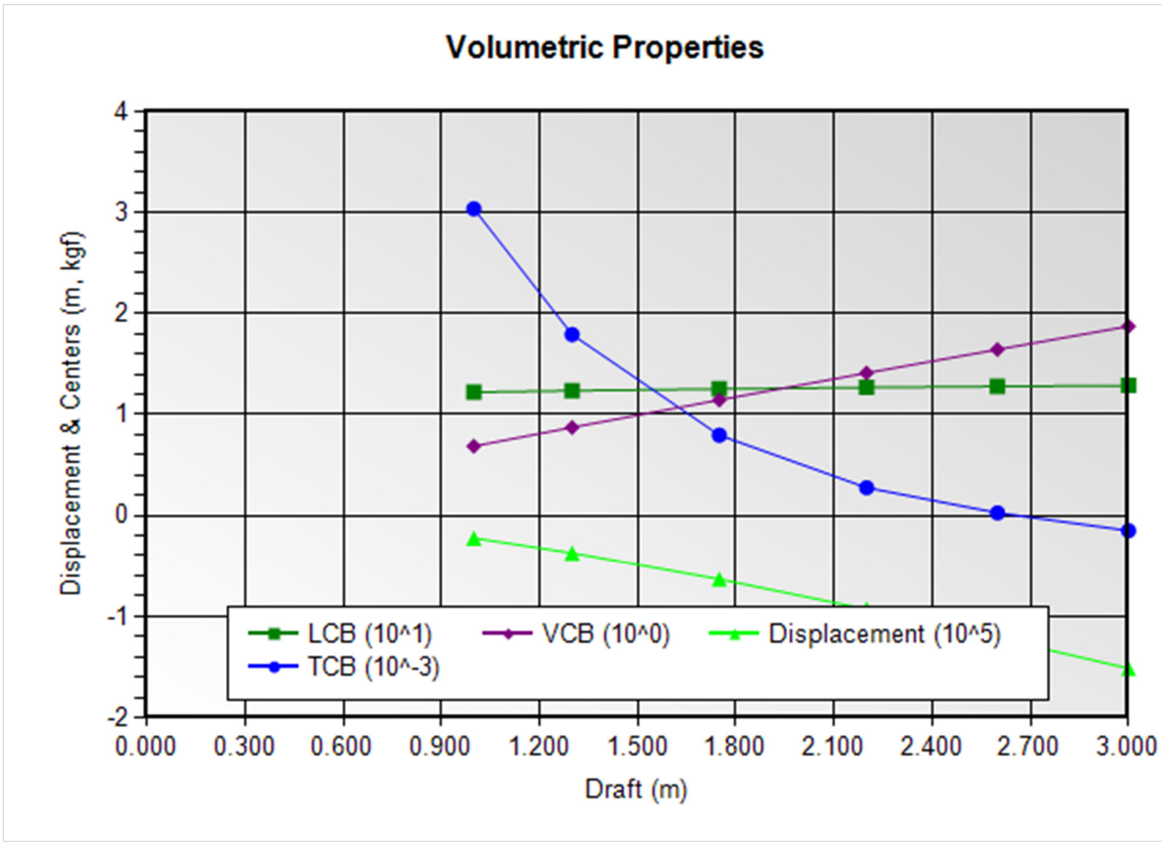
Volumetric Properties
Displacement & Centers (m, kgf)
Draft (m)
LCB (10^1)
VCB (10^0)
Displacement (10^5)
TCB (10^-3)
4
3
2
1
0
-1
-2
0.000
0.300
0.600
0.900
1.200
1.500
1.800
2.100
2.400
2.700
3.000

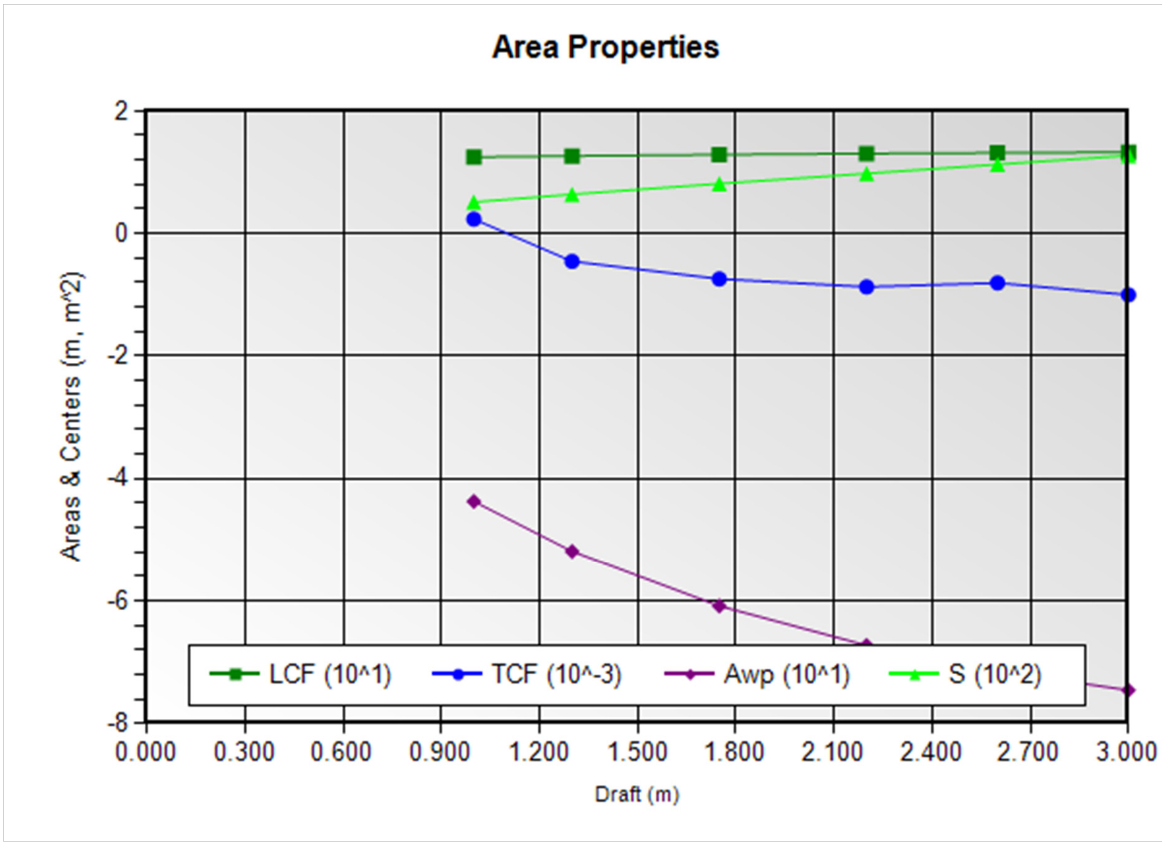
Area Properties
Areas & Centers (m, m^2)
Draft (m)
LCF (10^1)
TCF (10^-3)
Awp (10^1)
S (10^2)
2
0
-2
-4
-6
-8
0.000
0.300
0.600
0.900
1.200
1.500
1.800
2.100
2.400
2.700
3.000

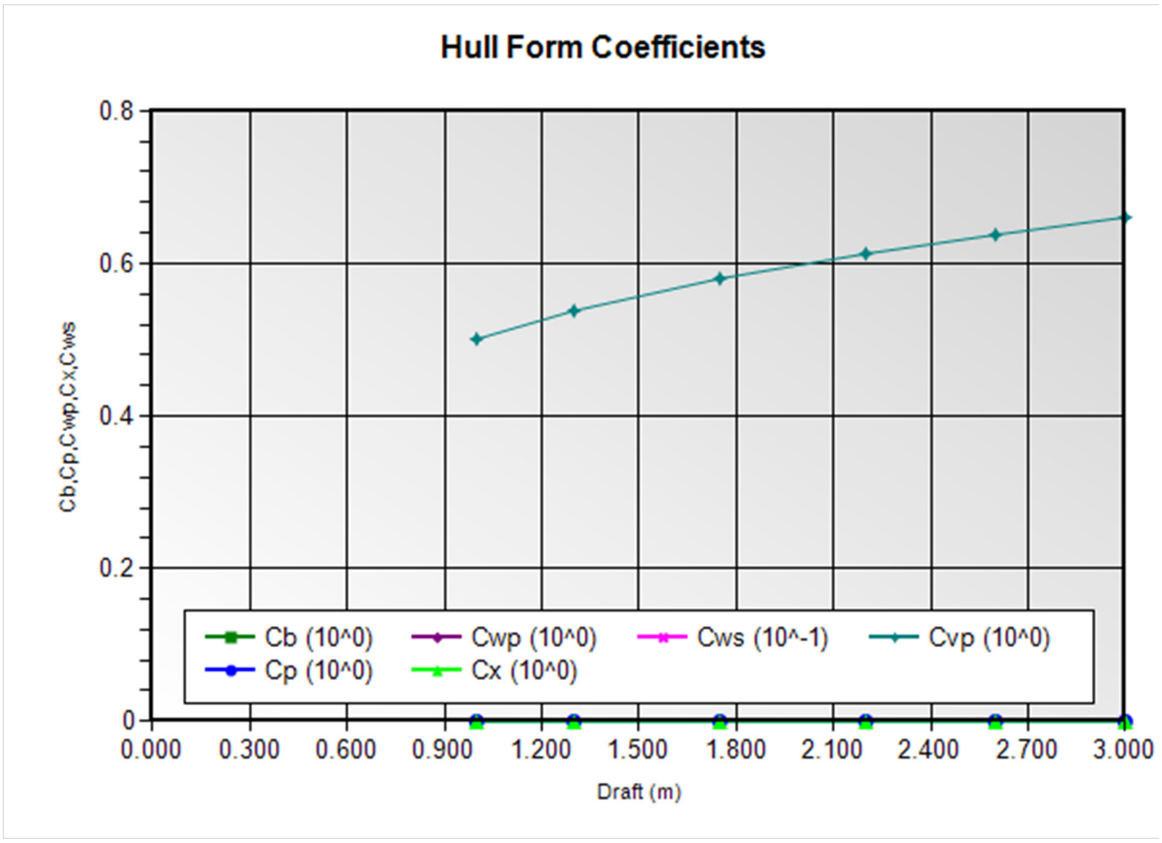
Hull Form Coefficients
0.8
0.6
0.4
0.2
0
Cb,Cp,Cwp,Cx,Cws
Cb (10^0)
Cwp (10^0)
Cws (10^-1)
Cvp (10^0)
Cp (10^0)
Cx (10^0)
0.000
0.300
0.600
0.900
1.200
1.500
1.800
2.100
2.400
2.700
3.000
Draft (m)

Condition Name=Condition 6,Model Sinkage=3.00,Model Trim=0.00,Model Heel=0.00

General Info

Analysis Type	FixedFlotationPlane	Up Direction = Positive_Z
		Fwd Direction = Negative_X

Surface Meshing Parameters

Density	1	Minimum edge length	0.0001 m
Maximum angle	0	Maximum edge length	0 m
Maximum aspect ratio	0	Max distance, edge to surf.	0 m
Minimum initial grid quads	0	Jagged seams	False
Refine mesh	True	Simple planes	True

Load Condition Parameters

Model Sinkage	3.000	m
Model Trim	0.000	deg
Model Heel	0.000	deg
VCG	None available	m
Fluid Type	Seawater	
Fluid Density	1025.900	kg/m^3
Mirror Geometry	False	

Resultant Model Attitude

Heel Angle	0.000 deg	Sinkage	3.000 m
Trim Angle	0.000 deg		

Overall Dimensions

Length Overall, LOA	16.798 m	Loa / Boa	2.265
Beam Overall, Boa	7.416 m	Boa / D	1.660
Depth Overall, D	4.467 m		

Waterline Dimensions

Waterline Length, Lwl	16.013 m	Lwl / Bwl	2.191
Waterline Beam, Bwl	7.307 m	Bwl / T	2.436
Navigational Draft, T	2.999 m	D / T	1.489

Volumetric Values

Displacement Weight	-151474.958 kgf	Displ-Length Ratio			-1028.081
Volume	-147.651 m^3				
LCB	12.864 m	FB/Lwl	0.463	AB/Lwl	0.537
TCB	0.000 m	TCB / Bwl			0.000
VCB	1.872 m				
Wetted Surface Area	127.256 m^2				
Moment To Trim	-586.144 kgf-m/cm				

Waterplane Values

Waterplane Area, Awp	-74.541 m^2				
LCF	13.267 m	FF/Lwl	0.488	AF/Lwl	0.512
TCF	-0.001 m	TCF / Lwl			0.000
Weight To Immerse	-764.720 kgf/cm				

Sectional Parameters

Ax	0.000 m^2		
Ax Location	0.000 m	Ax Location / Lwl	0.000

Hull Form Coefficients

Cb	-0.421	Cx	0.000
Cp	0.000	Cwp	-0.637
Cvp	0.660	Cws	NaN

Static Stability Parameters

I(transverse)	-219.100 m^4	I(longitudinal)	-914.916 m^4
BMt	1.484 m	BMl	6.196 m
GMt	None Available m	GMl	None Available m
Mt	0.356 m	Ml	5.069 m

Yassiada 7th century AD

The Yassiada 7th century AD lines plans were published in Steffy (2006: 81).

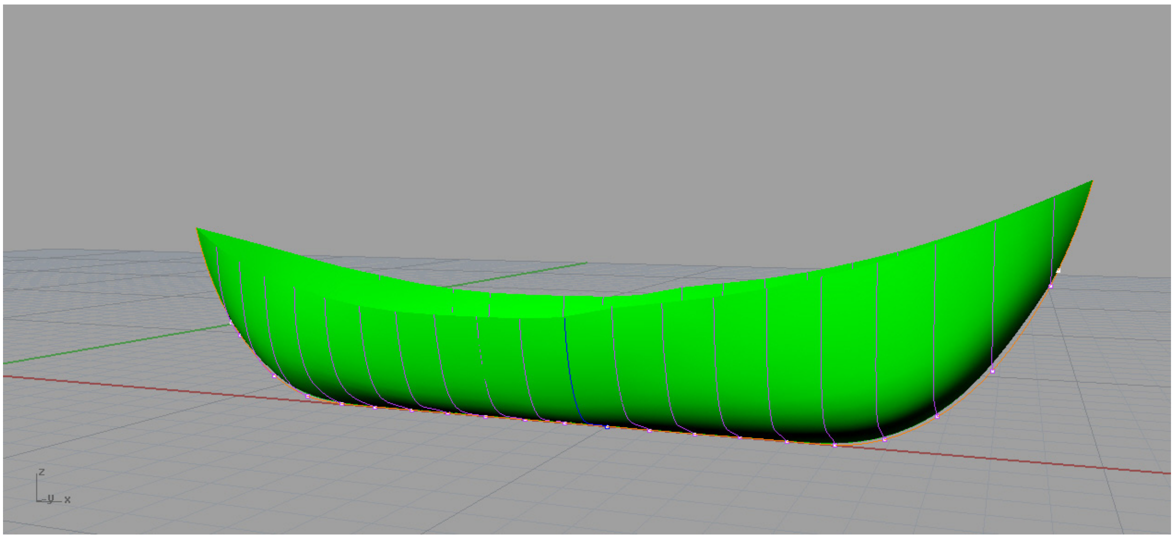

Condition Summary

Load Condition Parameters

Condition	Weight / Sinkage	LCG / Trim	TCG / Heel	VCG (m)
Condition 7	2.200 m	0.000 deg	0.000 deg	None available
Condition 6	2.000 m	0.000 deg	0.000 deg	None available
Condition 5	1.750 m	0.000 deg	0.000 deg	None available
Condition 4	1.400 m	0.000 deg	0.000 deg	None available
Condition 3	1.200 m	0.000 deg	0.000 deg	None available
Condition 2	0.700 m	0.000 deg	0.000 deg	None available
Condition 1	0.200 m	0.000 deg	0.000 deg	None available

Resulting Model Attitude and Hydrostatic Properties

Condition	Sinkage (m)	Trim(deg)	Heel(deg)	Ax(m^2)
Condition 7	2.200	0.000	0.000	0.00
Condition 6	2.000	0.000	0.000	0.00
Condition 5	1.750	0.000	0.000	0.00
Condition 4	1.400	0.000	0.000	0.00
Condition 3	1.200	0.000	0.000	0.00
Condition 2	0.700	0.000	0.000	0.00
Condition 1	0.200	0.000	0.000	0.00

Condition	Displacement Weight (kgf)	LCB(m)	TCB(m)	VCB(m)	Wet Area (m^2)
Condition 7	-108917.601	19.245	0.000	1.333	111.579
Condition 6	-94863.696	19.237	0.000	1.219	103.369
Condition 5	-77895.650	19.225	0.000	1.076	93.145
Condition 4	-55509.867	19.200	0.000	0.874	78.844
Condition 3	-43598.725	19.179	0.000	0.757	70.611
Condition 2	-17677.787	19.080	0.000	0.459	48.822
Condition 1	-1429.671	18.872	0.000	0.136	15.758

Condition	Awp(m^2)	LCF(m)	TCF(m)	VCF(m)
Condition 7	-69.418	19.306	0.000	2.200
Condition 6	-67.523	19.297	0.000	2.000
Condition 5	-64.715	19.289	0.000	1.750
Condition 4	-59.766	19.280	0.000	1.400
Condition 3	-56.248	19.271	0.000	1.200
Condition 2	-43.634	19.198	0.000	0.700
Condition 1	-14.896	18.877	0.000	0.200

Condition	BMt(m)	BMl(m)	GMt(m)	GMl(m)
Condition 7	0.929	14.094	None Available	None Available
Condition 6	1.003	15.408	None Available	None Available
Condition 5	1.112	17.419	None Available	None Available
Condition 4	1.305	21.297	None Available	None Available
Condition 3	1.448	24.445	None Available	None Available
Condition 2	1.962	39.674	None Available	None Available
Condition 1	1.339	121.232	None Available	None Available

Condition	Cb	Cp	Cwp	Cx	Cws	Cvp
Condition 7	-0.545	0.000	-0.785	0.000	NaN	0.695
Condition 6	-0.540	0.000	-0.790	0.000	NaN	0.684
Condition 5	-0.533	0.000	-0.796	0.000	NaN	0.670
Condition 4	-0.521	0.000	-0.806	0.000	NaN	0.646
Condition 3	-0.509	0.000	-0.810	0.000	NaN	0.629
Condition 2	-0.447	0.000	-0.794	0.000	NaN	0.563
Condition 1	-0.337	0.000	-0.727	0.000	NaN	0.465

Notes

1. Locations such as the center of buoyancy and center of flotation are measured from the origin in the Rhinoceros world coordinate system.

2. The orientation of the model for an Orca3D hydrostatics solution is defined in terms of “sinkage,” “trim,” and “heel.” The sinkage value represents the depth of the body origin (i.e. the Rhino world origin) below the resultant flotation plane, and is sometimes referred to as "origin depth." Heel and trim represent angular rotations about the Rhino longitudinal and transverse axes, respectively, and are taken in that order. For a more detailed description of these terms see the Orca3D documentation.

3. Hull form coefficients are non-dimensionalized by the waterline length.

4. Calculation of Cp and Cx use Orca sections to determine Ax. If no Orca sections are defined, these values will be reported as zero.

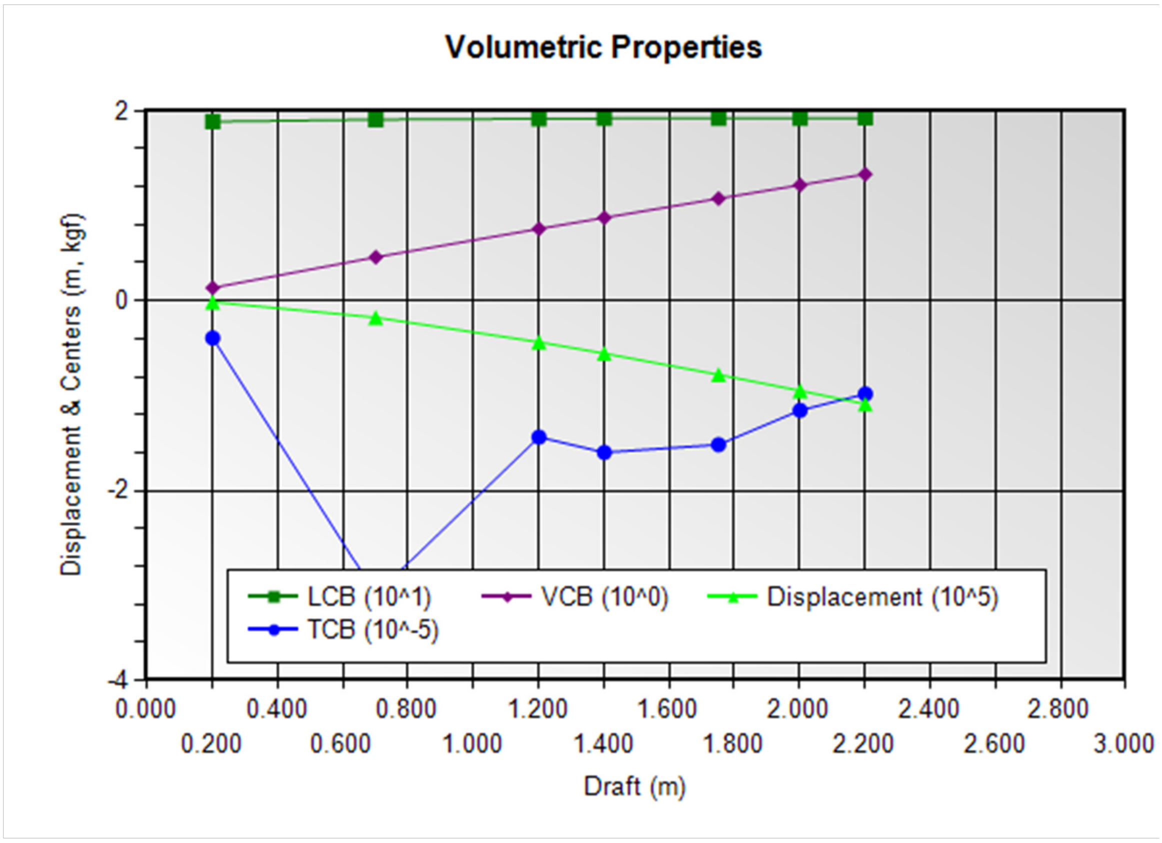
Volumetric Properties
Displacement & Centers (m, kgf)
2
0
-2
-4
0.000
0.200
0.400
0.600
0.800
1.000
1.200
1.400
1.600
1.800
2.000
2.200
2.400
2.600
2.800
3.000
Draft (m)
LCB (10^1)
VCB (10^0)
Displacement (10^5)
TCB (10^-5)

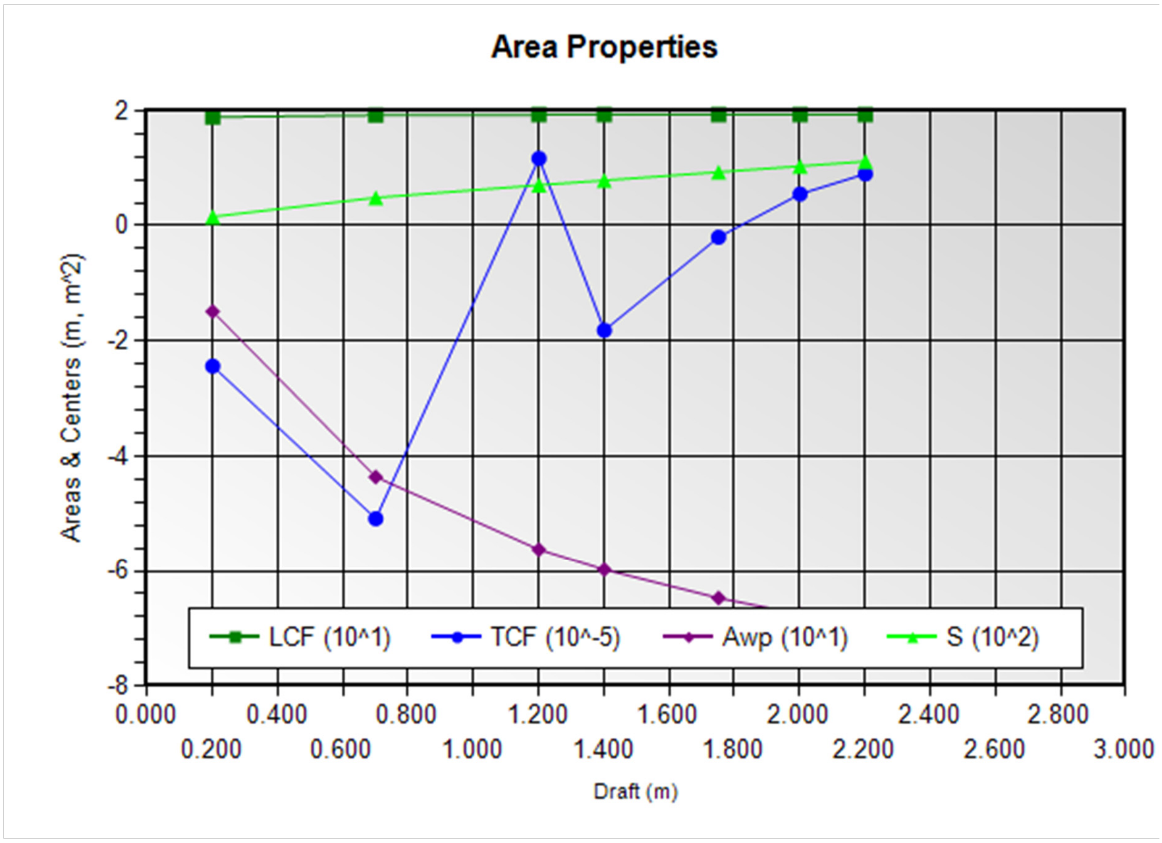
Area Properties
Areas & Centers (m, m^2)
2
0
-2
-4
-6
-8
0.000
0.200
0.400
0.600
0.800
1.000
1.200
1.400
1.600
1.800
2.000
2.200
2.400
2.600
2.800
3.000
Draft (m)
LCF (10^1)
TCF (10^-5)
Awp (10^1)
S (10^2)

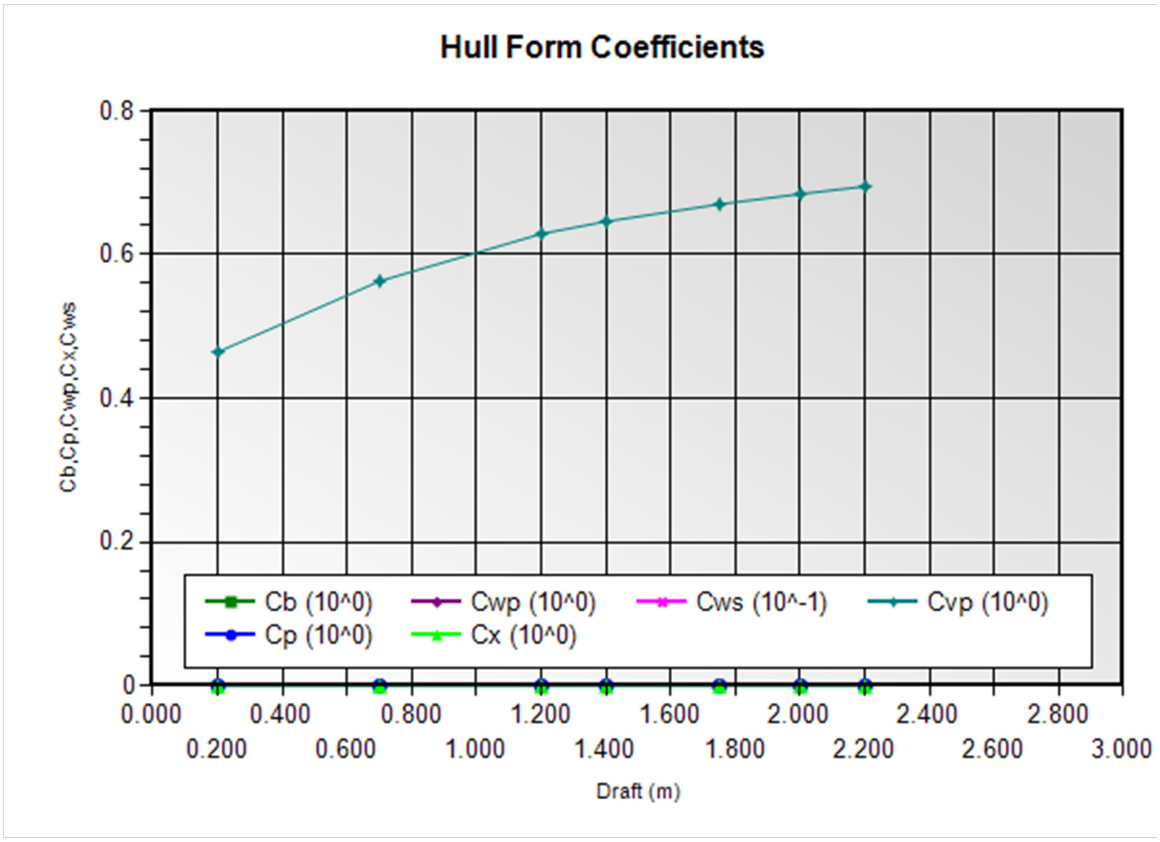
Hull Form Coefficients
Cb,Cp,Cwp,Cx,Cws
0.8
0.6
0.4
0.2
0
Cb (10^0)
Cwp (10^0)
Cws (10^-1)
Cvp (10^0)
Cp (10^0)
Cx (10^0)
0.000
0.400
0.800
1.200
1.600
2.000
2.400
2.800
0.200
0.600
1.000
1.400
1.800
2.200
2.600
3.000
Draft (m)

Condition Name=Condition 7,Model Sinkage=2.20,Model Trim=0.00,Model Heel=0.00

General Info

Analysis Type	FixedFlotationPlane	Up Direction = Positive_Z
		Fwd Direction = Negative_X

Surface Meshing Parameters

Density	1	Minimum edge length	0.0001 m
Maximum angle	0	Maximum edge length	0 m
Maximum aspect ratio	0	Max distance, edge to surf.	0 m
Minimum initial grid quads	0	Jagged seams	False
Refine mesh	True	Simple planes	True

Load Condition Parameters

Model Sinkage	2.200 m
Model Trim	0.000 deg
Model Heel	0.000 deg
VCG	None available m
Fluid Type	Seawater
Fluid Density	1025.900 kg/m^3
Mirror Geometry	False

Resultant Model Attitude

Heel Angle	0.000 deg	Sinkage	2.200 m
Trim Angle	0.000 deg		

Overall Dimensions

Length Overall, LOA	20.886 m	Loa / Boa	4.238
Beam Overall, Boa	4.929 m	Boa / D	0.910
Depth Overall, D	5.415 m		

Waterline Dimensions

Waterline Length, Lwl	18.587 m	Lwl / Bwl	3.906
Waterline Beam, Bwl	4.758 m	Bwl / T	2.161
Navigational Draft, T	2.201 m	D / T	2.460

Volumetric Values

Displacement Weight	-108917.601 kgf	Displ-Length Ratio			-472.692
Volume	-106.168 m^3				
LCB	19.245 m	FB/Lwl	0.517	AB/Lwl	0.483
TCB	0.000 m	TCB / Bwl			0.000
VCB	1.333 m				
Wetted Surface Area	111.579 m^2				
Moment To Trim	-825.903 kgf-m/cm				

Waterplane Values

Waterplane Area, Awp	-69.418	m^2				
LCF	19.306	m	FF/Lwl	0.521	AF/Lwl	0.479
TCF	0.000	m	TCF / Lwl			0.000
Weight To Immerse	-712.161	kgf/cm				

Sectional Parameters

Ax	0.000	m^2		
Ax Location	0.000	m	Ax Location / Lwl	0.000

Hull Form Coefficients

Cb	-0.545	Cx	0.000
Cp	0.000	Cwp	-0.785
Cvp	0.695	Cws	NaN

Static Stability Parameters

I(transverse)	-98.610	m^4	I(longitudinal)	-1496.377	m^4
BMt	0.929	m	BMl	14.094	m
GMt	None Available	m	GMl	None Available	m
Mt	0.062	m	Ml	13.227	m

Serce Limani

Reconstruction of the Serce Limani shipwreck from Steffy 2006: fig. 4.9.

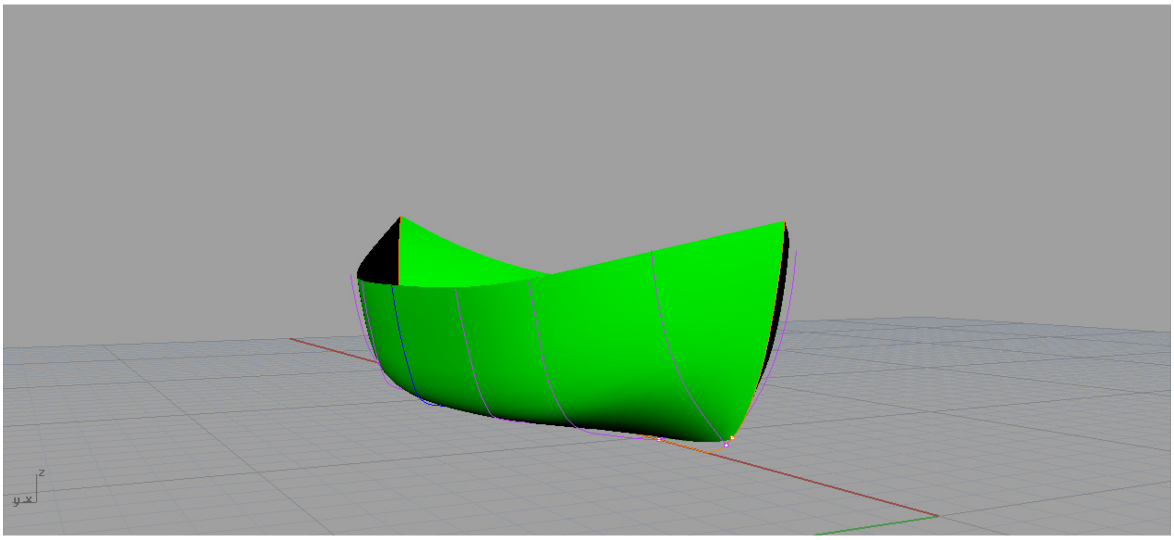

Condition Summary

Load Condition Parameters

Condition	Weight / Sinkage	LCG / Trim	TCG / Heel	VCG (m)
Condition 5	2.500 m	0.000 deg	0.000 deg	None available
Condition 4	2.000 m	0.000 deg	0.000 deg	None available
Condition 3	1.500 m	0.000 deg	0.000 deg	None available
Condition 2	1.000 m	0.000 deg	0.000 deg	None available
Condition 1	0.400 m	0.000 deg	0.000 deg	None available

Resulting Model Attitude and Hydrostatic Properties

Condition	Sinkage (m)	Trim(deg)	Heel(deg)	Ax(m^2)
Condition 5	2.500	0.000	0.000	0.00
Condition 4	2.000	0.000	0.000	0.00
Condition 3	1.500	0.000	0.000	0.00
Condition 2	1.000	0.000	0.000	0.00
Condition 1	0.400	0.000	0.000	0.00

Condition	Displacement Weight (kgf)	LCB(m)	TCB(m)	VCB(m)	Wet Area (m^2)
Condition 5	-312890.996	17.485	0.005	1.400	226.551
Condition 4	-236893.496	17.500	0.006	1.127	198.734
Condition 3	-164645.060	17.515	0.008	0.853	170.882
Condition 2	-97430.676	17.535	0.009	0.576	142.062
Condition 1	-28067.894	17.592	0.014	0.239	100.009

Condition	Awp(m^2)	LCF(m)	TCF(m)	VCF(m)
Condition 5	-151.372	17.422	0.001	2.500
Condition 4	-144.770	17.451	0.002	2.000
Condition 3	-136.569	17.475	0.004	1.500
Condition 2	-124.615	17.496	0.006	1.000
Condition 1	-96.655	17.537	0.010	0.400

Condition	BMt(m)	BMl(m)	GMt(m)	GMl(m)
Condition 5	2.093	17.140	None Available	None Available
Condition 4	2.494	21.005	None Available	None Available
Condition 3	3.177	27.069	None Available	None Available
Condition 2	4.482	38.123	None Available	None Available
Condition 1	9.651	78.685	None Available	None Available

Condition	Cb	Cp	Cwp	Cx	Cws	Cvp
Condition 5	-0.597	0.000	-0.741	0.000	NaN	0.806
Condition 4	-0.589	0.000	-0.739	0.000	NaN	0.798
Condition 3	-0.573	0.000	-0.731	0.000	NaN	0.783
Condition 2	-0.542	0.000	-0.711	0.000	NaN	0.762
Condition 1	-0.454	0.000	-0.641	0.000	NaN	0.708

Notes

1. Locations such as the center of buoyancy and center of flotation are measured from the origin in the Rhinoceros world coordinate system.

2. The orientation of the model for an Orca3D hydrostatics solution is defined in terms of “sinkage,” “trim,” and “heel.” The sinkage value represents the depth of the body origin (i.e. the Rhino world origin) below the resultant flotation plane, and is sometimes referred to as "origin depth." Heel and trim represent angular rotations about the Rhino longitudinal and transverse axes, respectively, and are taken in that order. For a more detailed description of these terms see the Orca3D documentation.

3. Hull form coefficients are non-dimensionalized by the waterline length.

4. Calculation of Cp and Cx use Orca sections to determine Ax. If no Orca sections are defined, these values will be reported as zero.

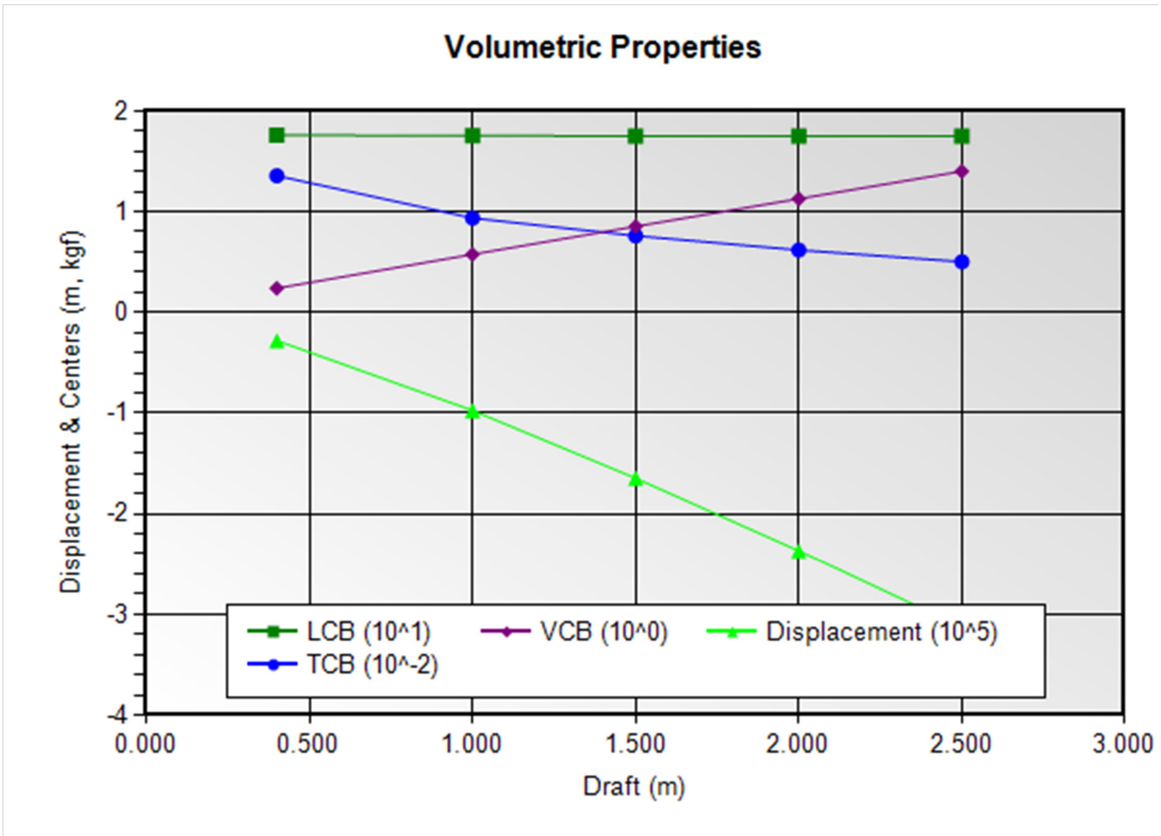
Volumetric Properties
Displacement & Centers (m, kgf)
Draft (m)
2
1
0
-1
-2
-3
-4
0.000
0.500
1.000
1.500
2.000
2.500
3.000
LCB (10^1)
VCB (10^0)
Displacement (10^5)
TCB (10^-2)

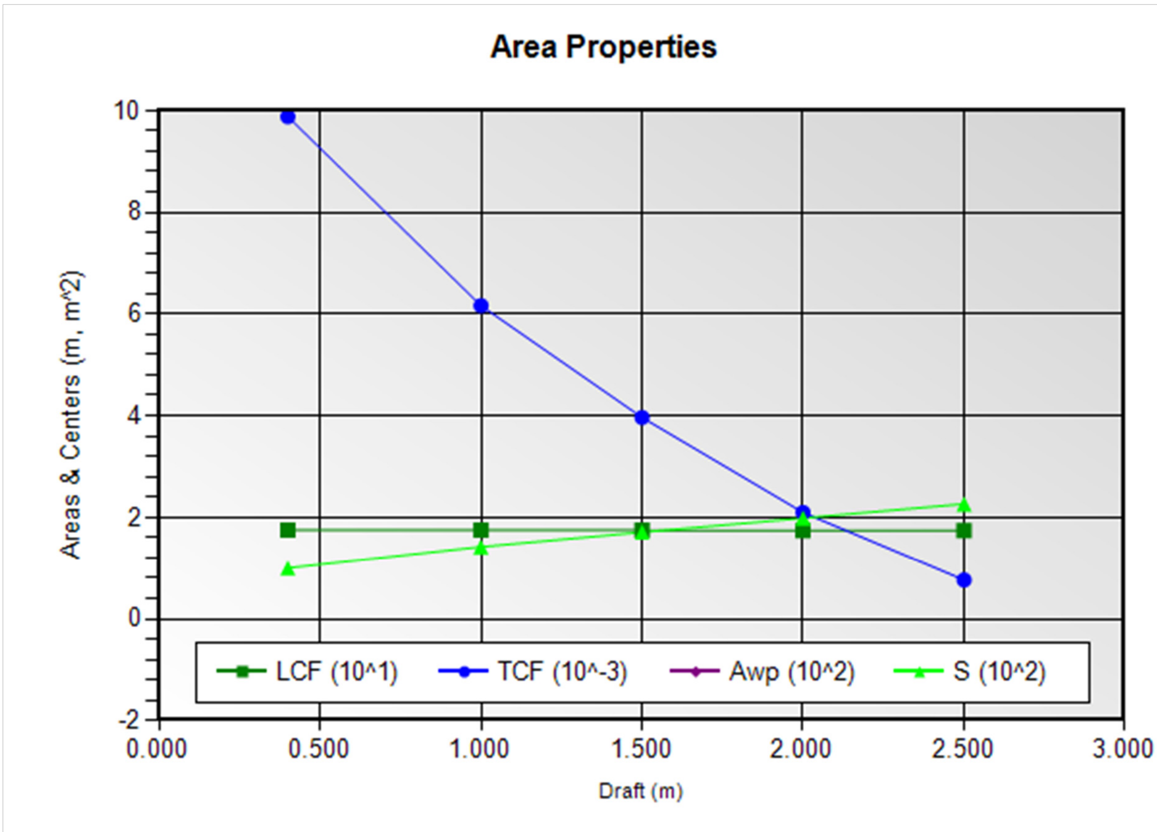
Area Properties
Areas & Centers (m, m^2)
Draft (m)
10
8
6
4
2
0
-2
0.000
0.500
1.000
1.500
2.000
2.500
3.000
LCF (10^1)
TCF (10^-3)
Awp (10^2)
S (10^2)

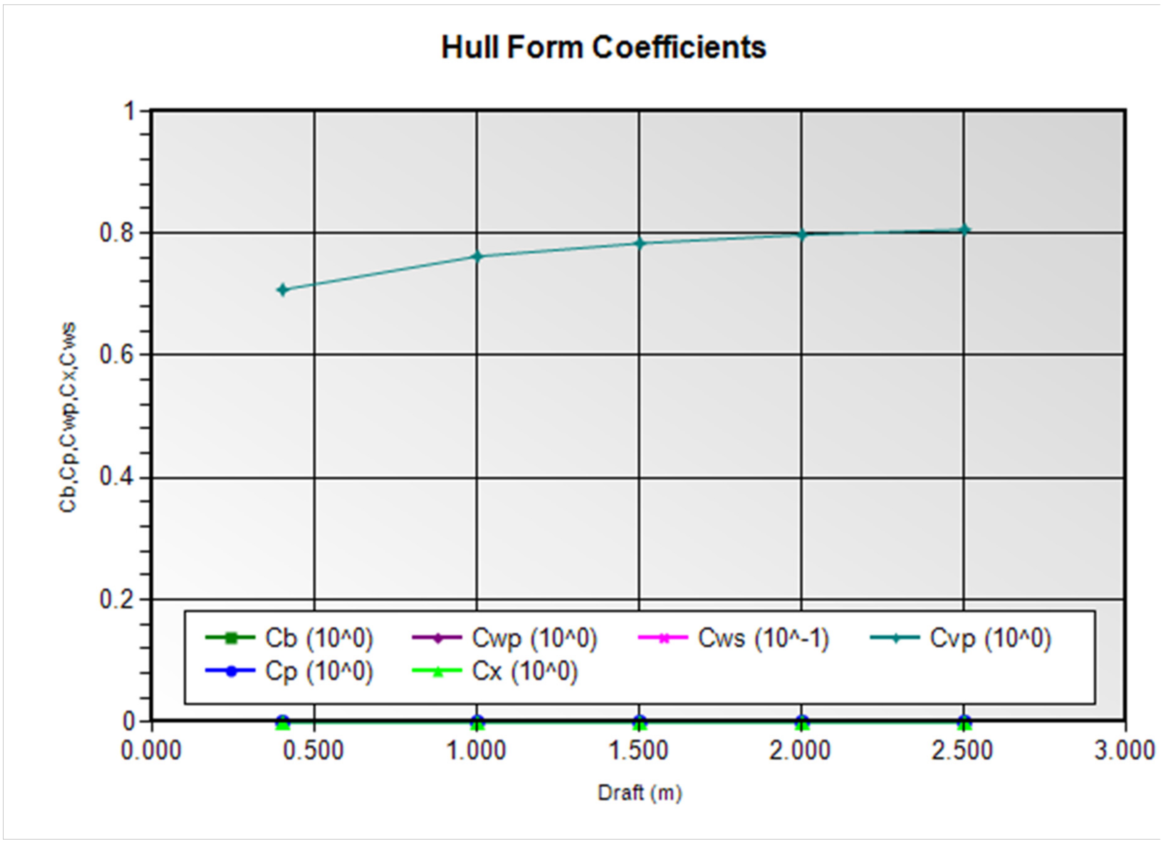
Hull Form Coefficients
Cb,Cp,Cwp,Cx,Cws
Draft (m)
Cb (10^0)
Cp (10^0)
Cwp (10^0)
Cx (10^0)
Cws (10^-1)
Cvp (10^0)
0
0.2
0.4
0.6
0.8
1
0.000
0.500
1.000
1.500
2.000
2.500
3.000

Condition Name=Condition 5,Model Sinkage=2.50,Model Trim=0.00,Model Heel=0.00

General Info

Analysis Type	FixedFlotationPlane	Up Direction = Positive_Z
		Fwd Direction = Negative_X

Surface Meshing Parameters

Density	1	Minimum edge length	0.0001 m
Maximum angle	0	Maximum edge length	0 m
Maximum aspect ratio	0	Max distance, edge to surf.	0 m
Minimum initial grid quads	0	Jagged seams	False
Refine mesh	True	Simple planes	True

Load Condition Parameters

Model Sinkage	2.500 m
Model Trim	0.000 deg
Model Heel	0.000 deg
VCG	None available m
Fluid Type	Seawater
Fluid Density	1025.900 kg/m^3
Mirror Geometry	False

Resultant Model Attitude

Heel Angle	0.000 deg	Sinkage	2.500 m
Trim Angle	0.000 deg		

Overall Dimensions

Length Overall, LOA	25.862 m	Loa / Boa	2.999
Beam Overall, Boa	8.624 m	Boa / D	1.341
Depth Overall, D	6.429 m		

Waterline Dimensions

Waterline Length, Lwl	25.109 m	Lwl / Bwl	3.085
Waterline Beam, Bwl	8.138 m	Bwl / T	3.255
Navigational Draft, T	2.500 m	D / T	2.572

Volumetric Values

Displacement Weight	-312890.996 kgf	Displ-Length Ratio			-550.880
Volume	-304.992 m^3				
LCB	17.485 m	FB/Lwl	0.493	AB/Lwl	0.507
TCB	0.005 m	TCB / Bwl			0.001
VCB	1.400 m				
Wetted Surface Area	226.551 m^2				
Moment To Trim	-2135.936 kgf-m/cm				

Waterplane Values

Waterplane Area, Awp	-151.372 m^2				
LCF	17.422 m	FF/Lwl	0.490	AF/Lwl	0.510
TCF	0.001 m	TCF / Lwl			0.000
Weight To Immerse	-1552.925 kgf/cm				

Sectional Parameters

Ax	0.000 m^2		
Ax Location	0.000 m	Ax Location / Lwl	0.000

Hull Form Coefficients

Cb	-0.597	Cx	0.000
Cp	0.000	Cwp	-0.741
Cvp	0.806	Cws	NaN

Static Stability Parameters

I(transverse)	-638.478 m^4	I(longitudinal)	-5227.641 m^4
BMt	2.093 m	BMl	17.140 m
GMt	None Available m	GMl	None Available m
Mt	0.994 m	Ml	16.041 m

Ma'agan Mikhael

The Ma'agan Mikhael lines plans were drawn by Winters and Kahanov (2003: 130).

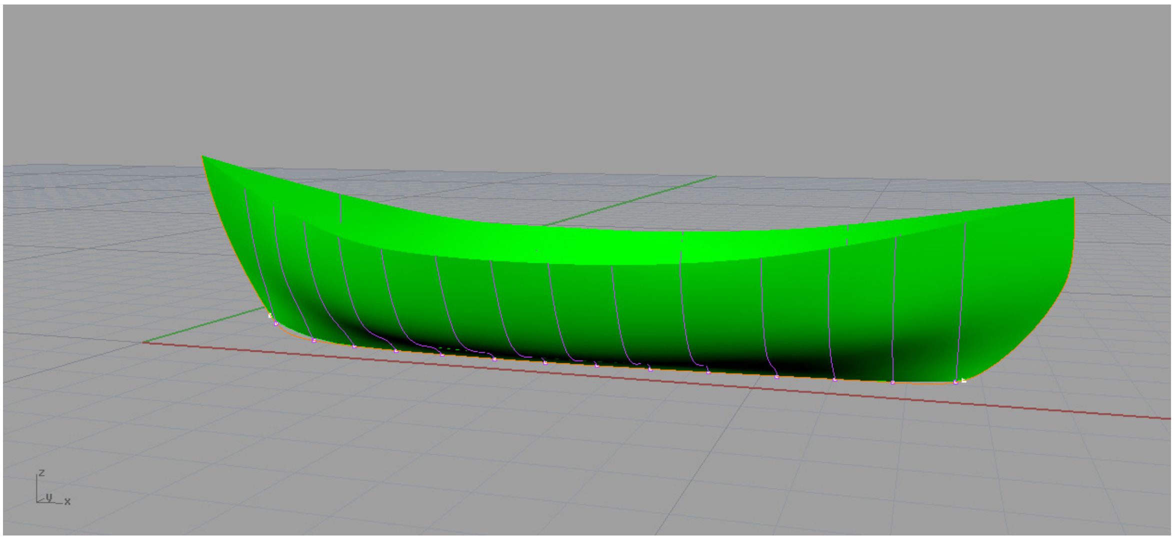

Condition Summary

Load Condition Parameters

Condition	Weight / Sinkage	LCG / Trim	TCG / Heel	VCG (m)
Condition 1	0.500 m	0.000 deg	0.000 deg	0
Condition 2	0.800 m	0.000 deg	0.000 deg	0
Condition 3	1.100 m	0.000 deg	0.000 deg	0
Condition 4	1.400 m	0.000 deg	0.000 deg	0
Condition 5	1.700 m	0.000 deg	0.000 deg	0

Resulting Model Attitude and Hydrostatic Properties

Condition	Sinkage (m)	Trim(deg)	Heel(deg)	Ax(m^2)
Condition 1	0.500	0.000	0.000	0.00
Condition 2	0.800	0.000	0.000	0.00
Condition 3	1.100	0.000	0.000	0.00
Condition 4	1.400	0.000	0.000	0.00
Condition 5	1.700	0.000	0.000	0.00

Condition	Displacement Weight (kgf)	LCB(m)	TCB(m)	VCB(m)	Wet Area (m^2)
Condition 1	1014.041	7.693	-0.289	0.403	7.742
Condition 2	3794.585	7.746	-0.467	0.592	13.009
Condition 3	7505.118	7.772	-0.557	0.771	17.303
Condition 4	11823.115	7.782	-0.617	0.947	21.374
Condition 5	16578.594	7.780	-0.663	1.121	25.402

Condition	Awp(m^2)	LCF(m)	TCF(m)	VCF(m)
Condition 1	6.858	7.744	-0.425	0.500
Condition 2	10.795	7.785	-0.600	0.800
Condition 3	13.161	7.803	-0.689	1.100
Condition 4	14.815	7.789	-0.751	1.400
Condition 5	16.031	7.762	-0.798	1.700

Condition	BMt(m)	BMl(m)	GMt(m)	GMl(m)
Condition 1	0.583	32.836	0.986	33.239
Condition 2	0.453	17.059	1.044	17.651
Condition 3	0.362	11.811	1.134	12.582
Condition 4	0.307	9.018	1.254	9.965
Condition 5	0.269	7.218	1.390	8.338

Condition	Cb	Cp	Cwp	Cx	Cws	Cvp
Condition 1	0.240	0.000	0.584	0.000	2.405	0.411
Condition 2	0.344	0.000	0.652	0.000	2.035	0.527
Condition 3	0.393	0.000	0.672	0.000	1.889	0.585
Condition 4	0.418	0.000	0.672	0.000	1.831	0.622
Condition 5	0.434	0.000	0.667	0.000	1.817	0.650

Notes

1. Locations such as the center of buoyancy and center of flotation are measured from the origin in the Rhinoceros world coordinate system.

2. The orientation of the model for an Orca3D hydrostatics solution is defined in terms of “sinkage,” “trim,” and “heel.” The sinkage value represents the depth of the body origin (i.e. the Rhino world origin) below the resultant flotation plane, and is sometimes referred to as "origin depth." Heel and trim represent angular rotations about the Rhino longitudinal and transverse axes, respectively, and are taken in that order. For a more detailed description of these terms see the Orca3D documentation.

3. Hull form coefficients are non-dimensionalized by the waterline length.

4. Calculation of Cp and Cx use Orca sections to determine Ax. If no Orca sections are defined, these values will be reported as zero.

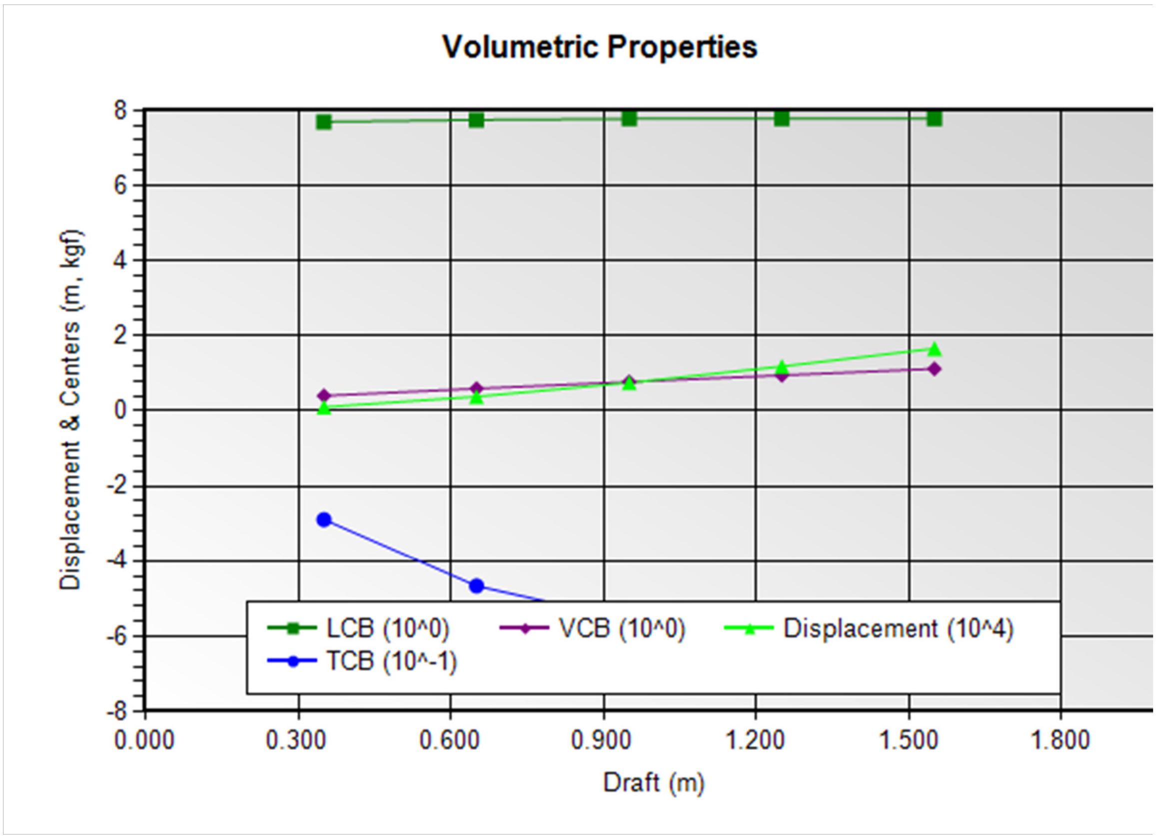

Volumetric Properties
Displacement & Centers (m, kgf)
8
6
4
2
0
-2
-4
-6
-8
0.000
0.300
0.600
0.900
1.200
1.500
1.800
Draft (m)
LCB (10^0)
VCB (10^0)
Displacement (10^4)
TCB (10^-1)

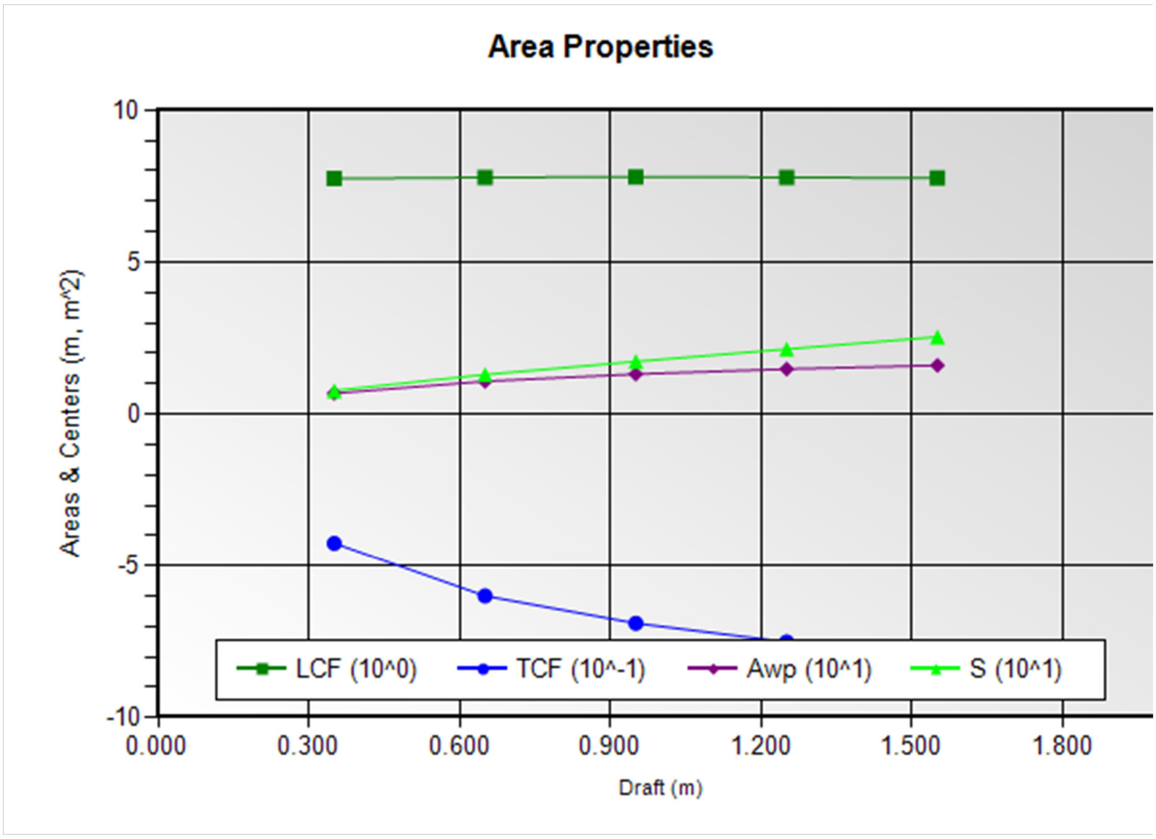

Area Properties
Areas & Centers (m, m^2)
10
5
0
-5
-10
0.000
0.300
0.600
0.900
1.200
1.500
1.800
Draft (m)
LCF (10^0)
TCF (10^-1)
Awp (10^1)
S (10^1)

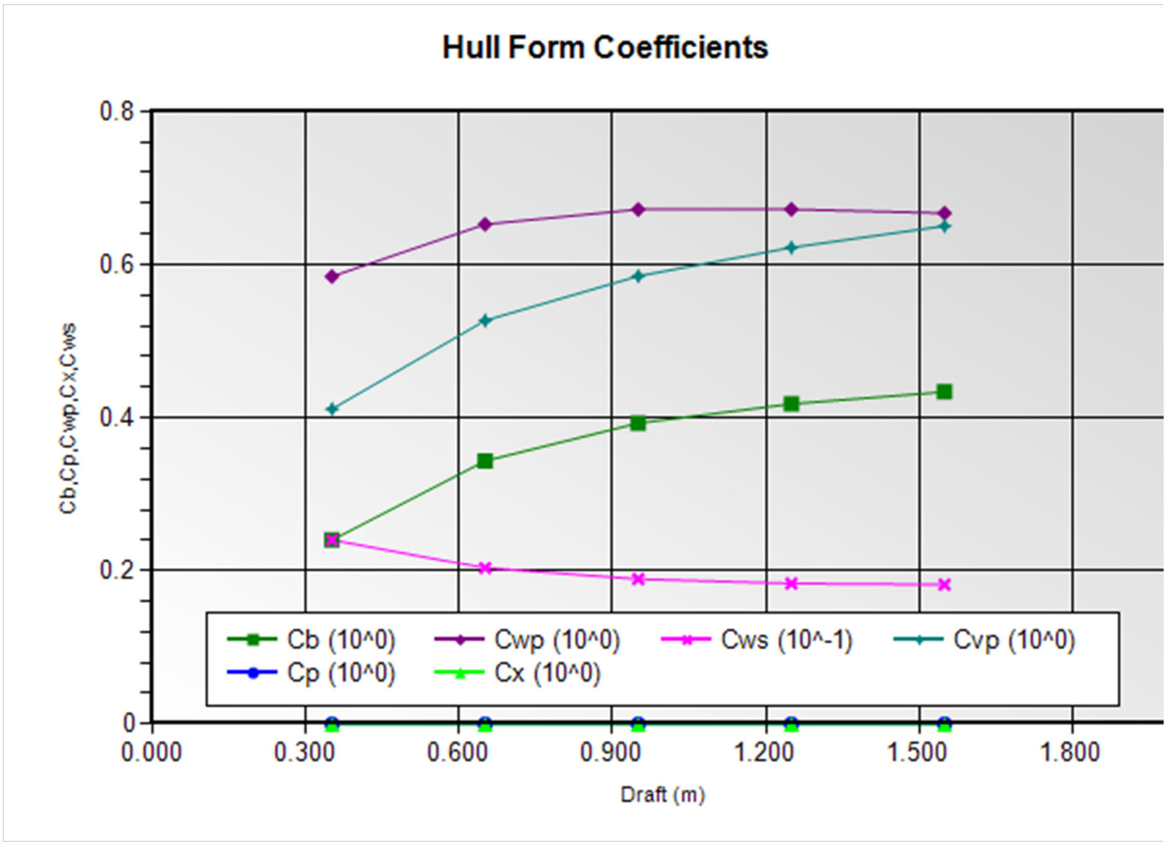

Hull Form Coefficients
0.8
0.6
0.4
0.2
0
Cb,Cp,Cwp,Cx,Cws
0.000
0.300
0.600
0.900
1.200
1.500
1.800
Draft (m)
Cb (10^0)
Cwp (10^0)
Cws (10^-1)
Cvp (10^0)
Cp (10^0)
Cx (10^0)

Condition Name=Condition 1,Model Sinkage=0.50,Model Trim=0.00,Model Heel=0.00

General Info

Analysis Type	FreeFloatEquilibrium	Up Direction = Positive_Z
		Fwd Direction = Negative_X

Surface Meshing Parameters

Density	1	Minimum edge length	0.0001 m
Maximum angle	0	Maximum edge length	0 m
Maximum aspect ratio	0	Max distance, edge to surf.	0 m
Minimum initial grid quads	0	Jagged seams	False
Refine mesh	True	Simple planes	True

Load Condition Parameters

Model Sinkage	0.500 m
Model Trim	0.000 deg
Model Heel	0.000 deg
VCG	0 m
Fluid Type	Seawater
Fluid Density	1025.900 kg/m^3
Mirror Geometry	False

Resultant Model Attitude

Heel Angle	0.000 deg	Sinkage	0.500 m
Trim Angle	0.000 deg		

Overall Dimensions

Length Overall, LOA	12.600 m	Loa / Boa	6.142
Beam Overall, Boa	2.051 m	Boa / D	0.708
Depth Overall, D	2.897 m		

Waterline Dimensions

Waterline Length, Lwl	10.485 m	Lwl / Bwl	9.366
Waterline Beam, Bwl	1.119 m	Bwl / T	3.195
Navigational Draft, T	0.350 m	D / T	8.268

Volumetric Values

Displacement Weight	1014.041 kgf	Displ-Length Ratio			24.518
Volume	0.988 m^3				
LCB	7.693 m	FB/Lwl	0.490	AB/Lwl	0.510
TCB	-0.289 m	TCB / Bwl			-0.258
VCB	0.403 m				
Wetted Surface Area	7.742 m^2				
Moment To Trim	32.146 kgf-m/cm				

Waterplane Values

Waterplane Area, Awp	6.858 m^2				
LCF	7.744 m	FF/Lwl	0.495	AF/Lwl	0.505
TCF	-0.425 m	TCF / Lwl			-0.041
Weight To Immerse	70.361 kgf/cm				

Sectional Parameters

Ax	0.000 m^2		
Ax Location	0.000 m	Ax Location / Lwl	0.000

Hull Form Coefficients

Cb	0.240	Cx	0.000
Cp	0.000	Cwp	0.584
Cvp	0.411	Cws	2.405

Static Stability Parameters

I(transverse)	0.577 m^4	I(longitudinal)	32.456 m^4
BMt	0.583 m	BMl	32.836 m
GMt	0.986 m	GMl	33.239 m
Mt	0.486 m	Ml	32.739 m

Nemi Ship 1

The Nemi Ship 1 lines were published by Bonino (1985:49).

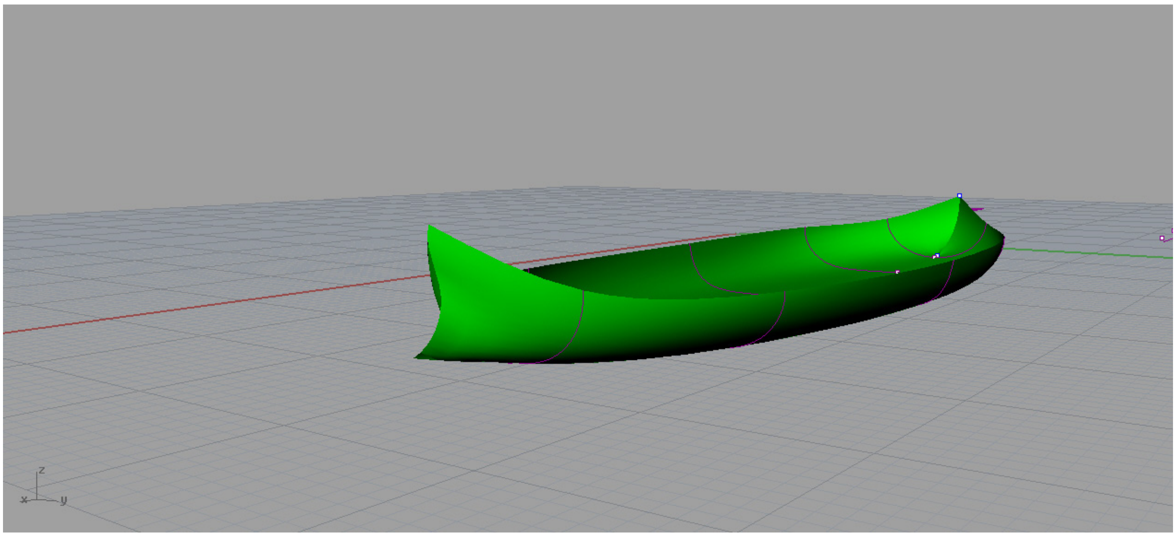

Condition Summary

Load Condition Parameters

Condition	Weight / Sinkage	LCG / Trim	TCG / Heel	VCG (m)
Condition 1	0.500 m	0.000 deg	0.000 deg	None available
Condition 2	1.000 m	0.000 deg	0.000 deg	None available
Condition 3	1.700 m	0.000 deg	0.000 deg	None available
Condition 4	1.800 m	0.000 deg	0.000 deg	None available
Condition 5	1.900 m	0.000 deg	0.000 deg	None available
Condition 6	2.000 m	0.000 deg	0.000 deg	None available
Condition 7	2.500 m	0.000 deg	0.000 deg	None available

Resulting Model Attitude and Hydrostatic Properties

Condition	Sinkage (m)	Trim(deg)	Heel(deg)	Ax(m^2)
Condition 1	0.500	0.000	0.000	0.00
Condition 2	1.000	0.000	0.000	0.00
Condition 3	1.700	0.000	0.000	0.00
Condition 4	1.800	0.000	0.000	0.00
Condition 5	1.900	0.000	0.000	0.00
Condition 6	2.000	0.000	0.000	0.00
Condition 7	2.500	0.000	0.000	0.00

Condition	Displacement Weight (kgf)	LCB(m)	TCB(m)	VCB(m)	Wet Area (m^2)
Condition 1	346525.027	48.703	30.999	0.242	748.017
Condition 2	761232.841	48.662	31.004	0.522	890.571
Condition 3	1417712.865	48.586	31.006	0.908	1026.249
Condition 4	1516224.791	48.578	31.006	0.963	1043.547
Condition 5	1615653.031	48.569	31.006	1.018	1060.586
Condition 6	1715922.464	48.560	31.006	1.072	1077.233
Condition 7	2227723.619	48.515	31.006	1.343	1157.031

Condition	Awp(m^2)	LCF(m)	TCF(m)	VCF(m)
Condition 1	739.837	48.782	31.000	0.500
Condition 2	863.810	48.533	31.000	1.000
Condition 3	955.746	48.453	31.000	1.700
Condition 4	964.968	48.438	31.000	1.800
Condition 5	973.566	48.421	31.000	1.900
Condition 6	981.343	48.402	31.000	2.000
Condition 7	1012.402	48.311	31.000	2.500

Condition	BMt(m)	BMl(m)	GMt(m)	GMl(m)
Condition 1	41.514	402.775	None Available	None Available
Condition 2	24.859	258.526	None Available	None Available
Condition 3	16.392	169.374	None Available	None Available
Condition 4	15.639	161.284	None Available	None Available
Condition 5	14.954	153.902	None Available	None Available
Condition 6	14.317	147.112	None Available	None Available
Condition 7	11.771	120.199	None Available	None Available

Condition	Cb	Cp	Cwp	Cx	Cws	Cvp
Condition 1	0.561	0.000	0.797	0.000	5.541	0.704
Condition 2	0.572	0.000	0.765	0.000	4.163	0.748
Condition 3	0.581	0.000	0.743	0.000	3.375	0.782
Condition 4	0.581	0.000	0.739	0.000	3.302	0.786
Condition 5	0.586	0.000	0.742	0.000	3.251	0.790
Condition 6	0.592	0.000	0.746	0.000	3.205	0.793
Condition 7	0.612	0.000	0.756	0.000	3.018	0.810

Notes

1. Locations such as the center of buoyancy and center of flotation are measured from the origin in the Rhinoceros world coordinate system.

2. The orientation of the model for an Orca3D hydrostatics solution is defined in terms of “sinkage,” “trim,” and “heel.” The sinkage value represents the depth of the body origin (i.e. the Rhino world origin) below the resultant flotation plane, and is sometimes referred to as "origin depth." Heel and trim represent angular rotations about the Rhino longitudinal and transverse axes, respectively, and are taken in that order. For a more detailed description of these terms see the Orca3D documentation.

3. Hull form coefficients are non-dimensionalized by the waterline length.

4. Calculation of Cp and Cx use Orca sections to determine Ax. If no Orca sections are defined, these values will be reported as zero.

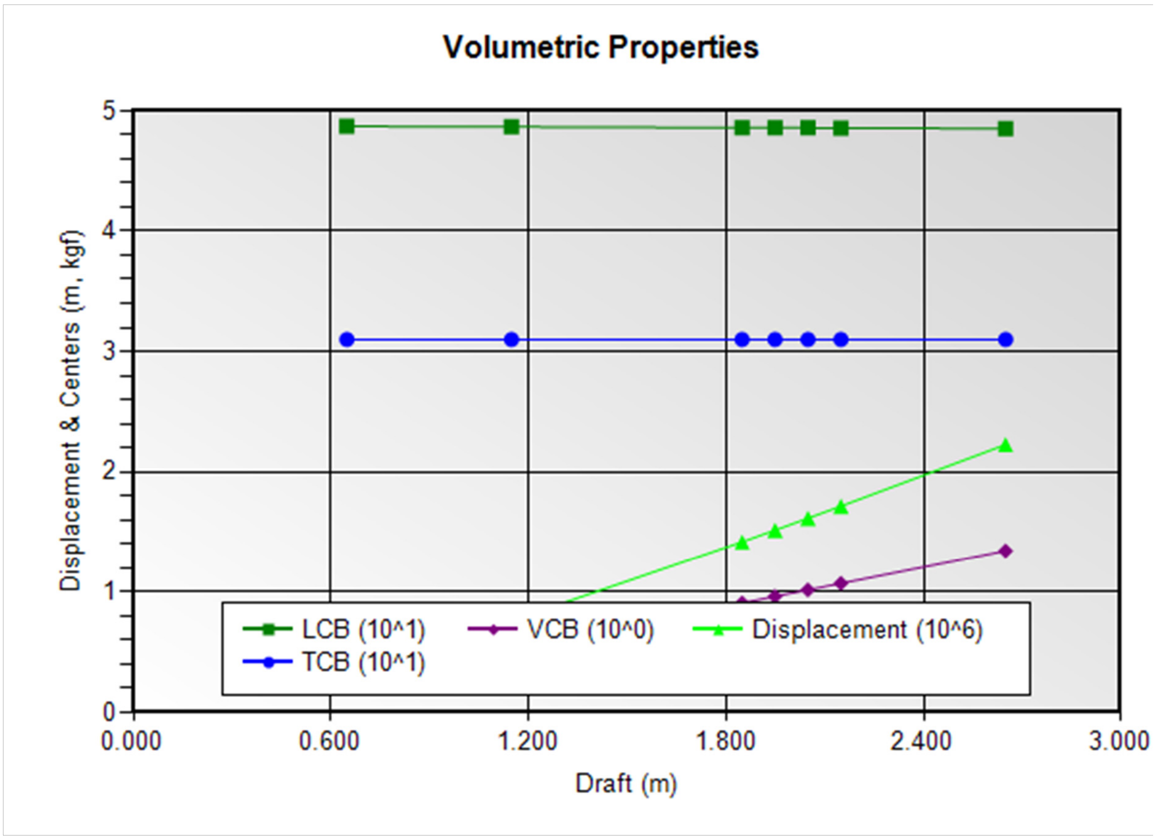

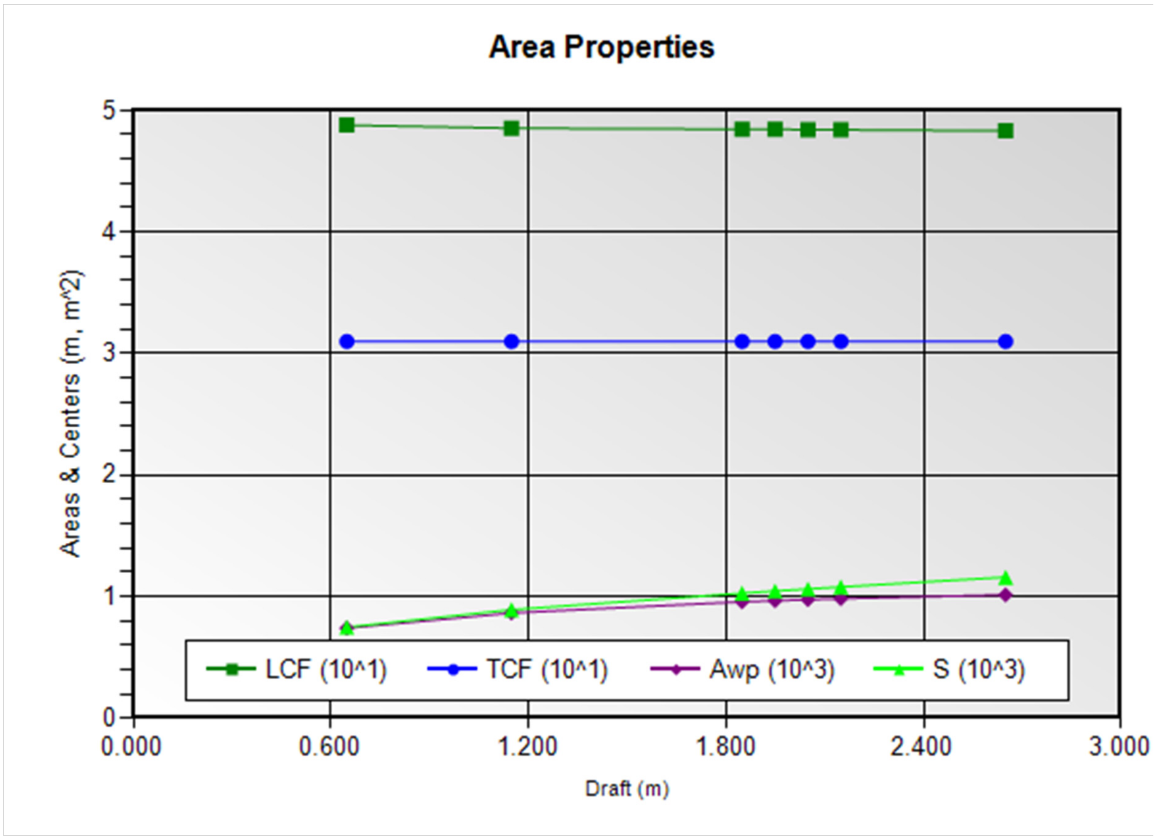
Area Properties
Areas & Centers (m, m^2)
Draft (m)
LCF (10^1)
TCF (10^1)
Awp (10^3)
S (10^3)

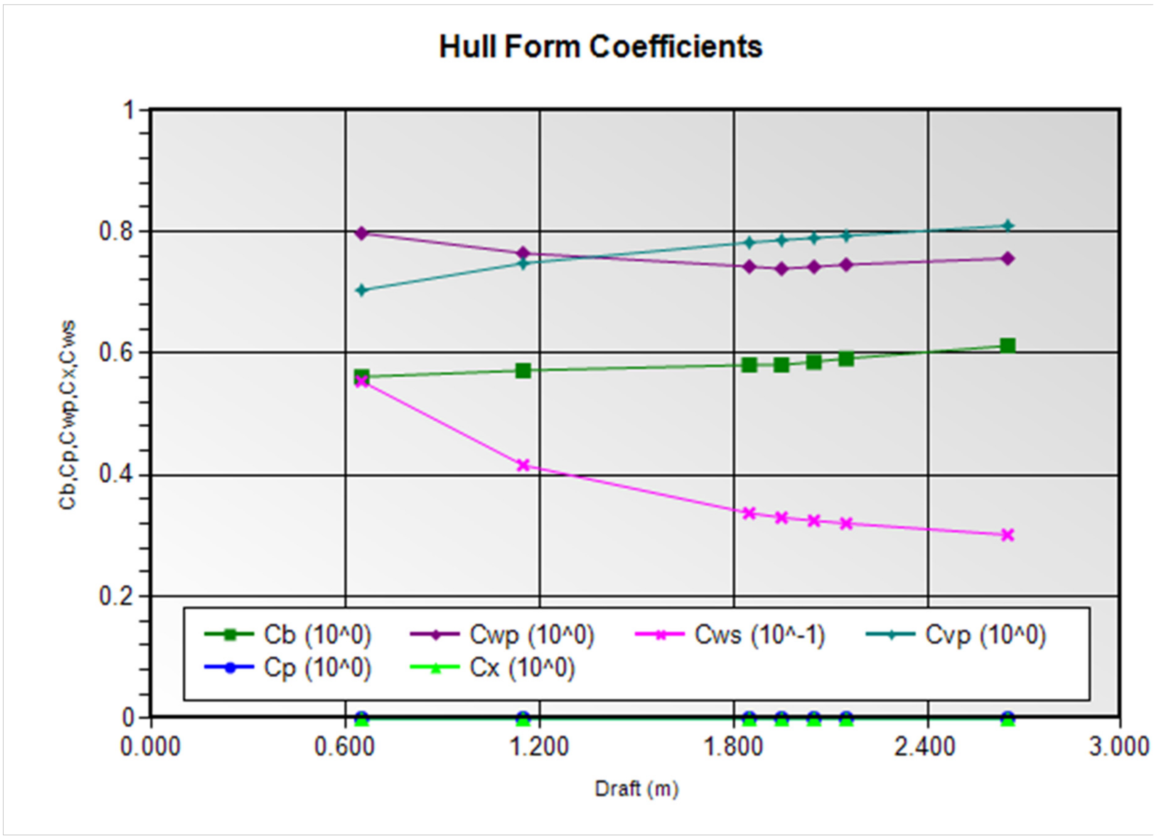
Hull Form Coefficients
Cb,Cp,Cwp,Cx,Cws
Draft (m)
Cb (10^0)
Cwp (10^0)
Cws (10^-1)
Cvp (10^0)
Cp (10^0)
Cx (10^0)

Pantano Longarini

The Pantano Longarini lines plans were published by Kampbell (2007:66).

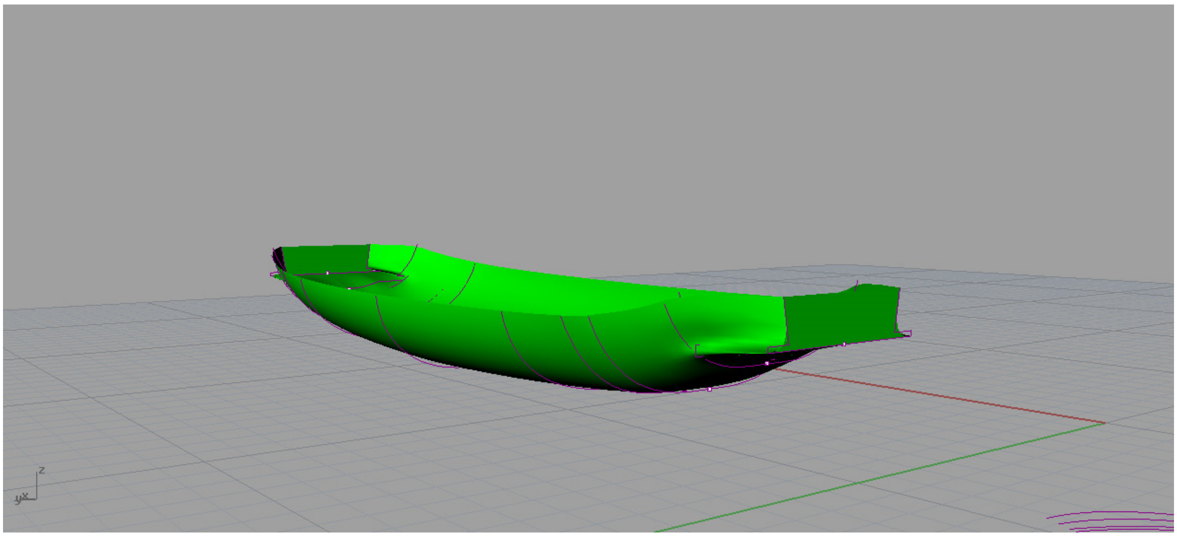

Condition Summary

Load Condition Parameters

Condition	Weight / Sinkage	LCG / Trim	TCG / Heel	VCG (m)
Condition 1	0.750 m	0.000 deg	0.000 deg	None available
Condition 2	1.450 m	0.000 deg	0.000 deg	None available
Condition 3	2.200 m	0.000 deg	0.000 deg	None available

Resulting Model Attitude and Hydrostatic Properties

Condition	Sinkage (m)	Trim(deg)	Heel(deg)	Ax(m^2)
Condition 1	0.750	0.000	0.000	0.00
Condition 2	1.450	0.000	0.000	0.00
Condition 3	2.200	0.000	0.000	0.00

Condition	Displacement Weight (kgf)	LCB(m)	TCB(m)	VCB(m)	Wet Area (m^2)
Condition 1	62469.529	17.626	6.528	0.479	139.540
Condition 2	179620.847	17.877	6.526	0.896	205.089
Condition 3	342083.060	17.989	6.524	1.344	278.632

Condition	Awp(m^2)	LCF(m)	TCF(m)	VCF(m)
Condition 1	135.085	17.874	6.527	0.750
Condition 2	187.563	18.109	6.523	1.450
Condition 3	237.993	18.066	6.522	2.200

Condition	BMt(m)	BMl(m)	GMt(m)	GMl(m)
Condition 1	8.361	68.476	None Available	None Available
Condition 2	5.788	44.542	None Available	None Available
Condition 3	4.425	41.537	None Available	None Available

Condition	Cb	Cp	Cwp	Cx	Cws	Cvp
Condition 1	0.536	0.000	0.844	0.000	3.891	0.635
Condition 2	0.565	0.000	0.854	0.000	3.132	0.662
Condition 3	0.545	0.000	0.840	0.000	2.821	0.649

Notes

1. Locations such as the center of buoyancy and center of flotation are measured from the origin in the Rhinoceros world coordinate system.

2. The orientation of the model for an Orca3D hydrostatics solution is defined in terms of “sinkage,” “trim,” and “heel.” The sinkage value represents the depth of the body origin (i.e. the Rhino world origin) below the resultant flotation plane, and is sometimes referred to as "origin depth." Heel and trim represent angular rotations about the Rhino longitudinal and transverse axes, respectively, and are taken in that order. For a more detailed description of these terms see the Orca3D documentation.

3. Hull form coefficients are non-dimensionalized by the waterline length.

4. Calculation of Cp and Cx use Orca sections to determine Ax. If no Orca sections are defined, these values will be reported as zero.

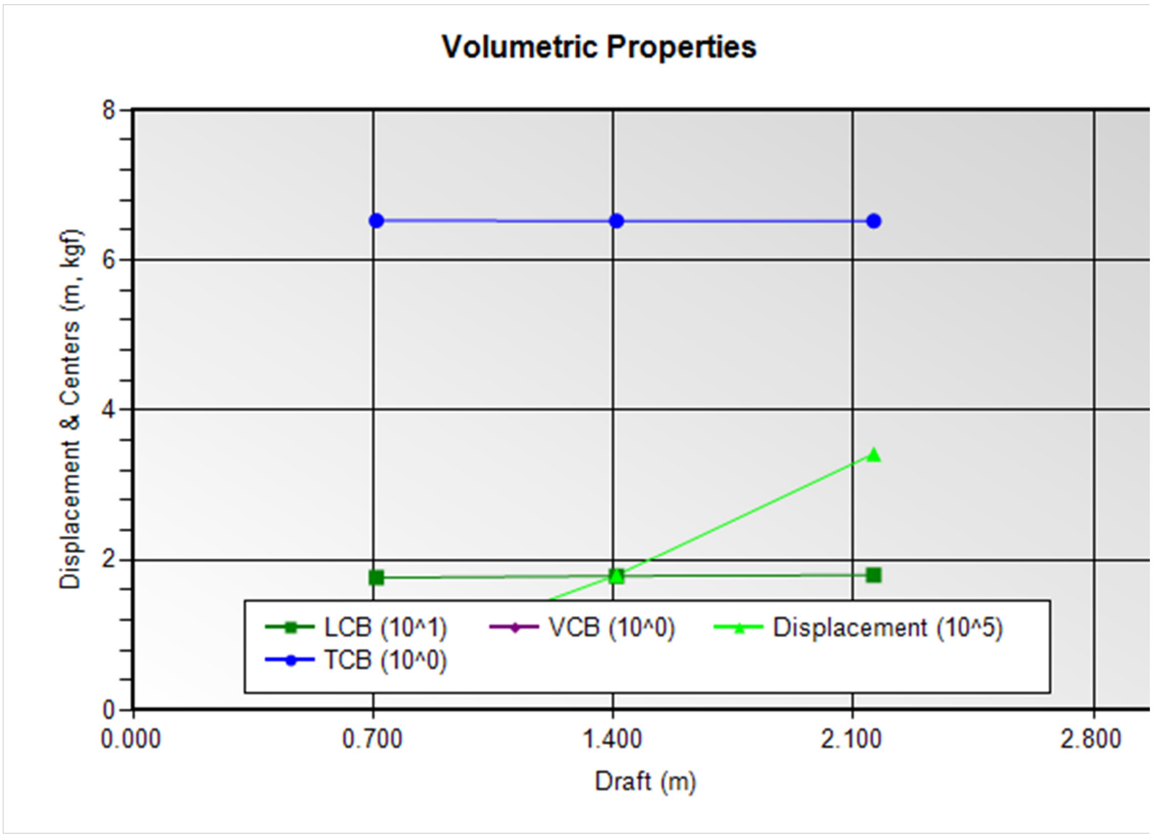
Volumetric Properties
Displacement & Centers (m, kgf)
Draft (m)
0.000
0.700
1.400
2.100
2.800
0
2
4
6
8
LCB (10^1)
VCB (10^0)
Displacement (10^5)
TCB (10^0)

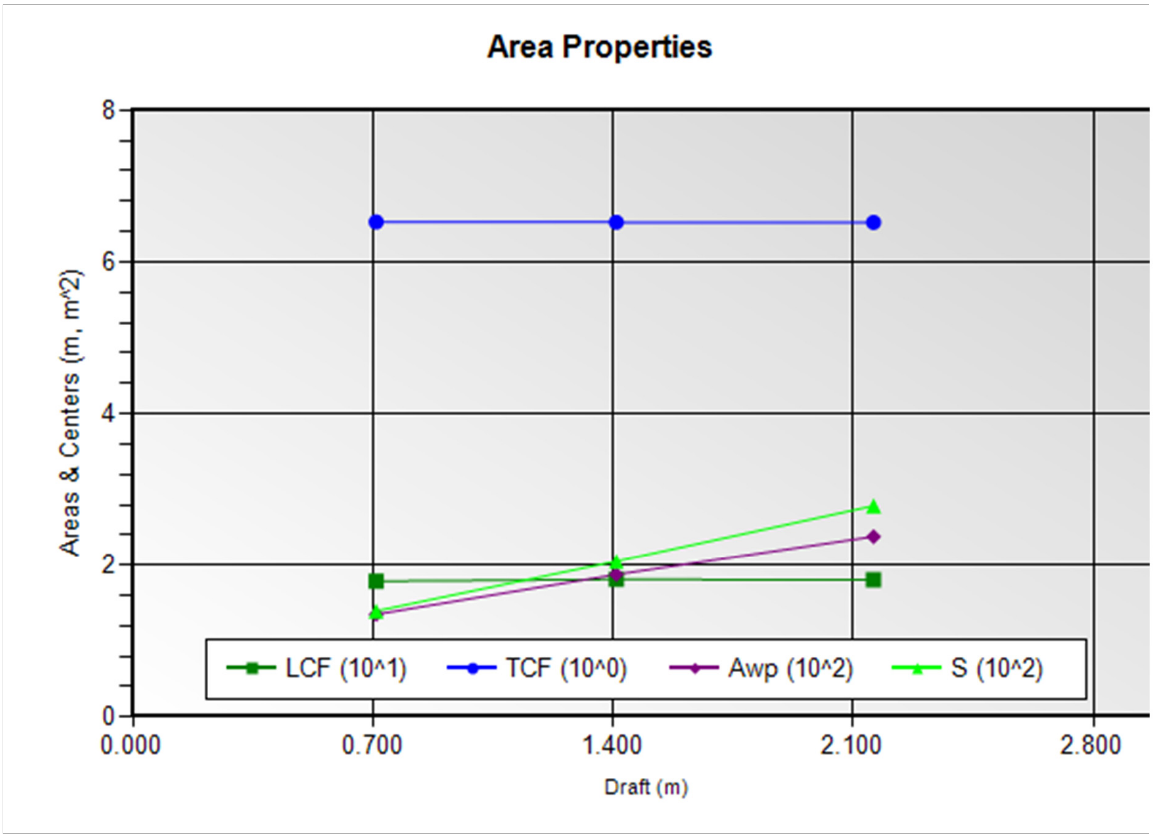
Area Properties
Areas & Centers (m, m^2)
Draft (m)
0.000
0.700
1.400
2.100
2.800
0
2
4
6
8
LCF (10^1)
TCF (10^0)
Awp (10^2)
S (10^2)

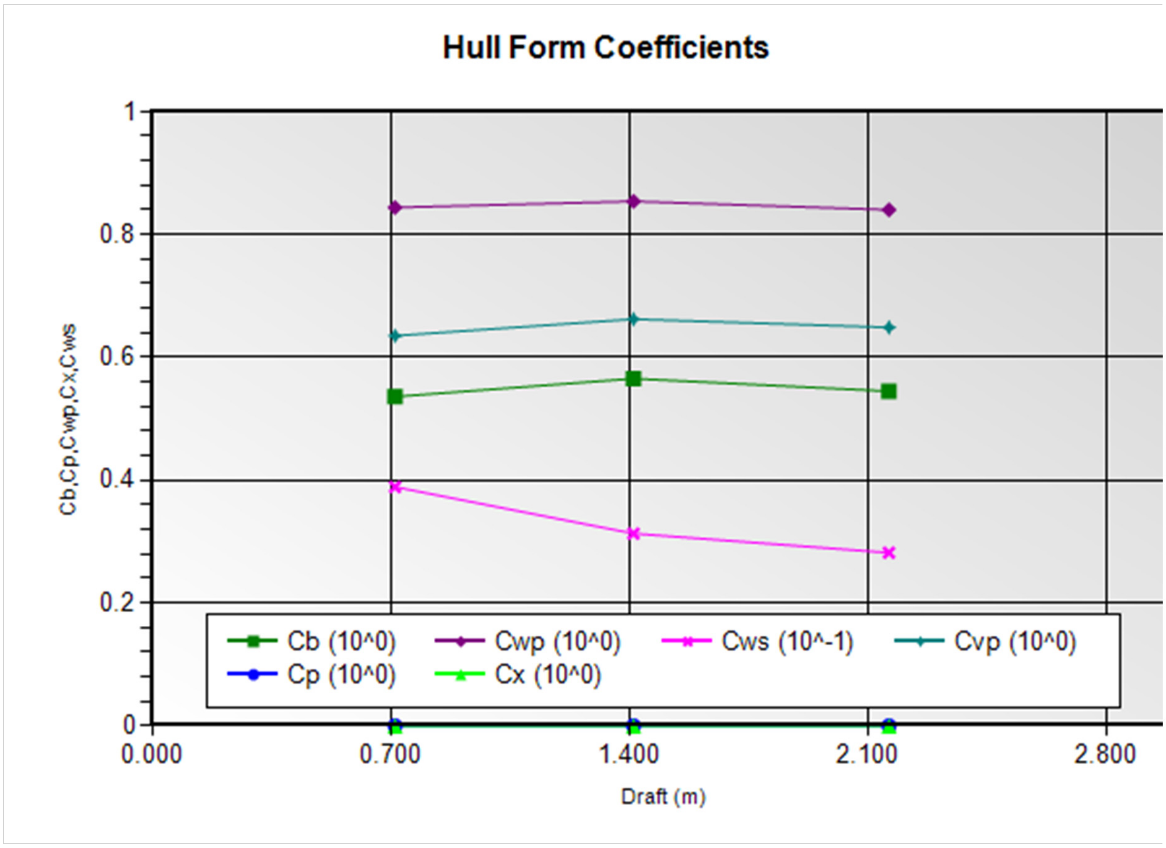
Hull Form Coefficients
1
0.8
0.6
0.4
0.2
0
Cb,Cp,Cwp,Cx,Cws
0.000
0.700
1.400
2.100
2.800
Draft (m)
Cb (10^0)
Cwp (10^0)
Cws (10^-1)
Cvp (10^0)
Cp (10^0)
Cx (10^0)

Port-Berteau 2

The lines plans for Port-Berteau 2 were published by Rieth *et al.* (2001: fig. 106).

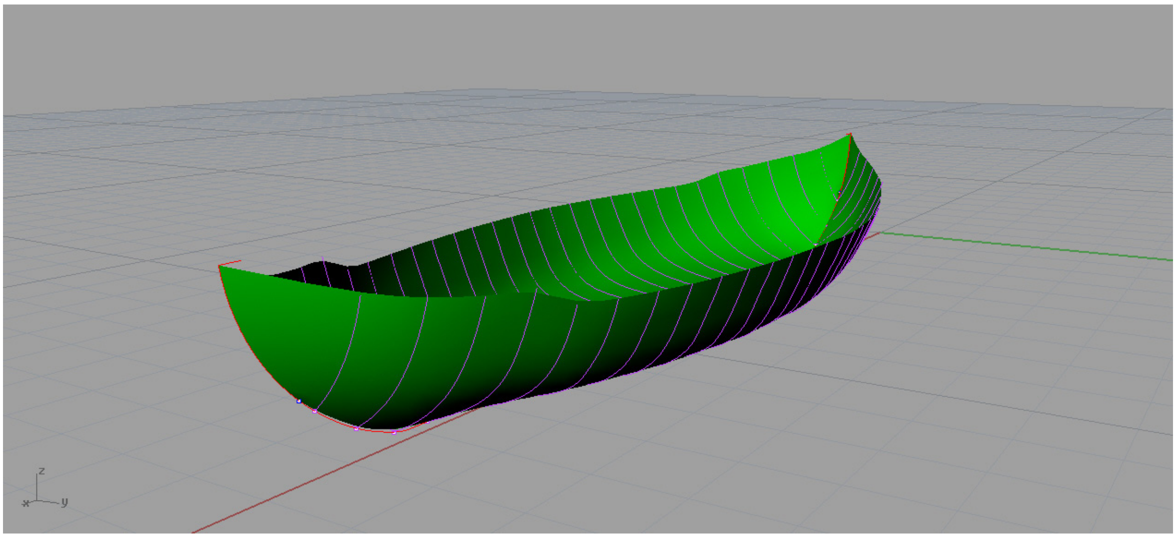

Condition Summary

Load Condition Parameters

Condition	Weight / Sinkage	LCG / Trim	TCG / Heel	VCG (m)
Condition 6	1.150 m	0.000 deg	0.000 deg	None available
Condition 5	0.950 m	0.000 deg	0.000 deg	None available
Condition 4	0.750 m	0.000 deg	0.000 deg	None available
Condition 3	0.550 m	0.000 deg	0.000 deg	None available
Condition 2	0.350 m	0.000 deg	0.000 deg	None available
Condition 1	0.150 m	0.000 deg	0.000 deg	None available

Resulting Model Attitude and Hydrostatic Properties

Condition	Sinkage (m)	Trim(deg)	Heel(deg)	Ax(m^2)
Condition 6	1.150	0.000	0.000	0.00
Condition 5	0.950	0.000	0.000	0.00
Condition 4	0.750	0.000	0.000	0.00
Condition 3	0.550	0.000	0.000	0.00
Condition 2	0.350	0.000	0.000	0.00
Condition 1	0.150	0.000	0.000	0.00

Condition	Displacement Weight (kgf)	LCB(m)	TCB(m)	VCB(m)	Wet Area (m^2)
Condition 6	-33300.381	9.188	-0.001	0.704	53.752
Condition 5	-25155.950	9.195	-0.001	0.591	47.511
Condition 4	-17552.624	9.202	-0.001	0.478	41.268
Condition 3	-10613.270	9.208	-0.001	0.365	34.750
Condition 2	-4609.447	9.208	-0.002	0.250	27.110
Condition 1	-388.614	9.221	-0.006	0.130	12.017

Condition	Awp(m^2)	LCF(m)	TCF(m)	VCF(m)
Condition 6	-40.916	9.163	-0.001	1.150
Condition 5	-38.434	9.172	-0.001	0.950
Condition 4	-35.589	9.184	-0.001	0.750
Condition 3	-31.859	9.200	0.000	0.550
Condition 2	-26.161	9.217	-0.001	0.350
Condition 1	-11.946	9.134	-0.004	0.150

Condition	BMt(m)	BMl(m)	GMt(m)	GMl(m)
Condition 6	1.412	12.028	None Available	None Available
Condition 5	1.626	14.245	None Available	None Available
Condition 4	1.979	17.678	None Available	None Available
Condition 3	2.577	23.879	None Available	None Available

Condition 2	3.793	39.304	None Available	None Available
Condition 1	5.520	166.236	None Available	None Available

Condition	Cb	Cp	Cwp	Cx	Cws	Cvp
Condition 6	-0.515	0.000	-0.688	0.000	NaN	0.748
Condition 5	-0.512	0.000	-0.691	0.000	NaN	0.741
Condition 4	-0.503	0.000	-0.692	0.000	NaN	0.728
Condition 3	-0.486	0.000	-0.689	0.000	NaN	0.705
Condition 2	-0.444	0.000	-0.674	0.000	NaN	0.659
Condition 1	-0.339	0.000	-0.648	0.000	NaN	0.523

Notes

1. Locations such as the center of buoyancy and center of flotation are measured from the origin in the Rhinoceros world coordinate system.

2. The orientation of the model for an Orca3D hydrostatics solution is defined in terms of “sinkage,” “trim,” and “heel.” The sinkage value represents the depth of the body origin (i.e. the Rhino world origin) below the resultant flotation plane, and is sometimes referred to as "origin depth." Heel and trim represent angular rotations about the Rhino longitudinal and transverse axes, respectively, and are taken in that order. For a more detailed description of these terms see the Orca3D documentation.

3. Hull form coefficients are non-dimensionalized by the waterline length.

4. Calculation of Cp and Cx use Orca sections to determine Ax. If no Orca sections are defined, these values will be reported as zero.

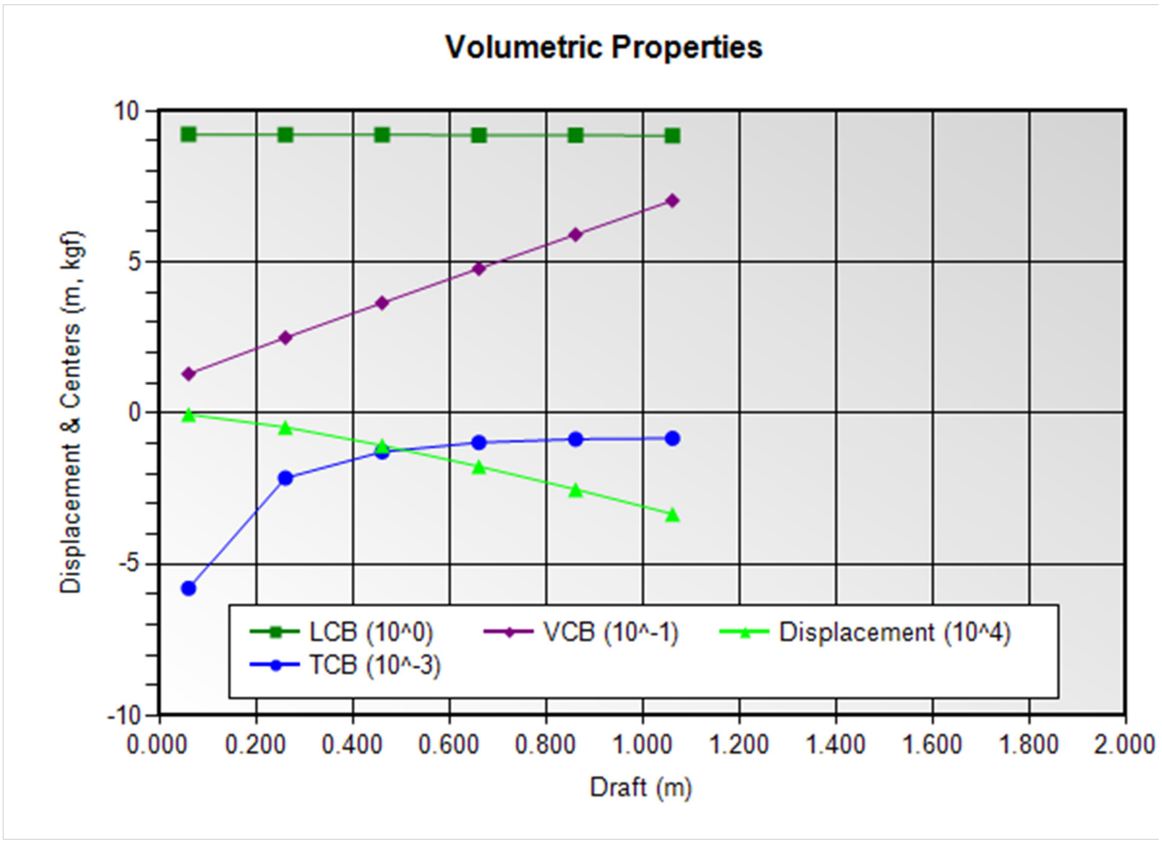
Volumetric Properties
Displacement & Centers (m, kgf)
Draft (m)
LCB (10^0)
VCB (10^-1)
Displacement (10^4)
TCB (10^-3)

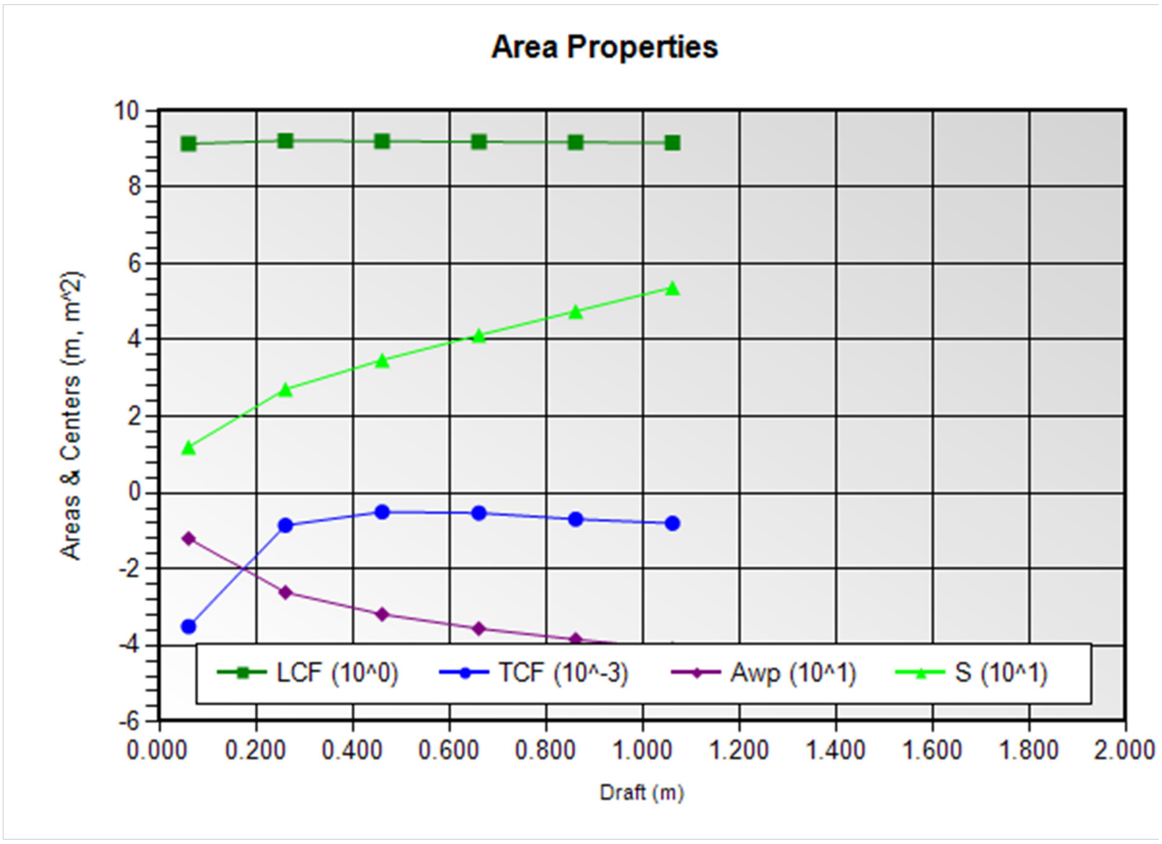
Area Properties
Areas & Centers (m, m^2)
Draft (m)
LCF (10^0)
TCF (10^-3)
Awp (10^1)
S (10^1)

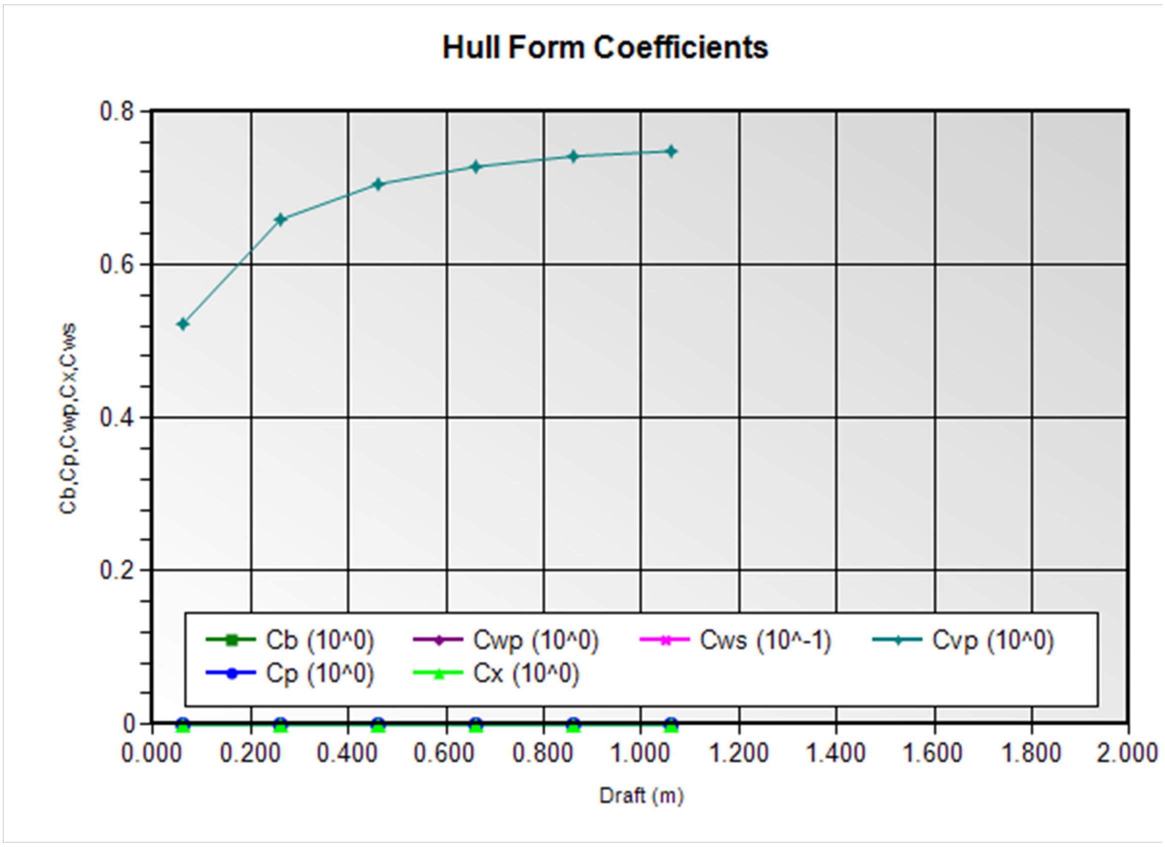
Hull Form Coefficients
0.8
0.6
0.4
0.2
0
Cb,Cp,Cwp,Cx,Cws
Cb (10^0)
Cwp (10^0)
Cws (10^-1)
Cvp (10^0)
Cp (10^0)
Cx (10^0)
0.000
0.200
0.400
0.600
0.800
1.000
1.200
1.400
1.600
1.800
2.000
Draft (m)

Pepper Wreck

The lines plans for the Pepper Wreck were published by Castro (2008).

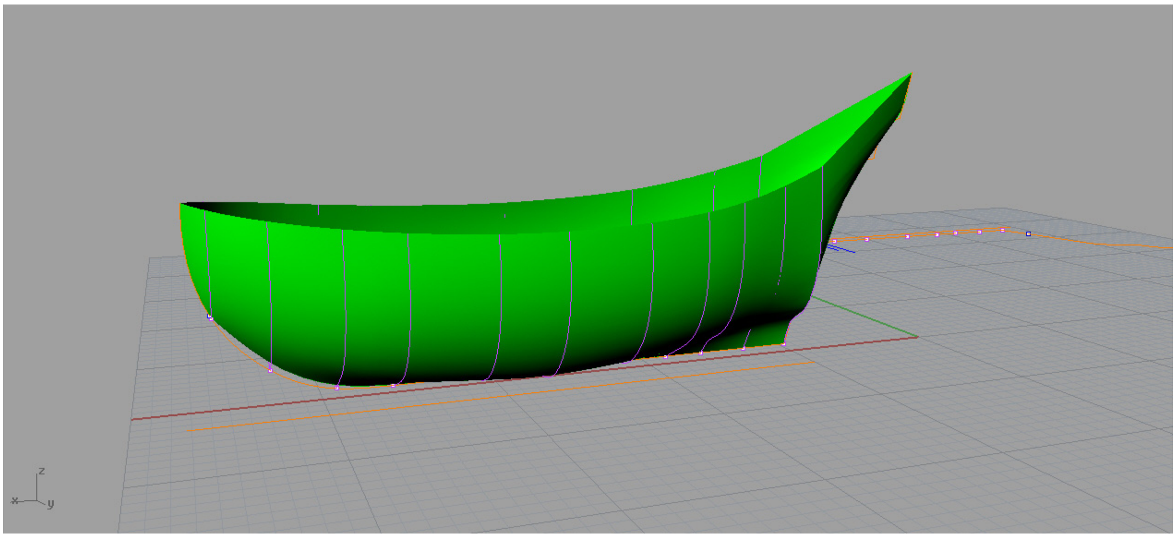

Condition Summary

Load Condition Parameters

Condition	Weight / Sinkage	LCG / Trim	TCG / Heel	VCG (m)
Condition 1	1.650 m	0.000 deg	0.000 deg	None available
Condition 2	3.250 m	0.000 deg	0.000 deg	None available
Condition 3	4.850 m	0.000 deg	0.000 deg	None available
Condition 4	6.450 m	0.000 deg	0.000 deg	None available

Resulting Model Attitude and Hydrostatic Properties

Condition	Sinkage (m)	Trim(deg)	Heel(deg)	Ax(m^2)
Condition 1	1.650	0.000	0.000	0.00
Condition 2	3.250	0.000	0.000	0.00
Condition 3	4.850	0.000	0.000	0.00
Condition 4	6.450	0.000	0.000	0.00

Condition	Displacement Weight (kgf)	LCB(m)	TCB(m)	VCB(m)	Wet Area (m^2)
Condition 1	198949.829	27.211	-1.434	1.042	232.542
Condition 2	621715.716	26.893	-1.434	2.037	394.498
Condition 3	1178391.517	26.744	-1.434	2.999	538.470
Condition 4	1807750.660	26.719	-1.434	3.926	678.626

Condition	Awp(m^2)	LCF(m)	TCF(m)	VCF(m)
Condition 1	199.740	27.079	-1.434	1.650
Condition 2	306.466	26.555	-1.434	3.250
Condition 3	366.019	26.626	-1.434	4.850
Condition 4	396.962	26.701	-1.434	6.450

Condition	BMt(m)	BMl(m)	GMt(m)	GMl(m)
Condition 1	4.974	55.880	None Available	None Available
Condition 2	4.032	37.968	None Available	None Available
Condition 3	3.180	27.168	None Available	None Available
Condition 4	2.449	20.743	None Available	None Available

Condition	Cb	Cp	Cwp	Cx	Cws	Cvp
Condition 1	0.385	0.000	0.662	0.000	2.912	0.582
Condition 2	0.459	0.000	0.759	0.000	2.699	0.605
Condition 3	0.503	0.000	0.780	0.000	2.605	0.645
Condition 4	0.544	0.000	0.793	0.000	2.612	0.686

Notes

1. Locations such as the center of buoyancy and center of flotation are measured from the origin in the Rhinoceros world coordinate system.

2. The orientation of the model for an Orca3D hydrostatics solution is defined in terms of “sinkage,” “trim,” and “heel.” The sinkage value represents the depth of the body origin (i.e. the Rhino world origin) below the resultant flotation plane, and is sometimes referred to as "origin depth." Heel and trim represent angular rotations about the Rhino longitudinal and transverse axes, respectively, and are taken in that order. For a more detailed description of these terms see the Orca3D documentation.

3. Hull form coefficients are non-dimensionalized by the waterline length.

4. Calculation of Cp and Cx use Orca sections to determine Ax. If no Orca sections are defined, these values will be reported as zero.

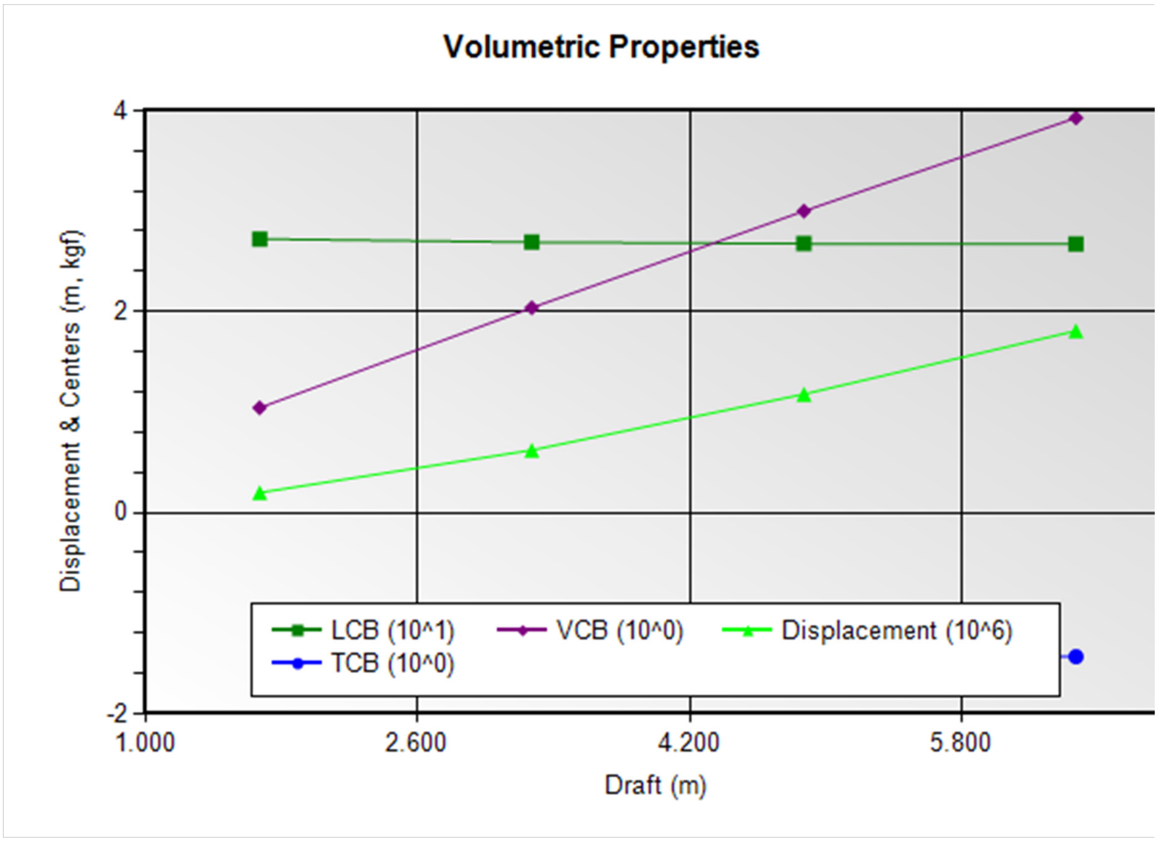

Cuttlebone

The lines plans of the cuttlebone are from Bonino (1985:49).

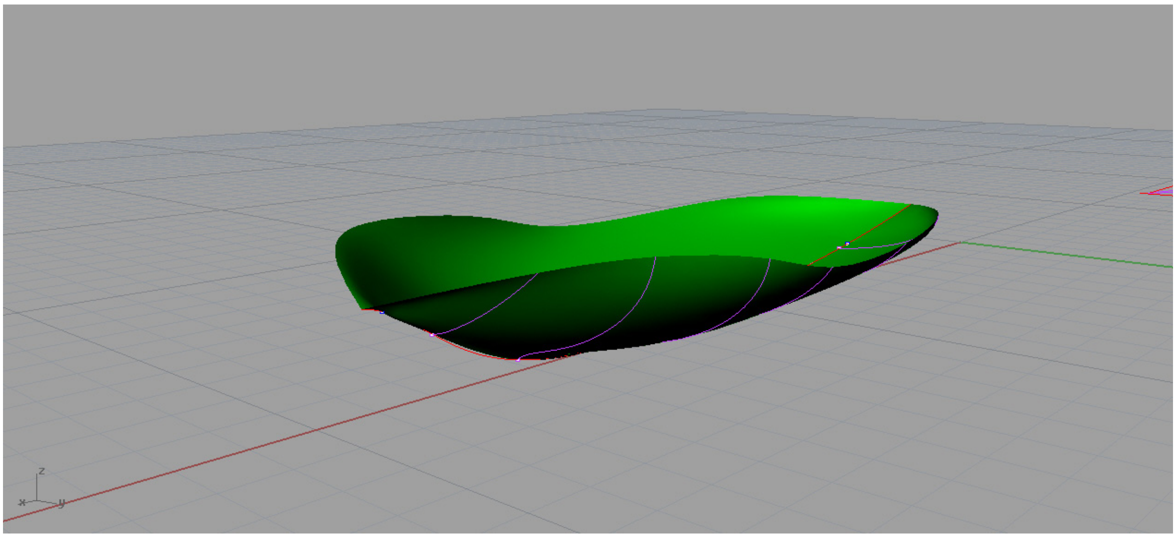

Condition Summary

Load Condition Parameters				
Condition	**Weight / Sinkage**	**LCG / Trim**	**TCG / Heel**	**VCG (m)**
Condition 1	1.000 m	0.000 deg	0.000 deg	None available
Condition 2	0.750 m	0.000 deg	0.000 deg	None available
Condition 3	0.500 m	0.000 deg	0.000 deg	None available
Condition 4	0.250 m	0.000 deg	0.000 deg	None available

Resulting Model Attitude and Hydrostatic Properties				
Condition	**Sinkage (m)**	**Trim(deg)**	**Heel(deg)**	**Ax(m^2)**
Condition 1	1.000	0.000	0.000	0.00
Condition 2	0.750	0.000	0.000	0.00
Condition 3	0.500	0.000	0.000	0.00
Condition 4	0.250	0.000	0.000	0.00

Condition	Displacement Weight (kgf)	LCB(m)	TCB(m)	VCB(m)	Wet Area (m^2)
Condition 1	-25812.474	12.158	0.044	0.691	58.473
Condition 2	-13729.555	12.498	0.044	0.523	42.579
Condition 3	-5435.372	12.898	0.044	0.353	26.198
Condition 4	-1015.350	13.408	0.044	0.179	10.677

Condition	Awp(m^2)	LCF(m)	TCF(m)	VCF(m)
Condition 1	-53.953	11.598	0.044	1.000
Condition 2	-39.910	11.999	0.044	0.750
Condition 3	-24.736	12.525	0.044	0.500
Condition 4	-9.905	13.160	0.044	0.250

Condition	BMt(m)	BMl(m)	GMt(m)	GMl(m)
Condition 1	3.795	22.454	None Available	None Available
Condition 2	3.911	23.112	None Available	None Available
Condition 3	3.739	22.874	None Available	None Available
Condition 4	2.950	21.835	None Available	None Available

Condition	Cb	Cp	Cwp	Cx	Cws	Cvp
Condition 1	-0.349	0.000	-0.750	0.000	NaN	0.466
Condition 2	-0.330	0.000	-0.740	0.000	NaN	0.446
Condition 3	-0.303	0.000	-0.709	0.000	NaN	0.427
Condition 4	-0.249	0.000	-0.625	0.000	NaN	0.398

Notes

1. Locations such as the center of buoyancy and center of flotation are measured from the origin in the Rhinoceros world coordinate system.

2. The orientation of the model for an Orca3D hydrostatics solution is defined in terms of “sinkage,” “trim,” and “heel.” The sinkage value represents the depth of the body origin (i.e. the Rhino world origin) below the resultant flotation plane, and is sometimes referred to as "origin depth." Heel and trim represent angular rotations about the Rhino longitudinal and transverse axes, respectively, and are taken in that order. For a more detailed description of these terms see the Orca3D documentation.

3. Hull form coefficients are non-dimensionalized by the waterline length.

4. Calculation of Cp and Cx use Orca sections to determine Ax. If no Orca sections are defined, these values will be reported as zero.

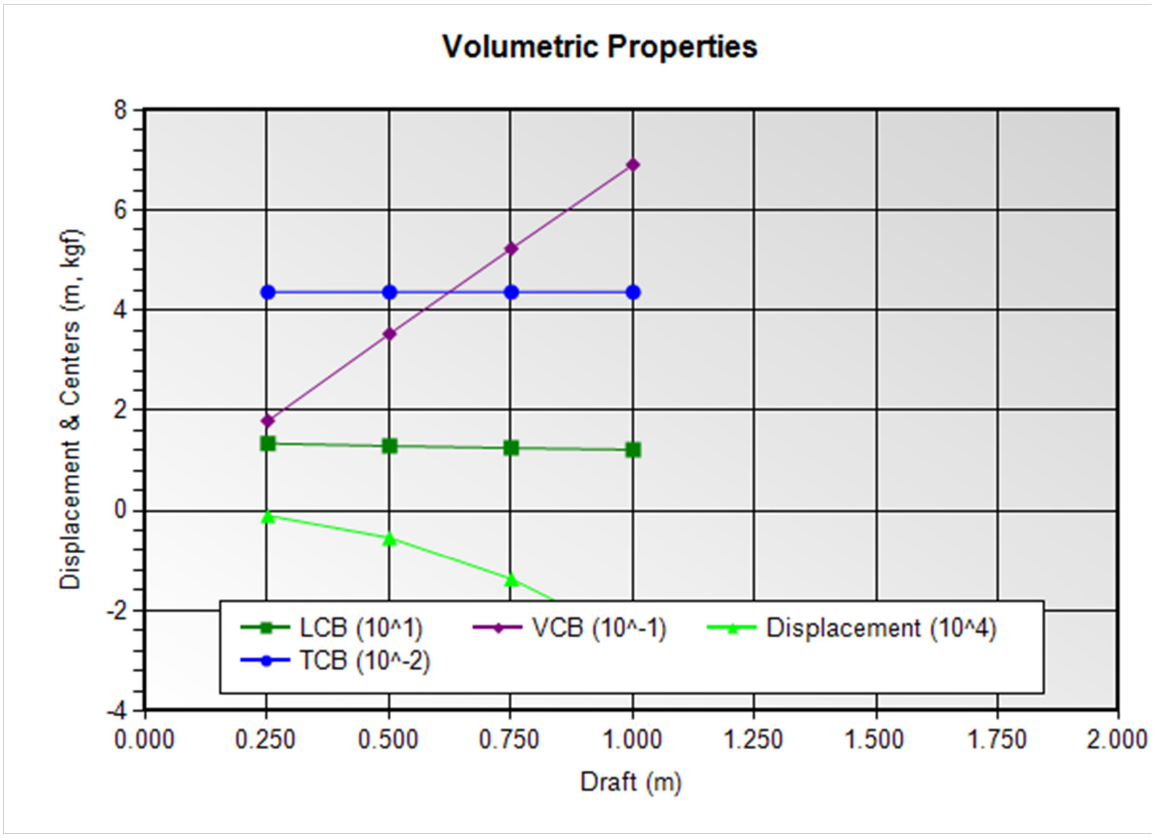

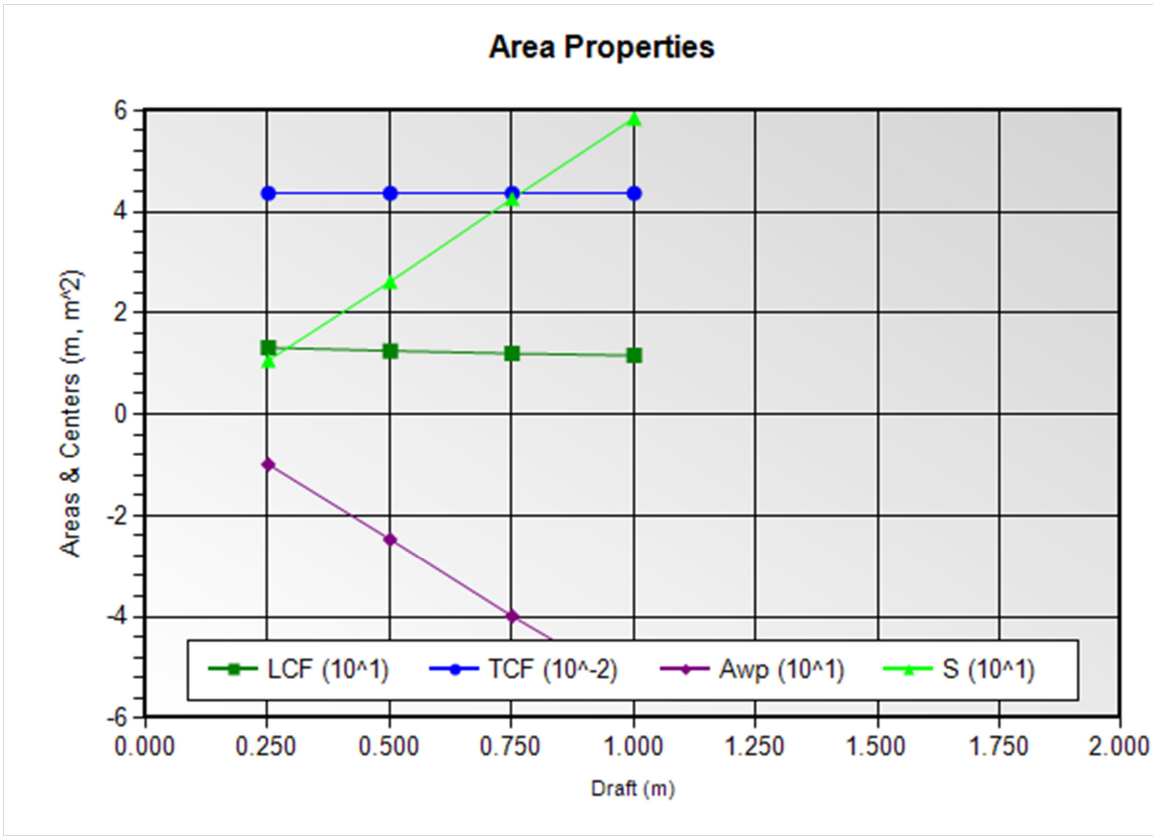

Area Properties
Areas & Centers (m, m^2)
6
4
2
0
-2
-4
-6
0.000
0.250
0.500
0.750
1.000
1.250
1.500
1.750
2.000
Draft (m)
LCF (10^1)
TCF (10^-2)
Awp (10^1)
S (10^1)

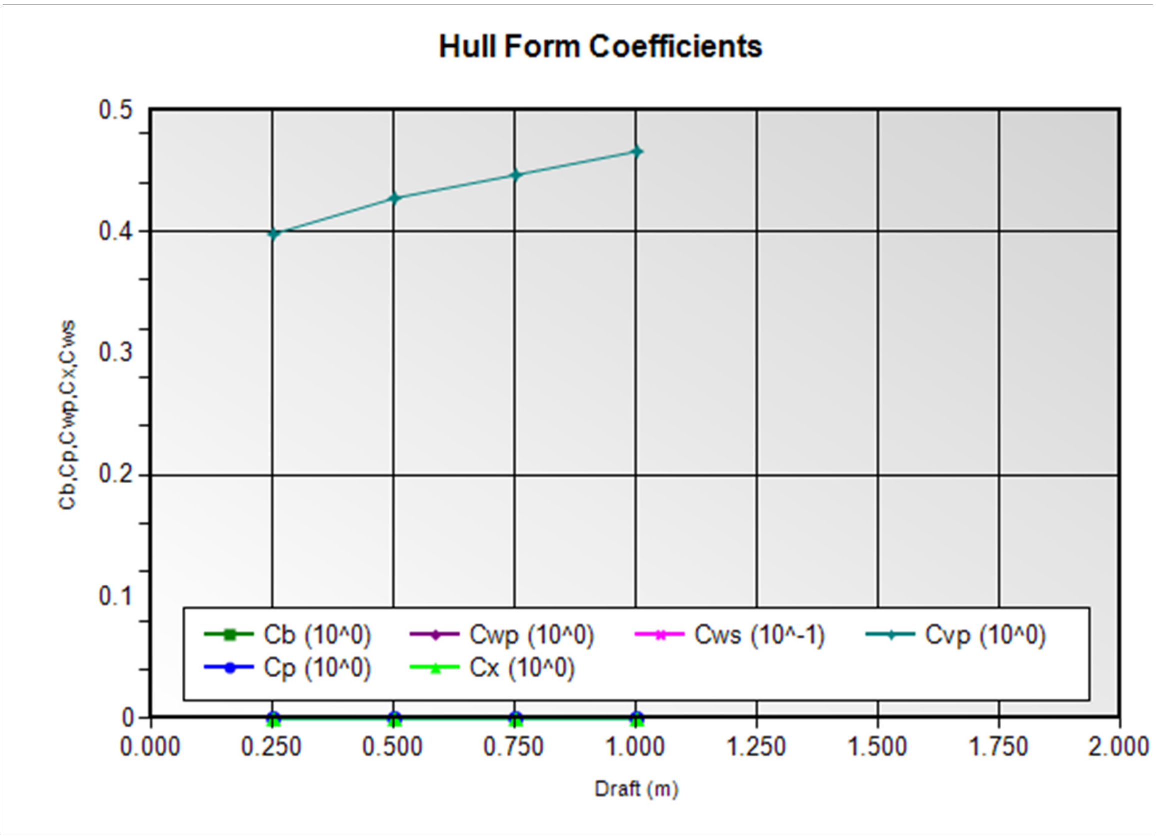

Hull Form Coefficients
Cb,Cp,Cwp,Cx,Cws
0.5
0.4
0.3
0.2
0.1
0
0.000
0.250
0.500
0.750
1.000
1.250
1.500
1.750
2.000
Draft (m)
Cb (10^0)
Cwp (10^0)
Cws (10^-1)
Cvp (10^0)
Cp (10^0)
Cx (10^0)

Glossary of Terms

Design Terms

Conceptual Design: A novel core concept, or fundamental principle, that characterizes a technology (Kroll et al. 2001: 1).

Design: The process of turning a concept into a physical entity. The product of cultural background, available materials, and previous experience.

Development: Change within a conceptual design framework. The core concept remains the same, but changes are made to increase variability whether improving efficiency for certain cultural or environmental conditions or stasis.

Emergent Phenomenon: A term coined by John Law to describe a technology that is greater than its parts (2012); see ***Gestalt***.

***Gestalt*:** German word used in psychology to mean “an organized whole that is perceived as more than the sum of its parts,” a concept that John Law applied to technology, notably ships (2012).

Innovation: The author argues that an innovation is the identification of a novel set of core concepts, or conceptual design. The amount to which the core concept differs from previous technologies determines the level of innovation.

Invention: The implementation of a new conceptual design as a material manifestation for the first time.

Technology: A conceptual development allowing for humans to affect their social and/or natural environments (agency manifest), according to the author’s proposed system of understanding technology as a material and immaterial hybrid.

Nautical Terms

Anchor: A device deployed from a vessel to keep it stationary.

> ***Ankura, ancora***: *ankura* (Greek) and *ancora* (Latin) refers to "bent" anchors, i.e. stocked anchors.
>
> **Crown:** "That portion of an anchor where its arms joined the shank" (Steffy 2006:266).
>
> ***Eunai:*** The earliest Greek term for an anchor, translating as "bed," and thought to describe stone bed-shaped weight-based anchors.
>
> **Fluke:** The widened distal end of an anchor's arms, either chisel or palm shaped, that grips the seafloor in crown-weighted anchors.
>
> **Palm:** "The triangular face of an anchor's fluke" (Steffy 2006:266).
>
> **Stock:** "A wooden, stone, or metal crosspiece near the top of and perpendicular to the shank" (Steffy 2006:267).
>
> **Tooth:** The narrowing point at the end of an anchor's arm that digs into the seafloor on a stock-weighted anchor, sometimes covered in iron or bronze to protect the wooden structure.

Ballast: "Heavy material, such as iron, lead, or stone, placed low in the hold to lower the center of gravity and improve stability" (Steffy 2006:267).

Butt Joint: "The union of two planks or timbers whose ends were cut perpendicularly to their lengths; sometimes called *carvel joint*" (Steffy 2006:268).

Cathead: A beam projecting from the side of a vessel to act as a crane and allow an anchor to be catted, or a loop was passed around one arm and hoisted on the railing or deck to secure the anchor from swinging.

Forefoot: "A curved piece between the forward end of the keel and the knee of the head" (Steffy 2006:271).

Frames: Internal timbers that provide transverse strengthening.

Hogging Truss: a form of longitudinal strengthening on ancient vessels, a hogging truss was a strong cable that connected to the bow and stern of a vessel to prevent sagging of the vessel's ends (Steffy 2006:273).

Keel and Keelplank: The primary structural longitudinal timber of a vessel on the bottom of the hull.

Keelson: "An internal longitudinal timber or line of timbers, mounted atop the frames along the centerline of the keel" (Steffy 2006:274).

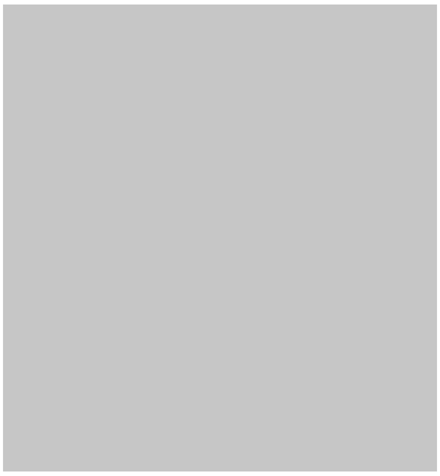

Mortise-and-Tenon Joint: "A union of planks or timbers by which a projecting piece (tenon) was fitted into one or more cavities (mortises) or corresponding size" (Steffy 2006:276).

Rabbet: "A groove or cut made in a piece of a timber in such a way that the edges of another piece could be fit into it to make a tight joint" (Steffy 2006:277).

Ram: "A strong projection on the bow of an ancient warship, usually sheathed in metal, used as a weapon to strike another vessel" (Steffy 2006:277).

Scarph: “An overlapping joint used to connect two timbers or planks without increasing their dimensions” (Steffy 2006:279).

Sewn Fastening: A method by which planks are lashed together rather than fastened with wood or metal fasteners. Example of ancient Egyptian sewn fastening (Mark 2009:Figure 7).

Strake: One of the timbers that forms the continuous hull planking on the exterior of a vessel.

Tuck: “The place where the ends of the bottom planks terminated under the stern or counter” (Steffy 2006:281).

Tumblehome: “The inward curvature of a vessel’s upper sides as they rose from the point of maximum breadth to the bulwarks” (Steffy 2006:281).

Wale: A thick strake of planking, or a belt of thick planking strakes, located along the side of a vessel for the purpose of girding and stiffening the outer hull” (Steffy 2006:281).

Bibliography

Abramzon, Mikhail G., and Vladimir D. Kuznetsov

2011 The Rebellion in Phanagoria in 63 BC: New Numismatic Evidence. *Ancient Civilizations from Scythia to Siberia* 17(1):75–110.

Adams, Jonathan R., Annita Antoniadou, Christopher O. Hunt, Paul Bennett, Ian W. Croudace, Rex N. Taylor, Richard B. Pearce, Graeme P. Earl, Nicholas C. Flemming, John Moggeridge, Timothy Whiteside, Kenneth Oliver, and Anthony J. Parker

2013 The Belgammel Ram, a Hellenistic-Roman Bronze Proembolion Found Off the Coast of Libya: Test Analysis of Function, Date and Metallurgy, with a Digital Reference Archive. *International Journal of Nautical Archaeology* 42(1):60–75.

van Alfen, Peter

1996 New light on the 7th-c. Yassi Ada shipwreck: capacities and standard sizes of LRA1 amphoras. *Journal of Roman Archaeology* 9: 189–213.

Aristophanes

2003 *The Birds and Other Plays*. Translated. Penguin Classics, New York.

Basch, Lucien

1987 *Le Musée Imaginaire de La Marine Antique*. Hellenic Institute for the Preservation of Nautical Tradition, Athens.

Bass, George F., Sheila Matthews, James W. Allan, and J. Richard Steffy

2004 *Serçe Limanı: An Eleventh-Century Shipwreck, Volume 1*. Texas A&M University Press, College Station.

Beltrame, Carlo

2002 *Vita di bordo in età romana*. Instituto Poligrafico e Zecca dello Stato, Rome.

Bilan Scientifique

1993 Bilan Scientifique du DRASM 1993. Ministrère de la Culture, Paris.

1998 *Bilan Scientifique du DRASM 1998*. Ministrère de la Culture, Paris.

2001 *Bilan Scientifique du DRASM 2001*. Ministrère de la Culture, Paris.

2002 *Bilan Scientifique du DRASM 2002*. Ministrère de la Culture, Paris.

2003 *Bilan Scientifique du DRASM 2003*. Ministrère de la Culture, Paris.

2005 *Bilan Scientifique du DRASM 2005*. Ministrère de la Culture, Paris.

Boardman, John

2011 *The Greeks Overseas: Their Early Colonines and Trade*. 4th editio. Thames and Hudson, London.

Bonino, Marco

1985 Notes on the Architecture of Some Roman Ships: Nemi and Fiumicino. In Tropis I, Harry Tzalas, editor, pp. 37–45. Hellenic Institute for the Preservation of Nautical Tradition, Piraeus.

Bound, Mensun

1989 The Carpenter's Calipers from the Pre-Classical Wreck at Campese Bay, Island of Giglio, Northern Italy (C. 600 BC). In *Tropis III*, Harry Tzalas, editor, pp. 99–110. Hellenic Institute for the Preservation of Nautical Tradition, Athens.

Bouscaras, A.

1954 Recherches sous-marine d'Agde. *Revue d'Etudes Lingures* 20:47-54.

Brather, S.

1994 *Wood Conservation Report*. Brandenburg.

Brouskari, Maria

1985 *The Paul and Alexandra Canellopoulos Museum: A Guide*. Karydakis, Athens.

Buccellato, Cecilia A., and Sebastiano Tusa

2013 The Acqualadroni Ram Recovered Near the Strait of Messina, Sicily: Dimensions, Timbers, Iconography and Historical Context. *International Journal of Nautical Archaeology* 42(1):76–86.

Calligas, Peter

1996 Bronze Ram of a Ship. In *Tropis IV*, Harry Tzalas, editor, pp. 129–141. Hellenic Institute for the Preservation of Nautical Tradition, Athens.

Campbell, Duncan B.

2006 *Besieged: Siege Warfare in the Ancient World*. Osprey Publishing, Oxford.

Carlson, Deborah N.

2009 Seeing the Sea: Ships' Eyes in Classical Greece. *Hesperia* 78(3):347–365.

Carlson, Deborah N., and William Aylward

2010 The Kızılburun Shipwreck and the Temple of Apollo at Claros. *American Journal of Archaeology* 114(1):145–159.

Caruso, F., M. L. Saladino, A. Spinella, C. di Stefano, P. Tisseyre, S. Tusa, and E. Caponetti

2011 Physico-Chemical Characterization of the Acqualadrone Rostrum. *Archaeometry* 53(3):547–562.

Casson, Lionel

1995 *Ships and Seamanship in the Ancient World*. 2nd edition. The Johns Hopkins University Press, Baltimore.

Casson, Lionel, and J. Richard Steffy

1991 *The Athlit Ram*. Lionel Casson and J. Richard Steffy, editors. Texas A&M University Press, College Station.

Castro, Filipe

2008 In Search of Unique Iberian Ship Design Concepts. *Historical Archaeology* 42(2):63–87.

Charlin, G., J. M. Gassend and R. Lequement

1978 L'épave antique de la baie de Cavalière (Le Lavandou, Var). *Archaeonautica* 2(1): 9-93.

Christie's

2004a A Roman Bronze Alloy Prow of a Ship: Circa 1st-2nd Century A.D. http://www.christies.com/lotfinder//a-roman-bronze-alloy-prow-of-a-4265332-details.aspx.

2004b A Roman Bronze Alloy Prow of a Ship: Circa 1st Century B.C./A.D. http://www.christies.com/lotfinder//a-roman-bronze-alloy-prow-of-a-4265333-details.aspx.

Craddock, Paul T.

1986 Three Thousand Years of Copper Alloys. B. van Zelst, editor, pp. 59–67. Boston Museum of Fine Arts, Boston.

Current World Archaeology

2015 Turkey's Largest Ancient Shipyard. *Current World Archaeology* November.

Dangréaux, B.

1993 Balise de Rabiou. *Bilan Scientifique du DRASM 1993*. Ministrère de la Culture, Paris.

2012 L'épave de la Tour Fondue (Presqu'île de Giens, Var), un bâtiment de cabotage dans la seconde moitié du IIIe siècle avant J. -C. *Cahiers d'Archéologie Subaquatique* 19: 5-36.

van Duivenvoorde, Wendy

2012The Anchor of the 3rd-Century-BC Ship from Kyrenia, Cyprus: A one-armed wooden anchor with a lead-filled stock. *International Journal of Nautical Archaeology* 41(2):397-407.

Dumas, Frédéric

1972 *30 Siècles Sous le Mer*. Famont, Geneva.

Dumontier, M. and J. P. Joncheray

1991 L'épave romaine du Miladou. *Cahiers d'Arch*éologie Subaquatique 10:125-174.

Frank, Patrick, Francesco Caruso, and Eugenio Caponetti

2012 Ancient Wood of the Acqualadrone Rostrum: Materials History through Gas Chromatography/Mass Spectrometry and Sulfur X-Ray Absorption Spectroscopy. *Analytical Chemistry* 84:4419–4428.

Freschi, A.

1997Gasr Ed-Dauun. *Rinvenimenti Subacquei a Milazzo e il Relitto di Punta Mazzo*, G. Tigano, editor, pp. 60-65. Messina.

Frost, Honor

1975 Another Punic Wreck in Sicily: Its Ram. 2. The Ram from Marsala. *International Journal of Nautical Archaeology* 4(2):219–228.

1982 On a Sacred Cypriot Anchor. In *Archéologie Au Levant*, Jean Pouilloux, editor, pp. 161–166. Maison de l'Orient et de la Méditerranée, Lyon.

Galili, E., and Y. Sharvit

1998 Ashqelon, North, Underwater and Coastal Survey. *Hadashot Arkheologiyot Excavations and Surveys in Israel* 18:155.

1999 Underwater survey in the Mediterranean 1992-1996. *Hadashot Arkheologiyot Excavations and Surveys in Israel* 19:96-101.

Galili, E., V. Sussman, G. Stiebel, and B. Rosen

2010 A Hellenistic/Early Roman Shipwreck Assemblage off Ashkelon, Israel. *International Journal of Nautical Archaeology* 39(1):125–145.

Garlan, Y.

1994 Warfare. In *The Cambridge Ancient History: The Fourth Century BC*, D M Lewis, John Boardman, Simon Hornblower, and M Ostwald, editors, pp. 678–692. Cambridge.

Gauthier, B.

1992Cap Gros C. *Bilan Scientifique du DRASM 1992*, pp. 55. Ministrère de la Culture, Paris.

Gianfrotta, P.

1981 Il commercio del marmo. *Mondo Archeologico* 57:27-31.

Gianfrotta, P. and P. Pomey

1980 *Archeologia Subacquea*. Mondadori, Milan.

Gibbins, D.

1997 More Underwater Finds of Roman Medical Equipment. *Antiquity* 71:457-459.

Göttlicher, Arvid

1978 *Materialien Für Ein Corpus Der Schiffsmodelle Im Altertum*. Verlag Philipp von Zabern, Mainz am Rhein.

Günsenin, Nergis

1998 Récentes découvertes sur l'île de Marmara (Proconnèse) à l›époque byzantine. *Archaeonautica* 14(1):309-316.

Hadas, Gideon, Nili Liphschitz, and Georges Bonani

2005 Two Ancient Wooden Anchors from Ein Gedi, on the Dead Sea, Israel. *International Journal of Nautical Archaeology* 34(2):299-307.

Hadjidaki, Elpida

1996 Underwater Excavations of a Late Fifth Century Merchant Ship at Alonnesos, Greece: The 1991-1993 Seasons. *Bulletin de Correspondance Hellénique* 12(2):561-593.

Harpster, Matthew B.

2005 Dowels as a Means of Edge-to-Edge Joinery in the 9th-Century AD Vessel from Bozburun, Turkey. *International Journal of Nautical Archaeology* 34(1):88–94.

Hasslöf, Olof

1972 Main Principles in the Technology of Ship-Building. In *Ships and Shipyards, Sailors, and Fishermen: Introduction to Maritime Ethnography*, Olof Hasslöf, H Henningsen, and A E Christensen, editors. University of Copenhagen Press, Copenhagen.

Haynes, Denys

1992 *The Technique of Greek Bronze Statuary*. Verlag Philipp von Zabern, Mainz am Rhein.

Hocker, Frederick M.

2004 Shipbuilding: Philosophy, Practice, and Research. In *The Philosophy of Shipbuilding: Conceptual Approaches to the Study of Wooden Ships*, Frederick M. Hocker and Cheryl A. Ward, editors, pp. 1–11. Texas A&M University Press, College Station.

Hockmann, Olaf

1987 Roman Danube Vessels from Oberstimm, Germany. In *Tropis II*, Harry Tzalas, editor, pp. 215–224. Hellenic Institute for the Preservation of Nautical Tradition, Athens.

Johnston, Paul Forsythe

1985 *Ship and Boat Models in Ancient Greece*. Naval Institute Press, Annapolis.

Joncheray, J.P.

1975 L'épave "C" de La Chrétienne. *Premier Supplément Aux Cahiers d'Archéologie Subaquatique* 4.

1994 L'épave Dramont C. *Cahiers d'Archéologie Subaquatique* 12(1):5–51.

Jurišić, Mario

2000*Ancient Shipwrecks of the Adriatic: Maritime Transport During the First and Second Centuries AD*. BAR International Series 828. Archaeopress, Oxford.

Kahanov, Ya'acov and Elisha Linder

2003 *The Ma'agan Mikhael Ship: The Recovery of a 2400-Year-Old Merchantman*. Volume 1. Israel Exploration Society, Jerusalem.

Kahanov, Ya'acov and Jeffrey Royal

2001 Analysis of Hull Remains of the Dor D Vessel, Tantura Lagoon, Israel. *International Journal of Nautical Archaeology* 30(2):257-265.

Kallipolitis, V.

1972 Artemision. *Athens Annals of Archaeology* 5:419-426.

Kampbell, Sarah M.

2007 The Pantano Longarini Shipwreck: A Reanalysis. MA thesis, Anthropology, Texas A&M University.

Kapitän, Gerhard

1983 A toothed gear and water-drawing pendulum from the Mahdia wreck. *International Journal of Nautical Archaeology* 12(2):145-153.

Kuhn, Thomas

2012 *The Structure of Scientific Revolutions*. 4th edition. University of Chicago Press, Chicago.

Lattanzi, Giovanni

2007 *Navi e Città Sommerse*. Laterza, Rome.

Leidwanger, Justin

2007 Two Late Roman Wrecks from Southern Cyprus. *International Journal of Nautical Archaeology* 36(2):308-316.

Leake, William Martin

1843 On the Brazen Prow of an Ancient Ship of War. *Transactions of the Royal Society, Second Series* 1(1):246–253.

Liou, B.

1973 Recherches Archéologiques Sous-Marine. *Gallia* 31(2):571-608.

Liou, Bernard, and Jean-Marie Gassend

1990 L'Epave Saint-Gervais 3 a Fos-Sur-Mer. *Archeonautica* 10:157–264.

Long, L.

1993Arles IV. *Bilan Scientifique du DRASM 1993,* pp. 30-31. Ministrère de la Culture, Paris.

1996 Saintes Maries de la Mer 3. *Bilan Scientifique du DRASM 1996,* pp. 42. Ministrère de la Culture, Paris.

Maffre, Frédéric

2004 Le Monnayage de Pharnabaze Frappé Dans L'atelier de Cyzique. *Numismatic Chronicle* 164(1):1–24.

Mark, Samuel

2009 The Construction of the Khufu I Vessel (c.2566 BC): A Re-Evaluation. *International Journal of Nautical Archaeology* 38(1):133–152.

Marlier, S.

2008Architecture et espace de navigation des navires à dolia. *Archeonautica* 15:176-192.

Marsden, Peter

1994 *Ships of the Port of London*. English Heritage, London.

Mattusch, Carol C.

1988 *Greek Bronze Statuary: From the Beginnings through the Fifth Century BC*. Cornell University Press, Ithaca.

McCann, A. M. and J. Freed

1994 *Deep Water Archaeology: A Late-Roman Ship from Carthage and an Ancient Trade Route Near Skerki Bank Off Northwest Sicily*. Journal of Roman Archaeology, Ann Arbor.

McCann, A. M. and J. P. Oleson

2004 Deep-Water Shipwrecks Off Skerki Bank: The 1997 Survey. *Journal of Roman Archaeology*, Supplementary Series No. 58.

Morrison, John S.

1995 Hellenistic Oared Warships 399-31 BC. In *The Age of the Galley: Mediterranean Oared Vessels Since Pre-Classical Times*, Robert Gardiner and John S. Morrison, editors, pp. 66–77. Conway Maritime Press, London.

Murray, William M.

1991 The Provenience and Date: The Evidence of the Symbols. In *The Athlit Ram*, Lionel Casson and J. Richard Steffy, editors, pp. 51–66. Texas A&M University Press, College Station.

Murray, William M., and Photios M. Petsas

1989 *Octavian's Campsite Memorial for the Actian War*. The American Philosophical Society, Philadelphia.

Negueruela, I.

2005 Coagmenta Punicana E Bagli: La Costruzione Navale a Fasciame Portante Tra I Fenici Del VIIe S. a.C. In *Mare, Uomini, E Merci Nel Meditteraneo Antico*, B.M. Giannattasio, C. Canepa, L. Grasso, and E. Piccardi, editors, pp. 22–41. All'Insegna del Giglio, Florence.

Neilson, Harry R.
2002 A terracotta phallus from Pisa Ship E: more evidence for the Priapus deity as protector of Greek and Roman navigators. *International Journal of Nautical Archaeology* 31(2):248-253.

Oron, Asaf
2001 The Athlit Ram: Classical and Hellenistic Bronze Casting Technology. Texas A&M.
2006 The Athlit Ram Bronze Casting Reconsidered: Scientific and Technical Re-Examination. *Journal of Archaeological Science* 33(1):63–76.

Parker, A. J.
1976 Il relitto romano delle colonne a Camarina. *Sicilia Archeologica* 9:25-29.
1992 *Ancient Shipwrecks of the Mediterranean and the Roman Provinces*. BAR Intern. Archeopress, Oxford.

Papathanassopoulos, G.
1980 Greece: Underwater Surveys in 1979. *International Journal of Nautical Archaeology* 9(2): 164-167.

Picozzi, S.
1988 La nave romana di Grado. *Subacqueo* 16(1):46-50.

Polzer, Mark
2004 An Archaic Laced Hull in the Aegean: The 2003 Excavation and Study of the Pabuç Burnu Ship Remains. *INA Quarterly* 31(3):3-11.

Pomey, Patrice
1982 Le Navire Romain de La Madrague De Giens. *Comptes Rendus Des Séances de l'Académie Des Inscriptions et Belles-Lettres* 126(1):133–154.
1988 Principes et Methodes de Construction En Architecture Navale Antique. *Navires et Commerces de La Mediterranee Antique* 33(3):397–412.
2002 Une Nouvelle Tradition Technique D'Assemblage Antique: L'Assemblage de La Membrure Par Ligatures et Chevilles. In *Tropis VII*, Harry Tzalas, editor, pp. 597–604. Hellenic Institute for the Preservation of Nautical Tradition, Athens.

Pomey, Patrice and Frédéric Guibal
1996 Dendrochronologie et Dendromorphologie des épaves Antiques de Méditerranée. *Bilan Scientifique du DRASSM 1994*, pp. 56. Ministère de la Culture, Paris.

Pomey, Patrice, Yaacov Kahanov, and Eric Rieth

2012 Transition from Shell to Skeleton in Ancient Mediterranean Ship-Construction: Analysis, Problems, and Future Research. *International Journal of Nautical Archaeology* 41(2):235–314.

Popular-Archaeology

2014 Ancient Naval Ram Found in Phanagoria Reveals History of Popular Unrest in 63 B.C. http://popular-archaeology.com/issue/06052014/article/ancient-naval-ram-found-in-phanagoria-reveals-history-of-popular-unrest-in-63-b-c.

Pridemore, Matthew G.

1996 The Form, Function, and Interrelationships of Naval Rams: A Study of Naval Rmas from Antiquity. MA thesis, Anthropology, Texas A&M University, College Station.

Pulak, Cemal

1998The Uluburun Shipwreck: An Overview. *International Journal of Nautical Archaeology* 27(3):188–224.

Purpura, G.

1987 Rinvenimenti sottomarini nella Sicilia occidentale. *Archeologia Subacquea* 3(37-38):139-160.

Raban, Avner

1969The finds from the Undersea Site at Hof HaCarmel. *Sefunim* 2:62-69.

Rash, Kimberly Paige

2012 Reconstructing the Assemblage of Iron Artifacts from the Late Hellenistic Shipwreck at Kizilburun, Turkey. MA thesis, Anthropology, Texas A&M University, College Station.

Rendini, P.

1982Monte Argentario: Isola del Giglio. Archeologia Subacquea in Toscana. *Bollettino d'arte* (Sup. 4):43-44.

Rieth, E., C. Carrierre-Desbois, and V. Serna

2001 *L'épave de Port Berteau II (Charente-Maritime): Un Caboteur Fluvio- Maritime Du Haut Moyen Âge et Son Contexte Nautique*. Maison des Sciences de l'Homme, Paris.

Royal, Jeffrey

2006 The 2005 Remote-Sensing Survey of the South-Eastern Bozburun Peninsula, Turkey: Shipwreck Discoveries and their Analyses. *International Journal of Nautical Archaeology* 35(2):195-217.

2008 Albanian Coastal Survey Project: 2008 Field Season. *INA Annual*: 21-25.

Ruscito, S.

1982 SOS Naufragio a Commachio. *Archaeologia Viva* 1:19-36.

Salvi, D.
1992 Da Carthago Nova verso i porti del Mediterraneo: il naufragio di un carico di lingotti di piombo. *Bollettino di Archeologia* 16-18:237-248.

Santamaria, Claide
1995 L'épave *Dramont « E » à Saint-Raphaël (Ve siècle ap. J.-C.). Archaeonautica* 13.

Sciallano, M.
1995La Giraglia. *Bilan Scientifique du DRASM 1993*, pp. 60. Ministrère de la Culture, Paris.

Sekunda, N. V.
1994 Classical Warfare. In *The Cambridge Ancient History: Plates to Volume V and VI*, John Boardman, editor, pp. 167–194. Cambridge University Press, Cambridge.

Speziale, G.C.
1931 The Roman Anchors Found at Nemi. *Mariner's Mirror* 17(4):309–320.

Steffy, J. Richard
1985 The Kyrenia Ship: An Interim Report on Its Hull Construction. *American Journal of Archaeology* 89(1):71–101.
1991 The Ram and Bow Timbers: A Structural Interpretation. In *The Athlit Ram*, Lionel Casson and J. Richard Steffy, editors, pp. 6–39. Texas A&M University Press, College Station.
2006 *Wooden Ship Building and the Interpretation of Shipwrecks*. 3rd edition . Texas A&M University Press, College Station.

Steinhauer, George
2001 *The Archaeological Museum of Piraeus*. Latsis Group, Athens.

Strauss, Julia
2013 Shipwrecks Database: The Oxford Roman Economy Project. Database Version 1.0. oxrep.classics.ox.ac.uk/databases/shipwrecks_database/ (accessed 10 May 2016).

Tchernia, André
1969 Recherches archéologiques sous-marine. *Gallia* 27(2):465-499.

Throckmorton, Peter
1970 *Shipwrecks and Archaeology*. Little and Brown, Boston.
1985 The Torre Sgaratta Ship. In *Tropis I*, Harry Tzalas, editor, pp. 263–274. Hellenic Institute for the Preservation of Nautical Tradition, Athens.

Torr, Cecil

1894 *Ancient Ships*. Cambridge University Press, Cambridge.

Touchais, G.

1985Chronique des fouilles et découvertes archéologiques en Grèce en 1984. *Bulletin de Correspondance Hellénique* 109:759-862.

Trethewey, Ken

2001 Lead anchor-stock cores from Tektas Burnu, Turkey. *International Journal of Nautical Archaeology* 30(1):109-114.

Trendall, A. D., and Alexander Cambitoglou

1982 *The Red-Figured Vases of Apulia*. Clarendon Press, Oxford.

Tupper, E.C., and K.J. Rawson

2001 *Basic Ship Theory*. 5th edition. Butterworth-Heinemann, Oxford.

Tusa, Sebastiano, and Jeffrey Royal

2012 The Landscape of the Naval Battle at the Egadi Islands (241 B.C.). *Journal of Roman Archaeology* 25(1):7–48.

Varoufakis, George

2007 The Bronze Ram of Nicopolis: A New Generation of Naval Weapons of the 1st Century BC. In *Nicopolis B: Proceedings of the Second International Nicopolis Symposium*, Konstantinos L. Zachos, editor, pp. 453–460. Vol. 1. Actia Nicopolis Foundation, Preveza.

Wachsmann, Shelley

2013 *The Gurob Ship-Cart Model and Its Mediterranean Context*. Texas A&M University Press, College Station.

Walters, H. B.

1899 *Catalogue of the Bronzes, Greek, Etruscan and Roman in the Department of Greek, Etruscan and Roman Antiquities, British Museum*. British Museum Press, London.

Whitehead, David, and P. H. Blyth

2004 *Athenaeus Mechanicus, On Machines*. Franz Steiner Verlag, Stuttgart.

Will, Elizabeth

1982 Greco-Italic Amphoras. *Hesperia* 51:338-356.

Winters, H., and Y. Kahanov

2003 Hull-Lines, Sea Worthiness, and Burden. T*he Ma'agan Mikhael Ship: The Recovery of a 2400-Year-Old Merchantman*, Volume 1, E. Linder and Y. Kahanov (eds.), pp. 130-133. Israel Exploration Society, Jerusalem.